MICROBIALLY INFLUENCED CORROSION STUDIES OF ENGINEERED BARRIER SYSTEM MATERIALS

Prepared for

U.S. Nuclear Regulatory Commission
Contract NRC–02–02–012

Center for Nuclear Waste Regulatory Analyses
San Antonio, Texas

SwRI Logo

MICROBIALLY INFLUENCED CORROSION STUDIES OF ENGINEERED BARRIER SYSTEM MATERIALS

Prepared for

U.S. Nuclear Regulatory Commission
Contract NRC–02–02–012

Prepared by

L. Yang
S. Birnbaum
G.A. Cragnolino

Center for Nuclear Waste Regulatory Analyses
San Antonio, Texas

July 2004

PREVIOUS REPORTS IN SERIES

Number	Name	Date Issued
CNWRA 91-004	A Review of Localized Corrosion of High-Level Nuclear Waste Container Materials—I	April 1991
CNWRA 91-008	Hydrogen Embrittlement of Candidate Container Materials	June 1991
CNWRA 92-021	A Review of Stress Corrosion Cracking of High-Level Nuclear Waste Container Materials—I	August 1992
CNWRA 93-003	Long-Term Stability of High-Level Nuclear Waste Container Materials: I—Thermal Stability of Alloy 825	February 1993
CNWRA 93-004	Experimental Investigations of Localized Corrosion of High-Level Nuclear Waste Container Materials	February 1993
CNWRA 93-014	A Review of the Potential for Microbially Influenced Corrosion of High-Level Nuclear Waste Containers	June 1993
CNWRA 94-010	A Review of Degradation Modes of Alternate Container Designs and Materials	April 1994
CNWRA 94-028	Environmental Effects on Stress Corrosion Cracking of Type 316L Stainless Steel and Alloy 825 As High-Level Nuclear Waste Container Materials	October 1994
CNWRA 95-010	Experimental Investigations of Failure Processes of High-Level Radioactive Waste Container Materials	May 1995
CNWRA 95-020	Expert-Panel Review of the Integrated Waste Package Experiments Research Project	September 1995
CNWRA 96-004	Thermal Stability and Mechanical Properties of High-Level Radioactive Waste Container Materials: Assessment of Carbon and Low-Alloy Steels	May 1996
CNWRA 97-010	An Analysis of Galvanic Coupling Effects on the Performance of High-Level Nuclear Waste Container Materials	August 1997
CNWRA 98-004	Effect of Galvanic Coupling Between Overpack Materials of High-Level Nuclear Waste Containers—Experimental and Modeling Results	March 1998

PREVIOUS REPORTS IN SERIES (continued)

Number	Name	Date Issued
CNWRA 98-008	Effects of Environmental Factors on Container Life	July 1998
CNWRA 99-003	Assessment of Performance Issues Related to Alternate Engineered Barrier System Materials and Design Options	September 1999
CNWRA 99-004	Effects of Environmental Factors on the Aqueous Corrosion of High-Level Radioactive Waste Containers—Experimental Results and Models	September 1999
CNWRA 2000-06 Revision 1	Assessment of Methodologies to Confirm Container Performance Model Predictions	January 2001
CNWRA 2001-003	Effect of Environment on the Corrosion of Waste Package and Drip Shield Materials	September 2001
CNWRA 2002-01	Effect of In-Package Chemistry on the Degradation of Vitrified High-Level Radioactive Waste and Spent Nuclear Fuel Cladding	October 2001
CNWRA 2002-02	Evaluation of Analogs for the Performance Assessment of High-level Waste Container Materials	March 2002
CNWRA 2003-01	Passive Dissolution of Container Materials—Modeling and Experiments	October 2002
CNWRA 2003-02	Stress Corrosion Cracking and Hydrogen Embrittlement of Container and Drip Shield Materials	October 2002
CNWRA 2003-05	Assessment of Mechanisms for Early Waste Package Failures	March 2003
CNWRA 2004-01	Effect of Fabrication Processes on Materials Stability—Characterization and Corrosion	October 2003
CNWRA 2004-02	Natural Analogs of High-Level Waste Container Materials—Experimental Evaluation of Josephinite	January 2004
CNWRA 2004-03	The Effects of Fabrication Processes on the Mechanical Properties of Waste Packages—Progress Report	July 2004

ABSTRACT

The performance of the waste package, the main component of the engineered barrier system of the potential high-level waste repository at Yucca Mountain, Nevada, is one of the principal factors in the U.S. Department of Energy (DOE) postclosure repository safety strategy. The waste package design for the license application consists of an outer disposal container made of Alloy 22 surrounding an inner container made of Type 316 nuclear grade stainless steel. Among the corrosion processes considered to be important in determining the performance of the waste package, microbially influenced corrosion deserves attention because of the ubiquitous nature of bacteria and the effects of bacterial metabolic products in creating aggressive local environments in the biofilms formed on metal surfaces by microorganisms. In this report, studies conducted by DOE on microbially influenced corrosion of Alloy 22 are reviewed, and the DOE model abstraction used in performance calculations is assessed. The results of initial experimental investigations conducted at the Center for Nuclear Waste Regulatory Analyses are presented. Electrochemical studies measuring galvanic coupling currents and repassivation potentials for Type 304 SS in aqueous chloride environments containing a slime former and a sulfate-reducing bacteria are reported. No effect of the sulfate-reducing bacteria on the repassivation potential was found, and higher anodic currents observed in forward polarization scans were attributed to the oxidation of reduced sulfur species adsorbed on the metal surface rather than metal corrosion. This explanation is suggested because similar anodic scans performed with platinum, which behaves as an inert metal, exhibited higher current densities in environments containing bacteria than in those in which the bacteria are absent. However, pitting corrosion of Type 304 SS was observed in a chloride solution containing the sulfate-reducing bacteria in a 160-day test. A set of long-term experiments is currently under way in which specimens of Alloy 22, Type 316L SS, and Alloy 825 are being exposed in parallel cells to aqueous solutions containing *Pseudomonas, Thiobacilli,* sulfate-reducing bacteria, plus *Vibrio Natriegens*, a slime former, or mixtures of these bacteria, to evaluate if localized corrosion could occur in these alloys. It is expected that this set of tests will help in evaluating the potential susceptibility to localized corrosion of this class of passive alloys at ambient temperatures.

CONTENTS

CONTENTS (continued)

FIGURES

FIGURES (continued)

TABLES

ACKNOWLEDGMENTS

This report was prepared to document work performed by the Center for Nuclear Waste Regulatory Analyses (CNWRA) for the U.S. Nuclear Regulatory Commission (NRC) under Contract No. NRC–02–02–012. The activities reported here were performed on behalf of the NRC Office of Nuclear Material Safety and Safeguards, Division of High-Level Waste Repository Safety. The report is an independent product of CNWRA and does not necessarily reflect the views or regulatory position of NRC.

The authors would like to thank S. Brossia for important contributions at the beginning of this study. The technical assistance and discussions with G. Becker (Applied Becker Consulting) in the microbial aspects of this work and the laboratory assistance by R.J. Dykstra and B. Derby are acknowledged. The authors acknowledge the technical review of D. Dunn, the programmatic review of B. Sagar, the editorial reviews of J. Pryor and C. Cudd, and the assistance of J. Gonzalez in preparing this report.

QUALITY OF DATA, ANALYSES, AND CODE DEVELOPMENT

DATA: All CNWRA-generated original data contained in this report meet quality assurance requirements described in the CNWRA Quality Assurance Manual. Experimental data have been recorded in CNWRA scientific notebook numbers 522, 287, and 604. Sources for other data should be consulted for determining the level of quality for those data.

ANALYSES AND CODES: No codes were used in the analyses contained in this report.

EXECUTIVE SUMMARY

The performance of the waste package, the main component of the engineered barrier system of the potential high-level waste repository at Yucca Mountain, Nevada, is one of the principal factors in the U.S. Department of Energy (DOE) postclosure safety strategy. The DOE reference waste package design to be included in the license application consists of an outer container made of Alloy 22, a highly corrosion-resistant nickel-chromium-molybdenum alloy, and an inner container made of Type 316 nuclear grade stainless steel (SS). For undisturbed repository conditions, corrosion of the container is expected to be the primary degradation process limiting the life of the waste package. Loss of containment as a result of corrosion will allow the release of radionuclides to the environment immediately surrounding the waste packages.

Among the various corrosion processes considered to be important to the degradation of waste packages, microbially influenced corrosion deserves attention because of the ubiquitous nature of bacteria and other microorganisms. In many circumstances, particularly for corrosion-resistant alloys such as stainless steels and nickel-chromium-molybdenum alloys, microbially influenced corrosion manifests itself primarily as localized corrosion in the form of pitting. The objective of the studies presented in this report is to quantify the effects of microbial activity on the corrosion of Alloy 22 and Type 316 SS. This report provides a review of the DOE model abstraction for the microbially influenced corrosion of Alloy 22 outer container and presents results of recent experimental work on the subject, mostly conducted using Type 304 SS, at the Center for Nuclear Waste Regulatory Analyses (CNWRA).

Because of the decay heat from radioactive waste, the temperature in the emplacement drift will increase, reaching a maximum value when the rate of heat generation equals the rate of heat loss to the surrounding rock. Thereafter, the temperature will decrease because of the decrease in the rate of heat generation. Concurrently, the relative humidity will gradually increase. According to the model estimations by DOE, for some waste packages the relative humidity on the waste package surface is expected to reach 90 percent, which is considered the threshold value for the microorganisms to be active, in approximately 200 to 300 years after emplacement. When the relative humidity on the waste package surfaces reaches 90 percent, the main source of water will be seepage into the emplacement drifts. The environmental conditions in terms of temperature, water, and nutrient availability for microbially influenced corrosion to occur will be established. At this point in the repository evolution, it is likely that extreme thermophilic bacteria capable of growth at temperatures above 70 °C [158 °F] will become established. Over time, as the temperature decreases, the microbial population will change to a population of moderate thermophilic bacteria {40 to 70 °C [104 to 158 °F} and then to a mesophilic population {below 40 °C [104 °F]}. The presence of sulfates, nitrates, and carbon dioxide in the seepage waters suggests that the composition of the aqueous environment in the emplacement drift is capable of supporting microbial growth.

The microorganisms associated with microbially influenced corrosion include algae, fungi, and bacteria; all of which are ubiquitous in nature. The role in microbially influenced corrosion of selected groups of bacteria including sulfate-reducing bacteria, *Thiobacillus, Pseudomonas,* iron- and manganese-oxidizing bacteria, and acid-producing bacteria, is briefly reviewed as an introduction to the bacteria identified by studies in the vicinity of Yucca Mountain and in the exploratory drift facility. Only generalizations of their specific metabolic behavior are presented, emphasizing that bacteria do not exist in pure cultures. Instead, communities of microbes

coexist and interact in complex ways. A range of candidate microbes able to promote microbially influenced corrosion were found to exist at Yucca Mountain such as acid-producing bacteria, exopolysaccharide-producing bacteria, iron-oxidizing bacteria, and sulfate-reducing bacteria. At Yucca Mountain, the microbial population is high enough to influence corrosion and nutrients are not limiting. Water, represented by relative humidity, is probably the dominant limiting factor controlling microbial growth.

In the studies on microbially influenced corrosion of Alloy 22 conducted by DOE, anodic current densities in the potentiodynamic polarization curves and corrosion rates using the linear polarization resistance method were higher in microbial environments than those obtained in microbe-free environments. In the CNWRA studies described in this report, higher anodic polarization current densities were obtained on both stainless steel and platinum electrodes in microbial environments compared to those observed in the microbe-free environments. Because platinum is not expected to corrode within the range of potentials included in the polarization scans, the higher anodic current densities observed on platinum and stainless steel electrodes are believed to be caused by the oxidation of adsorbed surface species produced by the microorganisms. The results from these initial CNWRA studies suggest that the higher corrosion rates for Alloy 22 measured by using the linear polarization resistance method may be an artifact caused by the oxidation of reduced species produced in the microbial environment rather than an increase in the uniform corrosion rate within the passive range caused by the activity of the microorganisms. DOE used a microbially influenced corrosion factor derived from the linear polarization resistance measurements to account for microbial activity in the model abstraction for the general corrosion of Alloy 22. This approach tends to overestimate the uniform corrosion rate and, therefore, can be considered a conservative approach if localized corrosion cannot be promoted by bacterial activity.

From the repassivation potential measurements performed by DOE and CNWRA in microbe-free environments, it can be concluded that the critical temperature for the localized corrosion of Alloy 22, even in concentrated chloride solutions without the presence of inhibiting anions may be high. Based on such repassivation potential measurements, DOE considered that Alloy 22 will not be susceptible to localized corrosion in environments characterized by the presence of microorganisms. However, many microorganisms found in the vicinity of Yucca Mountain are known to produce aggressive environments that could promote localized corrosion of stainless steels and relatively high corrosion-resistant nickel-based alloys. All the major groups of organisms identified as involved in microbially influenced corrosion include thermophilic microorganisms capable of growth at temperatures at or above 60 °C [140 °F] and some as high as 90 °C [194 °F].

From these initial CNWRA studies, it is apparent that the effect of microbial activity on the localized corrosion of passive metals such as Type 304 SS is not detectable in short-term tests using the repassivation potential technique. It appears that the high anodic polarization potentials required by the technique to initiate localized corrosion may affect bacterial activity or the concentration of potentially aggressive metabolic products. Even though pitting corrosion of Type 304 SS was observed in a chloride solution with the presence of sulfate-reducing bacteria in a 160-day immersion test, no lowering of the repassivation potential was observed in short-term electrochemical tests in the microbial environments. The repassivation potential method, based on the reverse potentiodynamic scan after initiation of localized corrosion at high anodic potentials, may not be adequate to quantify the effect of bacterial activity on localized corrosion. Therefore, it appears that in environments modified by bacterial metabolism, the

repassivation potential method may not be adequate to determine microbial effects on the susceptibility of localized corrosion of corrosion-resistant alloys such as Alloy 22, which is far more resistant to this form of corrosion than is Type 304 SS.

Long-term immersion tests, allowing sufficient time for creating occluded cell conditions in which the appropriate concentration of metabolic products can be reached, could provide a better assessment of the susceptibility to microbially influenced corrosion of a given corrosion-resistant alloy. For this reason, a set of long-term experiments with duplicate specimens made of heat-treated Alloy 22, Type 316L SS, and Alloy 825 is currently being conducted at CNWRA. These experiments are performed in parallel cells containing *Pseudomonas*, *Thiobacilli*, sulfate-reducing bacteria, plus *Vibrio Natriegens*, a slime former, or mixtures of these bacteria. At regular intervals, the specimens are from the test cells and examined with a scanning electron microscope for signs of localized corrosion.

The long-term immersion test solutions inoculated with Yucca Mountain rocks may not contain all the bacteria that are either native to the Yucca Mountain repository horizon or may be introduced into the repository during preclosure operations such as repository construction or waste emplacement. For this reason, it would be desirable to conduct long-term tests in solutions that contain all potential detrimental microorganisms that may be present at Yucca Mountain. Although this testing program may seem to be a rather cumbersome endeavor, performance confirmation activities should include this type of testing using not only mill-annealed specimens of Alloy 22 but also heat-treated and welded specimens.

1 INTRODUCTION

The performance of the engineered barriers in the potential Yucca Mountain repository, following emplacement of spent nuclear fuel and high-level waste, is extremely important to protect the public from any undue radiological risk before and after permanent closure, as stated by the U.S. Department of Energy (DOE) in its Repository Safety Strategy (CRWMS M&O, 2000a). The U.S. Nuclear Regulatory Commission (NRC) has published licensing requirements for disposal of high-level wastes at Yucca Mountain. According to 10 CFR Part 63, the engineered barrier system must be designed so that, working in combination with natural barriers, radiological exposures to the reasonably maximally exposed individual and release of radionuclides into the accessible environment are limited, as specified in 10 CFR 63.311. For these reasons, the performance of the waste package, the main component of the engineered barrier system, is one of the principal factors for the postclosure safety case (CRWMS M&O, 2000a). The reference waste package design to be included in the license application (Anderson, et al., 2003) consists of an outer container made of a highly corrosion-resistant nickel-chromium-molybdenum alloy, Alloy 22 (Ni-22Cr-13Mo-4Fe-3W), and an inner container made of Type 316 nuclear grade stainless steel (SS) (low C-high N-Fe-18Cr-12Ni-2.5Mo). For undisturbed repository conditions, corrosion is expected to be the primary degradation process limiting the life of the waste package. Loss of containment will allow the release of radionuclides to the environment immediately surrounding the waste packages.

In support of the NRC prelicensing activities on topics important to the postclosure performance of the proposed repository, the Center for Nuclear Waste Regulatory Analyses (CNWRA) is conducting an independent technical assessment of corrosion processes that may affect the integrity of the waste packages. The corrosion-related processes considered important to the degradation of the waste packages include dry-air oxidation, humid-air and uniform aqueous (general) corrosion, localized (pitting, crevice, and intergranular) corrosion, microbially influenced corrosion, stress corrosion cracking, and hydrogen embrittlement. Based on the available risk insights and the NRC ranking of waste package failure mode as having medium significance to waste isolation (NRC, 2004), the possibility of microbially influenced corrosion of the waste package needs to be considered as one of the corrosion processes that could adversely affect the life of the waste packages, influencing the corrosion morphology and the amount of water that can enter the waste package.

1.1 Objective

The objective of the studies presented in this report is to quantify the effects of microbial activity on the corrosion of Alloy 22 and Type 316L SS. A detailed review of the possibility of microbially influenced corrosion of the candidate and alternate container materials considered by DOE for the potential repository at Yucca Mountain was published several years ago by CNWRA (Geesey, 1993). One of that report conclusions was related to the lack of information on microbially influenced corrosion of nickel-based alloys containing chromium as the main alloying element. This report provides a review of the DOE model abstraction for microbially influenced corrosion of the Alloy 22 outer container and presents results of the recent experimental work conducted at CNWRA.

1.2 Scope and Organization of the Report

Corrosion processes potentially important in the degradation of the engineered barriers have been reviewed in the Integrated Issue Resolution Status Report (NRC, 2002) and are the subject of Subissue 1 for the waste package and Subissue 6 for the drip shield of the Container Life and Source Term Key Technical Issue (NRC, 2001). It is known that the failure mode of the waste package (e.g., localized corrosion promoted by microbial activity) is important for determining the amount of water that can enter the waste package, affecting the rate of release of radionuclides.

This report is organized into five chapters, including an introduction as Chapter 1. The design of the waste package, its emplacement in the drifts, and the temperature, relative humidity, and chemical composition of possible in-drift aqueous environments are discussed in Chapter 2. An overview of microbially influenced corrosion processes caused by different bacteria and a description of the bacteria found at Yucca Mountain are the subjects of Chapter 3. Chapter 4 provides a review of the DOE investigations on microbially influenced corrosion and a detailed description of the investigations being conducted at CNWRA. The chapter is completed with an assessment of the DOE approach and the implications of the results of current investigations. A summary of conclusions and recommendations for future work needed to provide technical assistance to NRC for the review of the license application is included in Chapter 5.

1.3 Relevant DOE and NRC Agreements

As noted, degradation processes of the waste package are considered in Subissue 1 of the Container Life and Source Term Key Technical Issue (NRC, 2001), and incorporated in the Degradation of Engineering Barriers Integrated Subissue (NRC, 2002). Through the process of prelicensing consultation for issue resolution between DOE and NRC, this subissue is considered closed-pending according to the DOE and NRC agreements. Agreements related to microbially influenced corrosion are listed in Table 1-1. Even though microbially influenced corrosion is not explicitly mentioned in the language of these agreements, the three agreements have aspects relevant to the effects of microbial activity on corrosion. Critical aspects of environmental composition affected by microbial activity, are included in CLST 1.01, because metabolic products can modify the waters in contact with the waste packages. Selective dissolution of Alloy 22 by microbial activity, particularly at welds, measurements of lineal polarization resistance to determine the increase of corrosion rates by microbially influenced corrosion and confirmation of the enhancement factor, are important subjects in the two other agreements listed in Table 1-1.

The information related to CLST.1.01 was provided by the DOE in Appendix A of the Technical Basis Document No. 5, In-Drift Chemical Environment (Bechtel SAIC Company, LLC, 2003a) and that related to CLST.1.03 in Appendix V of the Technical Basis Document No. 6, Waste Package and Drip Shield Corrosion (Bechtel SAIC Company, LLC, 2003b). No specific information related to CLST.1.03 has been provided yet. The two appendixes provided by DOE are currently under review by the NRC and CNWRA staffs. However, no information regarding the role of bacterial activity on the modification of the in-drift chemical environment is presented in the Appendix A whereas the information regarding corrosion rates measured by linear polarization resistance methods is very limited in the Appendix V, as noted in Chapter 4 of this report.

Table 1-1. DOE and NRC Agreements Related to This Report	
Agreement	**Agreement Statement**
CLST.1.01	Provide the documentation for Alloy 22 and titanium for the path forward items listed on slide 8 [establish credible range of brine water chemistry; evaluate effect of introduced materials on water chemistry; determine likely concentrations and chemical form of minor constituents in Yucca Mountain waters; characterize Yucca Mountain waters with respect to the parameters that define the type of brine that would evolve; evaluate periodic water drip evaporation]. DOE will provide the documentation in a revision to Analyses and Model Report Environment on the Surfaces of the Drip Shield and Waste Package Outer Barrier by license application.
CLST.1.02*	Provide the documentation for the path forward items listed on slide 12. (Surface elemental analysis of alloy test specimens is necessary for determination of selective dissolution; surface analysis of welded specimens for evidence of dealloying; continue testing including simulated saturated repository environment to confirm enhancement factor). DOE will provide the documentation in a revision to the Analyses and Model Report General and Localized Corrosion of Waste Package Outer Barrier by license application.
CLST.1.03*	Provide documentation that confirms the linear polarization resistance measurements with corrosion rate measurements using other techniques. DOE will provide the documentation in a revision to the Analyses and Model Report General and Localized Corrosion of Waste Package Outer Barrier by license application.

*Schlueter, J. "U.S. Nuclear Regulatory Commission/U.S. Department of Energy Technical Exchange and Management Meeting on Container Life and Source Term (September 12–13, 2000)." Letter (October 4) to S. Brocoum, DOE. Washington, DC: NRC. 2000. <www.nrc.gov/waste/hlw-disposal/public-involvement/mtg-archive.html#KTI>

2 WASTE PACKAGE AND IN-DRIFT ENVIRONMENTS

2.1 Waste Package Emplacement in the Drift

A cutaway view of the waste package and drip shield layout in the emplacement drifts is shown in Figure 2-1. Waste packages will contain several classes of waste forms, including commercial spent nuclear fuel, U.S. Department of Energy (DOE)-owned spent nuclear fuel and vitrified defense high-level waste inside pour canisters. Waste packages will rest on emplacement pallets placed on top of longitudinal and transverse support beams. The waste packages will be covered by an inverted U-shaped drip shield extended over the length of the emplacement drifts.

The waste packages will consist of an outer, weld-sealed Alloy 22 cylindrical container with an inner Type 316 nuclear grade stainless steel container (Anderson, et al., 2003). The Alloy 22 outer container is designed to provide corrosion resistance whereas mechanical strength will be provided by the thicker stainless steel inner container. The drip shield is designed to prevent seepage water from contacting the waste package and to provide additional protection to the waste package from mechanical loads as a consequence of rockfall. The drip shield will be

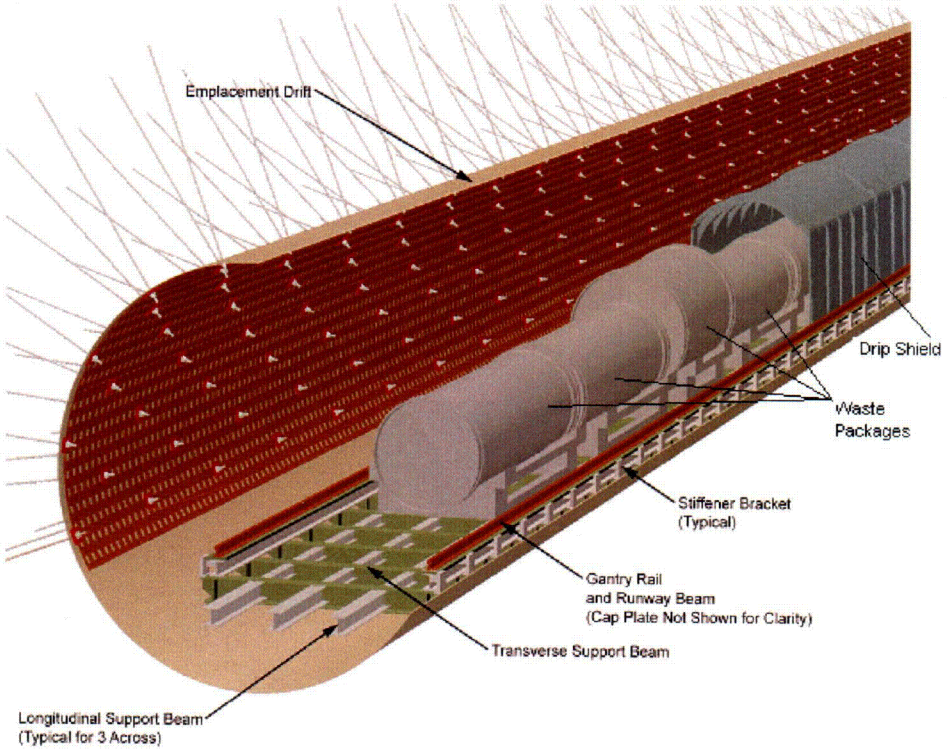

Figure 2-1. Cutaway View of Waste Package and Drip Shield Layout Within a Drift[1]

[1]Harrington, P. "Repository Design Status." *Presentation to the Nuclear Waste Technical Review Board Panel on the Engineered System, January 20, 2004.* Las Vegas, Nevada. 2004.

C01

fabricated from corrosion-resistant Titanium Grade 7 (Ti-0.15Pd) and reinforced with Titanium Grade 24 (Ti-6Al-4V-0.05Pd) structural members.

To accommodate the approximate 70,000 metric tons [77,162 short tons] of the high-level waste, the potential repository will consist of a series of drifts mined in parallel in the unsaturated zone at the proposed site at Yucca Mountain, approximately 300 m [984 ft] below the surface and approximately 300 m [984 ft] above the water table.

2.2 In-Drift Temperature and Humidity

Because of the decay heat from the radioactive waste, the drift will be heated after the emplacement of the waste packages. The temperatures of the drift and the waste package will depend on many factors such as the heat-generation rate, ventilation before permanent closure, position of the drip shield, and conductivity of the host rock. Because the drifts are parallel, the distance to the neighboring drifts will also affect the temperature. For example, the drifts near the edges of the repository will have lower temperatures than those in the center of the repository and the temperature at the end of the drifts will be lower than that at the center. Another factor that may affect substantially the temperature is related to the degradation of the drift as a result of rockfall, which may lead to the accumulation of rubble on the drip shield (Fedors, et al., 2004). Figure 2-2 shows the estimated ranges of temperature and relative humidity on the surfaces of the two classes of waste packages for a basecase scenario (no backfill, no drift degradation) (Bechtel SAIC Company, LLC, 2003a) as a function of time after the closure of the drifts. The peak temperatures are 182 and 169 °C [360 and 336 °F] for the hottest commercial spent nuclear fuel and defense high-level waste packages, respectively. The peak temperatures are 114 and 108 °C [237 and 226 °F] for the coolest commercial spent nuclear fuel and defense high-level waste packages, respectively. The relative humidities reach minimum values when the temperatures are at peak values. As the temperature decreases, the relative humidities increase.

Microbially influenced corrosion is unlikely during the low relative humidity and high-temperature phase because microorganisms would not be active during such conditions. However, as the temperature decreases and when the relative humidity reaches a threshold value (90 percent), certain microorganisms may become active and potentially cause microbially influenced corrosion of the engineered barrier system [CRWMS M&O, 2000b; Bechtel SAIC Company, LLC, 2003b,c). From the model-predicted relative humidity curves (Figure 2-2), microbially influenced corrosion may be a concern as early as 200 to 300 years after waste emplacement for some of the waste packages.

2.3 In-Drift Chemical Environments

Based on the thermal seepage model, DOE considers that when the drift temperature is above a threshold value of 100 °C [212 °F], no groundwater will reach the waste package or drip shield by seepage (Bechtel SAIC Company, LLC, 2003a). Above this threshold temperature, the chemical environment on the surfaces of the waste package and drip shield will be dominated by the chemistry of the dusts that may be deposited onto the waste package or the drip shield surfaces during the ventilation period or after the closure of the drift. The chemical environment will also depend on the ability of these dusts to form an aqueous solution in humid air by

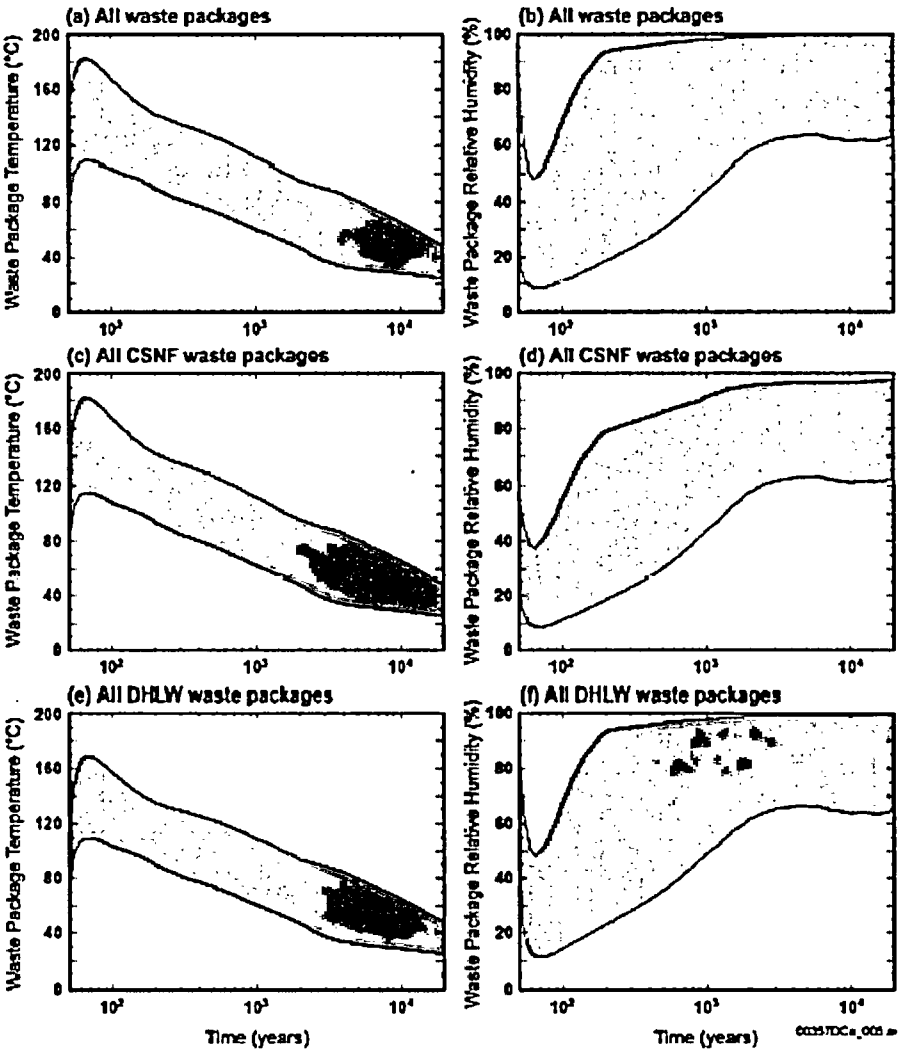

Figure 2-2. Estimated Ranges of Temperatures and Relative Humidities As a Function of Time on the Surfaces of the Different Types of Waste Packages (Bechtel SAIC Company, LLC, 2003c)

NOTE: For all waste packages [(a) and (b)], for all commercial spent nuclear fuel waste packages [(c) and (d)], and for all defense high-level waste packages [(e) and (f)]. The ranges include the lower, mean, and upper infiltration-flux cases and use the mean values of thermal conductivity for all model layer units, including the host-rock units.

deliquescence. Below this threshold temperature, groundwater modified by evaporation and precipitation may reach the waste package and drip shield by seepage and thus the chemistry of the groundwater will dominate the chemical environment on the surfaces of the waste package and drip shield.

As mentioned in Section 2.2, microorganisms can only be active at relatively low temperatures and high relative humidities (CRWMS M&O, 2000b; Bechtel SAIC Company, LLC, 2003b). The environment to consider for microbially growth should be that created by seepage water. DOE conducted evaporation modeling using EQ 3/6 and the chemical divide approach on a large number of waters considered representative of the seepage water compositions based on the thermal-hydrological-chemical model (Bechtel SAIC Company, LLC, 2003a). According to the final compositions of the evaporated waters, DOE grouped the groundwaters into 11 bins and used 11 waters representative of each of the 11 bins to encompass the range of seepage waters in the potential repository system (Bechtel SAIC Company, LLC, 2003a). Based on the number of waters in each bin and the number of chemistries each water represents, each bin is given a probability of occurrence.

Table 2-1 provides concentrations of the major cations and anions for 11 binned Yucca Mountain waters and their probabilities defined as a frequency of occurrence. Sulfate and nitrate are present in millimolar concentrations, which are concentrations capable of supporting microbial growth. Carbon dioxide is also present and could be a carbon source for autotrophs. This interpretation is supported by the findings of Davis, et al. (1998), who were successful in growing the native Yucca Mountain bacteria in 10 times the concentration of Yucca Mountain J–13 Well water without any additional carbon source. This observation suggests that the water chemistry derived from seepage into the drifts is capable of supporting microbial growth.

Table 2-1. Ranges of Seepage Water Compositions (mol/kg H_2O)* and Their Occurrence Probabilities†											
	Bin 1 Chemistry	Bin 2 Chemistry	Bin 3 Chemistry	Bin 4 Chemistry	Bin 5 Chemistry	Bin 6 Chemistry	Bin 7 Chemistry	Bin 8 Chemistry	Bin 9 Chemistry	Bin 10 Chemistry	Bin 11 Chemistry
Frequency (%)	1.36	3.53	3.26	11.68	7.34	2.17	6.79	5.98	15.76	2.72	39.40
pH	7.407	7.583	7.615	7.896	7.634	7.70	7.768	7.94	8.139	7.815	7.759
Ca^{2+}	1.75×10^{-2}	6.49×10^{-3}	2.14×10^{-3}	1.08×10^{-3}	1.36×10^{-3}	4.20×10^{-4}	4.46×10^{-4}	5.73×10^{-4}	7.24×10^{-5}	3.52×10^{-4}	3.34×10^{-4}
Mg^{2+}	1.70×10^{-5}	2.95×10^{-6}	4.13×10^{-6}	5.75×10^{-7}	1.13×10^{-5}	4.82×10^{-5}	5.52×10^{-5}	8.51×10^{-5}	2.54×10^{-7}	4.31×10^{-5}	6.34×10^{-6}
Na^{+}	3.89×10^{-3}	2.63×10^{-3}	2.67×10^{-3}	1.26×10^{-3}	5.53×10^{-3}	8.09×10^{-3}	7.65×10^{-3}	7.31×10^{-3}	4.27×10^{-3}	6.82×10^{-3}	4.80×10^{-3}
Cl	2.01×10^{-2}	5.02×10^{-3}	3.35×10^{-3}	1.03×10^{-3}	3.28×10^{-3}	3.32×10^{-3}	7.44×10^{-4}	5.61×10^{-4}	7.34×10^{-4}	6.00×10^{-4}	1.30×10^{-3}
$SiO_{2(aq)}$	9.42×10^{-3}	7.42×10^{-3}	6.96×10^{-3}	7.38×10^{-3}	1.22×10^{-2}	2.90×10^{-3}	2.46×10^{-3}	1.79×10^{-3}	4.15×10^{-3}	2.47×10^{-3}	1.19×10^{-2}
HCO_3	5.57×10^{-5}	9.06×10^{-5}	1.95×10^{-4}	1.64×10^{-4}	4.18×10^{-4}	2.93×10^{-3}	6.72×10^{-3}	6.92×10^{-3}	2.04×10^{-3}	5.74×10^{-3}	1.13×10^{-3}
SO_4^{2-}	8.87×10^{-3}	4.89×10^{-3}	1.50×10^{-3}	5.88×10^{-4}	1.77×10^{-3}	1.21×10^{-3}	4.12×10^{-4}	3.55×10^{-4}	1.18×10^{-4}	3.80×10^{-4}	7.29×10^{-4}
K^{+}	8.68×10^{-4}	5.40×10^{-4}	5.00×10^{-4}	2.38×10^{-4}	8.68×10^{-4}	6.25×10^{-4}	4.67×10^{-4}	2.76×10^{-4}	5.02×10^{-4}	4.17×10^{-4}	7.50×10^{-4}
AlO_2	3.27×10^{-8}	7.08×10^{-8}	5.02×10^{-8}	9.97×10^{-8}	8.03×10^{-10}	5.36×10^{-9}	3.62×10^{-9}	1.50×10^{-9}	6.09×10^{-8}	4.03×10^{-9}	1.42×10^{-9}
F^{-}	1.93×10^{-4}	2.46×10^{-4}	3.48×10^{-4}	4.28×10^{-4}	1.00×10^{-4}	8.26×10^{-4}	7.81×10^{-4}	6.43×10^{-4}	9.77×10^{-4}	8.61×10^{-4}	1.38×10^{-3}
NO_3	1.30×10^{-3}	5.46×10^{-4}	1.83×10^{-4}	1.33×10^{-4}	2.22×10^{-4}	1.04×10^{-4}	6.87×10^{-5}	3.97×10^{-5}	3.10×10^{-4}	4.25×10^{-5}	1.26×10^{-4}
$CO_2(g)$ (bar)	3.89×10^{-4}	4.93×10^{-4}	1.04×10^{-3}	4.88×10^{-4}	1.88×10^{-3}	7.06×10^{-3}	1.19×10^{-2}	6.34×10^{-3}	2.94×10^{-3}	9.19×10^{-3}	4.06×10^{-3}
$\log CO_2(g)$	-3.410	-3.307	-2.984	-3.312	-2.726	-2.151	-1.926	-2.198	-2.532	-2.037	-2.392

*Note: 1 mol/kg H_2O = 0.454 mol/lb H_2O.

†Bechtel SAIC Company, LLC. "Technical Basis Document No. 5: In-Drift Chemical Environment." Rev. 1. Las Vegas, Nevada: Bechtel SAIC Company, LLC. 2003.

3 MICROBIALLY INFLUENCED CORROSION PROCESSES AND YUCCA MOUNTAIN BACTERIA

3.1 Microbially Influenced Corrosion Processes

Microbially influenced corrosion may be defined as accelerated corrosion of susceptible metals as a result of the direct, indirect, or both, actions of microbial metabolism. In many circumstances, particularly for corrosion-resistant alloys such as stainless steels and nickel-chromium-molybdenum alloys, microbially influenced corrosion manifests itself primarily as localized corrosion in the form of pitting. The microorganisms associated with microbially influenced corrosion include algae, fungi, and bacteria; all of which are ubiquitous in nature. This section of the report addresses a select group of bacteria recognized as playing a significant role in microbially influenced corrosion (Davis, 2000; Maier, et al., 2000). Bachofen (1991, 1990), Geesey (1993), and Geesey and Cragnolino (1995) specifically discussed microbially influenced corrosion in nuclear waste disposal. The specific organisms addressed here include sulfate-reducing bacteria, *Thiobacillus, Pseudomonas*, iron- and manganese-oxidizing bacteria, and acid-producing bacteria. Each of these groups of organisms is represented in nature by great diversity and, as such, only generalizations of their specific metabolic behavior will be presented. It is also important to note that, in nature, bacteria do not exist in pure cultures. Instead, communities of microbes coexist and interact in complex ways that are poorly understood. Indeed, the details of the many mechanisms of microbially influenced corrosion are themselves poorly understood and provide for great debate. There are, however, general statements to be made regarding microbial metabolism that help elucidate microbial processes and the interaction between bacteria and their surroundings.

From the perspective of microbially influenced corrosion, bacteria may be grouped according to their terminal electron acceptors for metabolic respiration. Aerobes are organisms requiring oxygen as their terminal electron acceptor, whereas anaerobes use alternate electron acceptors and cannot grow in the presence of oxygen (although even obligate anaerobes can subsist in a dormant state in the presence of air). In addition, some bacteria are classified as microaerophilic (requiring very small concentrations of oxygen), and some are facultative anaerobes capable of respiring using oxygen when available, or an alternate electron acceptor when oxygen is absent (Ehrlich, 2002). For example, some soil *Pseudomonas* can utilize nitrate instead of oxygen during conditions of reduced oxygen concentrations (low E_h values). One possibly significant aspect of microbial metabolism with respect to microbially influenced corrosion is the need for a supply of mobile electrons, protons, or both, for metabolic activity.

Ehrlich (2002) provides an excellent summary of the bacterial electron transport system and its importance to microbial growth. In aerobic respiration, hydrogen atoms or electrons provide the reducing power for respiration through the oxidation of either organic compounds (heterotrophs) or inorganic compounds (chemotrophs). Anaerobic respiration employs similar strategies as aerobic bacteria, but uses compounds such as sulfate, elemental sulfur, nitrate, carbon dioxide, and ferric and manganese oxide compounds as their electron acceptors. Both groups of organisms have evolved specific enzymes and active sites in the cell envelope that transfer hydrogen atoms or electrons from otherwise insoluble substrates. Because these enzymes are located in the cell envelope, bacteria can make direct contact between the active enzymes and the substrate (e.g., a metal surface) (Ehrlich, 2002).

Bacteria store energy gained by their metabolism in high-energy phosphate bonds in the compound adenosine 5' -triphosphate (ATP). ATP produced through reaction between inorganic phosphate (P_i) and adenosine 5' -diphosphate (ADP) in the following energy-consuming reaction

$$ADP + P_i \rightarrow ATP$$

The energy required for this reaction is made possible by a charge separation between the interior and exterior of the cell. According to Ehrlich (2002), "... the charge separation results from the passage of electrons down the electron transport chain to oxygen, which is coupled concurrently with the pumping of protons across the plasma membrane from the cell interior to the cell periplasm or its equivalent." Ehrlich continues to explain that protons reenter the cell through an enzyme, ATPase, located in a specific position on the cell. Whereas proton reentry in aerobes is coupled with the reduction of oxygen to form water (as in the previous quote), in anaerobes, the protons are consumed in the reduction of the alternate electron acceptor (e.g., SO_4^{2-} for the sulfate-reducing bacteria). This active electron/proton transport system is common to all bacteria and may play a part in microbially influenced corrosion.

In addition to possible direct effects on metal resistance to corrosion, many possible indirect effects are associated with the production of metabolites, the waste products of microbial metabolism. Metabolic processes can alter the pH of the environment and can produce corrosive compounds such as hydrogen sulfide or sulfuric acid. The following sections briefly describe the metabolism and possible contributions to microbially influenced corrosion of specific bacteria.

Of importance to note is the inferred role of biofilms in corrosion. Biofilms are complex encrustations of slime on surfaces that consist of living cells, dead cells, extracellular polymer substances, and trapped particulates (Marshall, 1997). Biofilms produce microenvironments that permit closely spaced environmental extremes in pH, redox potential, and nutrient transport (Santegoeds, et al., 1998; Okabe, et al., 1999; Vroom, et al., 1999; Teilzel and Parsek, 2003). Biofilms are formed to enhance survival, but the microenvironments produced in the biofilm are highly variable and in some cases detrimental to metals. To determine the precise processes and interactions that take place within biofilms will require significant new research.

3.1.1 Corrosion by Sulfate-Reducing Bacteria

The many genera of sulfate-reducing bacteria constitute a group of bacteria that oxidize an organic substrate and use sulfate as their terminal electron acceptor. Common genera of the sulfate-reducing bacteria include *Desulfobacter*, *Desulfobulbus*, *Desulfococcus*, *Desulfomonas*, *Desulfonema*, *Desulfosarcina*, *Desulfotomaculum*, and *Desulfovibrio* (Maier, et al., 2000; Peck and LeGall, 1994; Postgate, 1979). The sulfate-reducing bacteria are obligate anaerobes responsible for the production of hydrogen sulfide; it is the hydrogen sulfide that makes their presence recognizable because hydrogen sulfide imparts an unpleasant rotten eggs odor. It is also this metabolite that is considered to be corrosive for metals such as copper and iron (Davis, 2000; Bradford, 2001). Sulfate-reducing bacteria span the temperature range from mesophilic {20 to 40 °C [68 to 104 °F]} to extreme thermophilic {temperatures above 80 °C [176 °F]} (Castro, et al., 2000; Stetter, 1988; Jorgensen, et al., 1992; Love, et al., 1993; Davis, et al., 1998; Liu, et al., 1997). Although not culturable, Jergensen, et al. (1992)

demonstrated sulfate-reducing bacteria metabolism at 106 °C [222 °F] at a deep-sea hydrothermal vent.

According to Dowling and Guezennec (1997), sulfate-reducing bacteria exist in biofilms that create the conditions for the establishment of occluded electrochemical cells depleted of oxygen. They stated that sulfate-reducing bacteria are obligate anaerobes but are oxygen tolerant and withstand small quantities of oxygen in the presence of oxygen-respiring aerobes. During these conditions, they state that corrosion is accomplished through two sets of coupled electrochemical charge transfer partial reactions. The first set of reactions takes place on the exposed metal surface (e.g., on steel) and is characterized by the reduction of oxygen coupled to metal dissolution and formation of a protective oxide film at pH above 8.4.

$$\text{Anode reaction: } 3Fe + 4H_2O \rightarrow Fe_3O_4 + 8H^+ + 8e^- \quad (3\text{-}1a)$$

$$2Fe + 3H_2O \rightarrow Fe_2O_3 + 6H^+ + 6e^- \quad (3\text{-}1b)$$

$$\text{Cathode reaction: } \tfrac{1}{2}O_2 + H_2O + 2e^- \rightarrow 2OH^- \quad (3\text{-}2)$$

The second set of reactions takes place in an occluded cell during anaerobic conditions where the anodic reaction is accelerated by the hydrogen cathodic reaction as indicated in the following reactions

$$\text{Anode reaction: } Fe^0 \rightarrow Fe^{2+} + 2e^- \quad (3\text{-}3)$$

$$\text{Cathode reaction: } 2H^+ + 2e^- \rightarrow H_2 \quad (3\text{-}4)$$

The significance of the biofilm in this corrosion reaction is emphasized by Hamilton (1995). The biofilm creates anaerobic microniches suitable for sulfate-reducing bacteria growth. Within this microniche, the sulfate-reducing bacteria use H_2 as an electron donor as part of their electron transport system; this removes hydrogen from the environment and provides a driving force for the anodic reaction.

$$Fe^{2+} + 2H_2O \rightarrow Fe(OH)_2 + H_2 \quad (3\text{-}5)$$

$$4H_2 + SO_4^{2-} \rightarrow H_2S + 2OH^- + 2H_2O \text{ (sulfate-reducing bacteria)} \quad (3\text{-}6)$$

$$H_2S + Fe^{2+} \rightarrow FeS + H_2 \quad (3\text{-}7)$$

In essence, the sulfate-reducing bacteria catalyzes the cathodic reaction through the reaction described in Eq. (3-6), promoting accelerated dissolution of the metal at the anode. Finally, sulfide is the end product of sulfate reduction; this sulfide reacts with Fe^{2+} to form FeS as an insoluble precipitate. The exact path of the reduction from sulfate to sulfide appears to differ in differing genera and is not completely understood. Ehrlich (2002) provides a good review of the problem. What is clear is that several sulfur-bearing intermediary compounds are produced during sulfate reduction. These intermediary compounds include sulfite (SO_3), bisulfite (HSO_3^-), trithionate ($S_3O_6^{2-}$), and thiosulfate ($S_2O_3^{2-}$). Among these anions, $S_2O_3^{2-}$ has been implicated in promoting localized corrosion of stainless steels in chloride solutions at potentials lower than the repassivation potential in plain chloride solutions (Newman, et al., 1982).

3.1.2 Corrosion by *Thiobacillus* (Iron-Oxidizing, Acid-Producing Bacteria)

The iron-oxidizing bacteria include the genera *Thiobacillus*, *Thiomicrospira*, and *Thiosphaera*. Of these, the *Thiobacillus* have received the greatest attention, largely because of their association with acid mine drainage. A common feature of these iron oxidizers is their ability to gain energy from the oxidation of reduced sulfur species to sulfate (yielding sulfuric acid), thereby producing acidic conditions. Nearly all members of the group grow autotrophically (an organism using CO_2 as its sole carbon source—synonymous with chemotrophy and lithotrophy), with some capable of growing heterotrophically (an organism that requires reduced organic carbon compounds for its metabolism) and mixotrophically (an organism that uses organic carbon as an energy source and an inorganic compound as its electronic donor). In addition to reduced sulfur compounds, some members of this group can utilize hydrogen, ferrous iron, and other reduced metal ions for their energy source. Carbon dioxide is the carbon source for the autotrophic forms while the heterotrophs are capable of using organic carbon. All members of the group are aerobic, requiring oxygen as their terminal electron acceptor. Although *Thiobacilli* are primarily mesophilic, some moderately thermophilic forms have been described in literature to grow at temperatures up to 65 °C [149 °F] (Halberg and Lindstrom, 1994; Shooner, et al., 1996; Takai, et al., 2001).

The most widely studied iron-oxidizing bacterium is the acidophilic *Thiobacillus ferrooxidans*, which derives its energy from the oxidation of ferrous iron, reduced forms of sulfur, metal sulfides, H_2, and formate (Ehrlich, 2002). When using hydrogen as an energy source, the enzyme hydrogenase is induced. *T. ferrooxidans* oxidizes ferrous iron at pH values ranging from 1 to 4.5 and can grow to a pH 6.

Research on the energetics of ferrous iron oxidation by *T. ferrooxidans* suggests that this oxidation is a poor energy source for carbon assimilation. Although free energy values calculated for the oxidation of Fe^{2+} vary somewhat with pH, the greatest variation in calculating iron oxidation energetics comes from the range of efficiencies determined for *T. ferrooxidans*. Using the highest efficiency reported by Ehrlich (2002), 20.5 percent, it would take 90.1 mol Fe^{2+} to assimilate 1 mol C. As efficiency decreases, the required amount of Fe^{2+} increases (Ehrlich, 2002).

The oxidation of iron by *T. ferrooxidans* involves an iron-oxidizing enzyme system that functions in the presence of sulfate. Although specific details of the system are debated, Figure 3-1 illustrates the enzyme-mediated process.

In summary, *Thiobacillus* species may be engaged in microbially influenced corrosion through a combination of active, enzyme-mediated ferrous iron oxidation and through acid production as a product of sulfide oxidation.

In addition to the *Thiobacillus* organisms, numerous additional bacteria and archaea are known to oxidize iron. Bacteria include *Leptospirillium, Metallogenium, Ferromicrobium acidophilum, Sulfobacillus thermosulfidooxidans, and Acidomicrobium ferrooxidans.* These bacteria are all acidophilic, favoring pH values below 6; the latter two organisms are thermophilic, with *Sulfobacillus thermosulfidooxidans* growing at temperatures to 60 °C [140 °F] (Ehrlich, 2002).

The archaea are represented by a number of both mesophilic (moderate temperature) and thermophilic organisms including *Ferroplasma acidphilum, Ferroplasma acidarmanus, Acidianus*

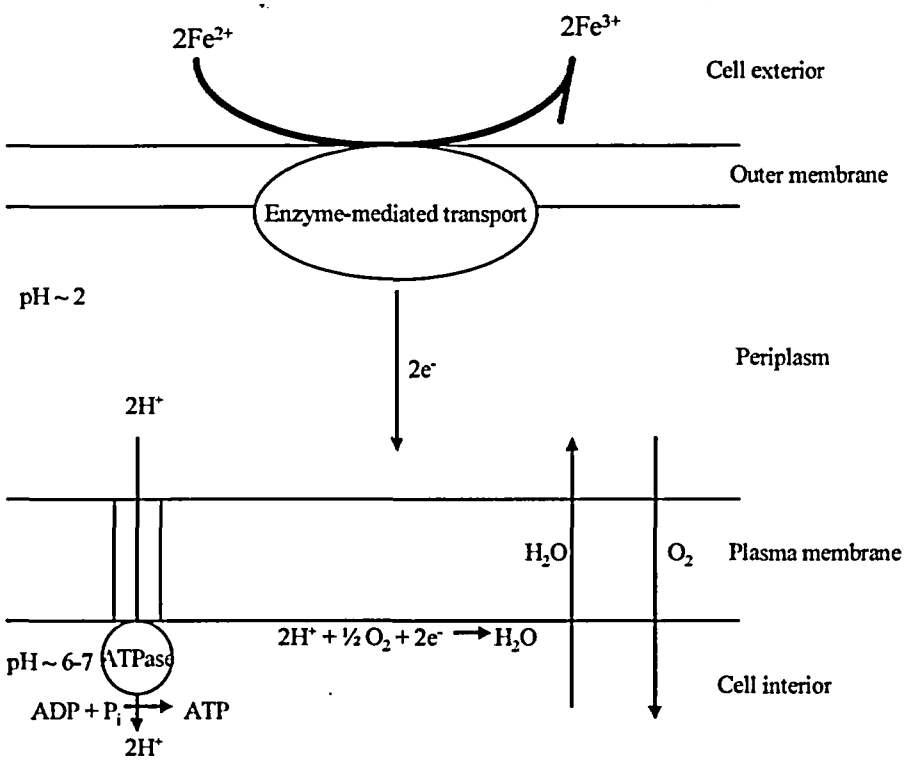

Figure 3-1. Proton and Electron Transport System Across a Cell Membrane in Iron Oxidizing Bacteria (Modified from Ehrlich, 2002) (Reproduced with Permission from Copyright Clearance Center)

brierleyi, and *Sulfolobus acidcaldarius*. As with the bacteria, these organisms favor extremely low pH environments. The latter two are thermophiles with *Acidianus brierleyi* capable of growing at temperatures to 90 °C [194° F] (Ehrlich, 2002).

In addition to the acid-producing/acid-tolerant iron oxidizers, there is a group of neutrophilic (preferring neutral pH environments) iron oxidizers. This group includes the microaerophilic *Gallionella* that grows at the interface between aerobic and anaerobic conditions. *Gallionella* uses CO_2 as its sole carbon source and gets its energy from ferrous iron. *Gallionella* has been implicated in numerous cases of microbially influenced corrosion of stainless steels (Tiller, 1983). Other neutrophilic iron oxidizers include the sheathed bacteria *Sphaerotilus, Leptothrix, Crenothrix Polyspora*, and *Clonothrix* (Ehrlich, 2002). The role that these organisms might play in microbially influenced corrosion is unclear.

3.1.3 Corrosion by *Pseudomonas*

Pseudomonas is a ubiquitous, diverse group of bacteria capable of existing in a broad range of environments including soils, rock matrices, and freshwater and marine water columns and sediments. These bacteria are capable of surviving on limited nutrients and can oxidize a wide range of organic substrates, making them extremely useful in bioremediation. Although the *Pseudomonads* are largely mesophilic, a small number of thermotolerant and thermophilic forms

have been identified (Manaia and Moore, 2002; Manaia, et al., 2003). In addition, thermophilic organisms with strong biochemical similarities to *Pseudomonas* species have been identified (Sanbongi, et al., 1989), perhaps suggesting mutation from an original *Pseudomonas* ancestor.

The primary role of the *Pseudomonas* species in microbially influenced corrosion is likely to be twofold. First, some members of the group are active slime formers and play an important role in biofilm formation. Owing to the abundance and diversity of this group and their ability to exist in extremely nutrient-poor environments, their contribution to biofilm formation may be considered a critical contribution to microbially influenced corrosion. In addition, some *Pseudomonas* species actively produce H_2O_2 as part of their metabolism. It is known that H_2O_2 can act as an oxidant, which can increase the corrosion potential to values higher than those observed in air-saturated solutions. Finally, as noted in Section 3.1.4, some *Pseudomonas* are capable of oxidizing manganese.

3.1.4 Corrosion by Manganese-Oxidizing Bacteria

Manganese is an important trace nutrient in biological systems playing a role as an activator in many enzymatic reactions. This role helps to explain why many taxonomically unrelated bacteria oxidize manganese. While some bacteria enzymatically oxidize manganese, others do so nonenzymatically. There are no demonstrably autotrophic manganese oxidizers; all known manganese oxidizers require organic carbon compounds. Some are mixotrophic and gain energy from manganese oxidation, while others are heterotrophic and do not get energy from manganese oxidation. They have been reported from all environments including desert varnish on rock surfaces, in soil, and in sediments and water column in both marine and lacustrine settings (Ehrlich, 2002).

Manganese oxidation takes place at near neutral pH, unlike iron oxidation, which is favored by acidic conditions. Although a broad range of bacteria is recognized to oxidize manganese enzymatically, these bacteria can be placed into one of three groups according to the enzymatic mechanisms. Group I manganese oxidizers oxidize dissolved Mn^{2+} using O_2 as their terminal electron acceptor. Some in this group conserve energy from manganese oxidation, while others do not. Group II manganese oxidizers oxidize prebound Mn^{2+} using O_2 as their terminal electron acceptor. Group III manganese oxidizers oxidize Mn^{2+} using H_2O_2 as their oxidant. All three groups are capable of contributing to microbially influenced corrosion.

Group I manganese oxidizers include bacteria in the genera *Pseudomonas, Leptothrix*, and *Bacillus*. Group II manganese oxidizers include bacteria in the genera *Arthrobacter*, *Oceanospirillum*, and *Vibrio*. Group III manganese oxidizers include bacteria in the genera *Metallogenium, Leptothrix*, and *Siderobacter*. Note that *Metallogenium* and *Leptothrix* are recognized as iron-oxidizing bacteria as well (Ehrlich, 2002).

Nonenzymatic manganese oxidation is favored by elevated Eh (greater than +500 mV) and mildly alkaline pH. Nonenzymatic manganese oxidation appears to be a result of bacterial metabolism of organic substrates such as citrate, lactate, malate, and gluconate. Some nonenzymatic manganese oxidizers are represented by *Pseudomonas*, *Arthobacter*, and *Actinomycetes* species (Ehrlich, 2002).

3.1.5 Corrosion by Acid-Producing Bacteria

The reduction in pH of the environment adjacent to a metal surface plays an important role in corrosion. Some microorganisms can alter the pH through the production of organic or inorganic acids. An example of the former is *Clostridum*, a common soil-borne bacterium some of which produce acetic acid, and of the latter *Thiobacillus* which, as described previously, is responsible for the production of sulfuric acid, a strong corrosive agent. Brock (1986) lists 11 species of thermophilic *Clostridum* capable of growing at temperatures up to 75 °C [167 °F]. Each organism produces acidic conditions in differing ways. The bacteria listed in Table 3-1 as acid producers, identified from Yucca Mountain, are heterotrophs that oxidize organic carbon sources producing different organic acids as part of their metabolism. Other microorganisms, while not actively involved in lowering the pH, are acidophilic and grow best in acidic conditions.

Table 3-1. Bacteria Isolated from Yucca Mountain Rock and Their Classification from a Microbially Influenced Corrosion Perspective*. (Reproduced with Permission from NACE International.)

Strain Number†	Species Identification	Classification
ESF–71h–RT–4	*Flavobacterium esteroaaromaticum*	Acid Producer
ESF–C1	*Cellulomonas flavigena*	Acid Producer
LB–71h–50–3	*Bacillus*	Acid Producer
Lban–U7	*Uncharacterized*	Acid Producer
LB–C1	*Uncharacterized*	Slime Producer
LB–71h–50–4	*Bacillus subtilus*	Slime Producer
LB–71h–50–6	*Bacillus sp.*	Slime Producer
LB–71h–RT–15	*Pseudomonas pseudoflava*	Slime Producer
Lban–U3	*Bacillus pantothentics*	Slime Producer
68	Uncharacterized	Iron Oxidizer
69	Uncharacterized	Iron Oxidizer
	Sulfate-Reducing Bacteria Collected From Yucca Mountain Site	Sulfate Reducer

*Lian, T., S. Martin, D. Jones, A. Rivera, and J. Horn. "Corrosion of Candidate Container Materials by Yucca Mountain Bacteria." Proceedings of the CORROSION '99 Conference. Paper No. 476. Houston, Texas: NACE International. 1999.

†The strain designations are described in Horn, et al., 1998, as follows:

ESF = Exploratory Studies Facility
LB = large block
an = isolated under anaerobic conditions
C = crushed rock isolate
U = uncrushed rock isolate
71h = isolated after 71 hours of growth
RT = room temperature isolate
50 = 50 °C isolate

Reference: Horn, J.M., A. Rivera, T. Lian, and D.A. Jones. "MIC Evaluation and Testing for the Yucca Mountain Repository." Proceedings of the CORROSION '98 Conference. Paper No. 152. Houston, Texas: NACE International. 1998.

A new bacterial kingdom, the *Acidobacterium*, has been identified and recognized as having great diversity, perhaps as great as the *Proteobacteria* (Barns, et al., 1999). A great deal of future study is required to determine the role that bacteria in this new kingdom might play in microbially influenced corrosion.

3.2 Yucca Mountain Bacteria

Geesey (1993), in a review describing subsurface microorganisms, pointed to the broad distribution of bacteria in every terrestrial and aquatic environment investigated. So, too, are there bacteria at Yucca Mountain and specifically within the Topopah Spring tuff layer, the potential repository horizon.

Many papers provide insight into the microbial population at Yucca Mountain (Stetzenbach, 1995; Castro, et al., 2004, 1998; Davis, et al., 1998; Horn, et al., 2003, 1998, 1996; Lian, et al., 1999a; and Pitonzo, et al., 2004). Although exact numbers of bacterial genera at Yucca Mountain are unknown, Stetzenbach (1995) reports that more than 1,100 bacterial isolates were collected during a 2-year period from 31 springs in the Yucca Mountain area. Horn, et al. (2003), employing the molecular techniques of 16sRNA, identified 200 clones representing 65 distinct organism types from Yucca Mountain lithologies. Using a culturing approach, many of these authors have been successful in isolating a diverse population of bacteria from Yucca Mountain rocks. However, it should be noted that a small proportion, as low as 1 percent, of the extant microbes in nature can be grown on any given growth medium (Horn, et al., 2003). Therefore, it is possible (and highly probable) that many other bacteria besides those already identified in the literature exist at Yucca Mountain.

Among the many isolated bacteria are numerous organisms recognized as playing a role in microbially influenced corrosion. Lian, et al. (1999a) selected specific organisms for their corrosion tests from a group suspected to be significant in microbially influenced corrosion. This suite of bacteria is presented in Table 3-1.

In Bechtel SAIC Company, LLC (2003c), DOE recognizes that nutrient requirements necessary to support growth of the native microflora are currently met at Yucca Mountain. Growth rates and cell density are generally low in the Yucca Mountain rock (when compared to surface soils), in large part owing to the general lack of nutrients, research indicates that all nutrients necessary to support microbial growth currently exist in the Yucca Mountain rocks, or will likely be introduced during repository construction (Castro, et al., 1998). Horn, et al. (2004, 2003) state that all the necessary nutrients exist in the rocks and that water is the only truly limiting factor thwarting microbial growth. Davis, et al., (1998) were able to grow bacteria from Yucca Mountain rocks using a ten-fold concentration of simulated J–13 Well water with no additional carbon source added. Bechtel SAIC Company, LLC (2003c) points out that the microbial population is already high enough to influence corrosion and that nutrients are not limiting. Bechtel SAIC Company, LLC (2003c) concurs that water, represented as relative humidity, is considered to be the limiting factor controlling microbial growth. According to Geesey (1993), a critical threshold value of relative humidity necessary to support microbial growth is 90 percent. This value, used in Bechtel SAIC Company, LLC (2003b), is considered to be conservative by DOE.

Table 3-2 summarizes the discussion of the major groups of organisms that may play a role in microbially influenced corrosion. These groups of organisms are represented by bacteria either

Table 3-2. Summary of Organisms That Have Been Isolated at Yucca Mountain or May Be Introduced During Construction and Their Potential Role in Corrosion			
Organism	**Aerobe/Anaerobe/ Electron Acceptor**	**Mesophilic/ Thermophilic**	**Potential Role in Corrosion**
Sulfate-reducing bacteria	Anaerobe/SO_4^{2-}	Mesophilic to thermophilic (*desulfotomaculum* to 85 °C [185 °F].	Production of H_2S and other reduced sulfur species ($S_2O_3^{2-}$)
Thiobacillus	Aerobe	Primarily mesophilic, some thermotolerant to moderately thermophilic {65 °C [149 °F]} species. Brock* lists three thermophilic species growing at 50–60 °C [122–140 °F].	Acid producer
Iron and manganese oxidizers	Aerobe	Primarily mesophilic, some thermotolerant to moderately thermophilic {55 °C [131 °F]} species. Some *Clostridium* species grow above 60 °C [140 °F] and one iron-oxidizing archaea grows at 90 °C [194 °F].	Oxidation of reduced iron and manganese
Slime formers (e.g., *Bacillus* and *Pseudomonas* species)	Aerobe and facultative anaerobes—facultative anaerobes use O_2 when available and an alternate electron acceptor (e.g., nitrate or Fe^{3+}) when O_2 is not available	Mesophilic to extreme thermophilic (*Pseudomonas* are thermotolerant to moderately thermophilic, some *Bacillus* species are extreme thermophiles).	Biofilm formation, some acid production

*Brock, T.D., ed. "Introduction: An Overview of Thermophiles." *Thermophiles: General, Molecular, and Applied Microbiology*. New York City, New York: John Wiley and Sons. p. 316. 1986.

currently extant at Yucca Mountain, or likely to be introduced owing to construction activities. Table 3-2 also identifies that each group contains organisms that are either moderate or extreme thermophiles capable of growing at elevated temperatures, often above 60 °C [140 °F]. Two studies address corrosion of carbon steel at elevated temperatures of 50 °C [122 °F] (Castro, et al., 2004, 1998), but none address the potential for microbially influenced corrosion of stainless steels at temperatures greater than 60 °C [140 °F]. Also noteworthy is the question of the origin of thermophile. Brock (1986) and Sundaram (1986) point to the likelihood that thermophilic bacteria form from mutation of mesophilic bacteria over time. This is supported by studies such as those by Sanbongi, et al. (1989) that reveal greater biochemical similarity between specific mesophilic and thermophilic organisms than between otherwise similar thermophiles.

It is clear from the literature that a range of candidate microbes able to promote microbially influenced corrosion exists at Yucca Mountain. Castro, et al. (2004, 1998), Horn, et al. (1998), Lian, et al. (1999a), and Pitonzo, et al. (2004) all conducted corrosion experiments using singly, or in consortium, acid-producing bacteria, exopolysaccharide-producing bacteria, iron-oxidizing bacteria and sulfate-reducing bacteria. Corrosion tests should explore the roles played by these organisms in microbially influenced corrosion of candidate waste container materials, both at ambient temperatures and, using appropriate thermophiles, at temperatures above 60 °C [140 °F].

4 MICROBIALLY INFLUENCED CORROSION INVESTIGATIONS FOR THE YUCCA MOUNTAIN PROJECT

4.1 DOE Investigations

The U.S. Department of Energy (DOE) conducted limited investigations on microbially influenced corrosion (Bechtel SAIC Company, LLC, 2003b,c; CRWMS M&O, 2000b). The studies on effects of microbial activity on the corrosion of Alloy 22 and other materials can be classified in two categories. One category of studies comprises the electrochemical tests in simulated groundwaters inoculated with Yucca Mountain bacteria (Horn, et al., 1998; Castro, et al., 1998; Lian, et al., 1999a,b; Pitonzo, et al., 2004). The other category of studies includes the immersion tests in a simulated groundwater incubated with crushed Yucca Mountain tuff (Horn, et al., 2001, 2000, 1999; Martin, et al., 2004). The experimental procedures and results are described in the following sections.

4.1.1 Electrochemical Studies in Simulated Yucca Mountain Water Inoculated with Yucca Mountain Bacteria

The electrochemical studies on the microbially influenced corrosion for the Yucca Mountain project include work performed using Alloy 22 and other alloys (Castro, et al., 1998; Lian, et al., 1999a,b; Horn, et al., 1998; Pitonzo, et al., 2004).

In the work by Lian, et al. (1999a,b), 12 strains of Yucca Mountain bacteria, including acid and slime producers and sulfate-reducing and iron-oxidizing bacteria, were used. Table 3-1 shows the 12 strains of Yucca Mountain bacteria that were isolated and used in the experiments. A schematic of the electrochemical cell is shown in Figure 4-1. The working electrode is located at the bottom of the cell facing upward and a platinum wire is used as a counterelectrode. Five materials were tested, including 1020 carbon steel, Alloys 400, 22, 625, and Type 304 SS. The tests were conducted at 22 °C [72 °F] in 100× simulated J–13 Well water, which was the composition adopted as a reference for corrosion testing in the Yucca Mountain project (Harrar, et al., 1990). The recipe for the preparation of the 100× simulated groundwater is given in Table 4-1.

Anodic polarization scans were performed for all the alloys using a potential scan rate of 0.167 mV/sec. No pitting corrosion was initiated in the cells with and without the bacteria for Alloys 22 and 625 and Type 304 SS. Anodic currents measured in the cells containing Yucca Mountain bacteria were significantly higher than those measured in the sterile cells at potentials

Table 4-1. Recipe of the 100× Water Used in the Microbially Influenced Corrosion Test* (g solute/L water)†

$NaHCO_3$	NaF	Na_2O_3Si	$MgSO_4$	Na_2SO_4	$NaNO_3$	KCl	$CaCl_2$	NaCl	H_2SO_4
10.7	0.32	0.04	0.05	1.67	0.88	0.64	0.05	0.57	0.02

*Lian, T., D. Jones, S. Martin, and J. Horn. "A Quantitative Assessment of Microbiological Contributions to Corrosion of Candiate Nuclear Waste Package Materials." Scientific Basis for Nuclear Waste Management XXII. Symposium Proceedings 556. D.J. Wronkiewicz and J. H. Lee, eds. Warrendale, Pennsylvania: Materials Research Society. pp. 1,175–1,182. 1999.
†1lb/ft^3 = 16 oz g/L.

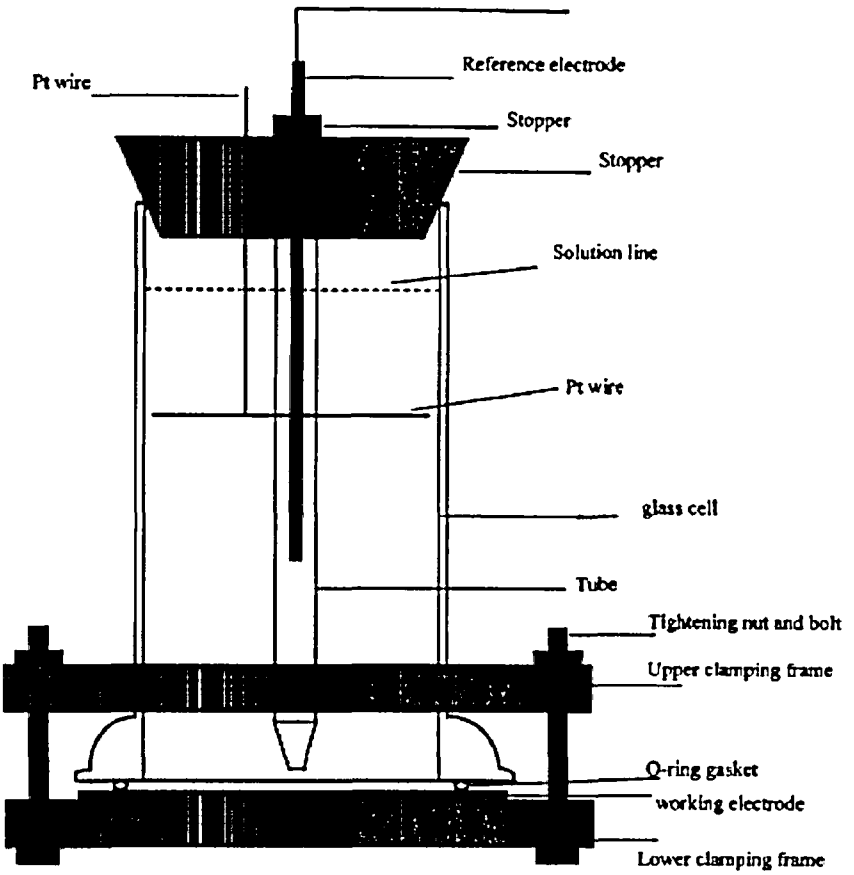

Figure 4-1. Electrochemical Cell Used in the Microbially Induced Corrosion Tests (Lian, et al., 1999). (Reproduced with Permission from NACE International.)

between the corrosion potentials (ranging from -0.15 to -0.66 V_{SCE}) and 0.3 V_{SCE} for all the Type 304 SS and Alloys 625 and 22 specimens. The corrosion rates of the different metals were measured using the linear polarization resistance method, and it was found that the rates in the inoculated cells were higher than those in the sterile cells for the different alloys during the 5-month exposure (Table 4-2) (Lian, et al., 1999a). These increases were attributed to the enhancement of general corrosion by bacterial activity. A term called microbially influenced corrosion factor, which is the ratio of the corrosion rate measured in the inoculated cell to the corrosion rate measured in the sterile cell, was introduced in the DOE model to account for the microbial influence on the general corrosion rate of Alloy 22 (Bechtel SAIC Company, LLC, 2003b,c):

Table 4-2. General Corrosion Rate and the Enhancement by Yucca Mountain Bacteria* (μm/yr)†					
	Carbon Steel 1020	Monel 400	Stainless Steel 304	Alloy 625	Alloy 22
Bacteria Cell‡	8.8	1.02	0.035	0.013	0.022
Sterile Cell‡	1.4	0.005	0.003	0.003	0.011

*Lian, T., S. Martin, S. Jones, D. Rivera, and J. Horn. "Corrosion of Candidate Container Materials by Yucca Mountain Bacteria." Proceedings of the CORROSION '99 Conference. Paper No. 476. Houston, Texas: NACE International. 1999.
†1 in/yr = 2.54×10^4 μm/yr
‡CRWMS M&O. "General Corrosion and Localized Corrosion of Waste Package Outer Barrier." ANL–EBS–MD–000003. Rev. 00. Las Vegas, Nevada: CRWMS M&O. 2000.

$$CR_{MIC} = CR_{st} \cdot f_{MIC} \quad (4\text{-}1)$$

where

CR_{MIC} — general corrosion rate in the inoculated cell
CR_{st} — general corrosion rate measured in the sterile cell
f_{MIC} — the microbially influenced corrosion (MIC) factor

The corrosion rates obtained in the solutions with and without the bacteria are shown in Table 4-2 (Lian, et al., 1999a). Based on the data shown in Table 4-2, the microbially influenced factor for Alloy 22 is 2.0 (Bechtel SAIC Company, LLC, 2003b,c).

In the 5-month exposure experiment (Lian, et al.,1999a), no localized corrosions in Alloy 22, Type 304 SS, and Alloy 625 specimens were observed. The aqueous media was analyzed by using inductively coupled plasma to determine the dissolution of metal-alloying elements. The contents of chromium and nickel in solution were not detectable in the sterile test cells. However, the chromium and nickel concentrations were 1.05 and 0.1 mg/L [6.55×10^{-5} and 6.242×10^{-6} lb/ft^3], respectively, in the test cell containing the microorganisms (Table 4-3). Similar increases in chromium and nickel also were shown for Type 304 SS and Alloy 625. The contents of nickel, chromium, and iron in Alloys 22 and 625 are approximately 60, 22, and 4 percent, whereas the content of molybdenum is approximately 13 and 9 percent. The data for these two alloys in Table 4-3 clearly show preferential dissolutions of chromium and iron in the presence of bacteria.

4.1.2 Immersion Studies in Simulated Yucca Mountain Groundwater Incubated with Yucca Mountain Tuff

The immersion studies were conducted in a simulated Yucca Mountain groundwater (excluding lithium, strontium, aluminum, iron, and silicon) that represents a ten fold concentration of J–13 Well water. Figure 4-2 shows the continuous flow-through configuration employed in the experiment (Martin, et al., 2004). The test specimens were placed in a 500-mL [0.13-gal] glass vessel containing crushed Yucca Mountain tuff. A constant flow of the simulated groundwater from a 1-L [0.26-gal] reservoir {2-L [0.53-gal] reservoir in earlier experiment} (Horn, et al., 2000),

Table 4-3. Dissolution of Metals in Test Solutions After a 5-Month Exposure* (mg/L)†				
Vessel Conditions/ Material	**Iron**	**Chromium**	**Nickel**	**Molybdenum**
Unexposed J–13 Supplemented Medium	0.25	Not detectable	Not detectable	Not detectable
Sterile 304 Stainless Steel	0.31	Not detectable	Not detectable	Not detectable
Bacteria + 304 Stainless Steel	0.57	1.03	0.04	Not detectable
Sterile 625	0.31	Not detectable	Not detectable	Not detectable
Bacteria + 625	0.33	1.07	0.12	Not detectable
Sterile C-22	0.42	Not detectable	Not detectable	Not detectable
Bacteria + C-22	0.32	1.05	0.1	Not detectable

*Lian, T., S. Martin, S. Jones, D. Rivera, and J. Horn. "Corrosion of Candidate Container Materials by Yucca Mountain Bacteria." Proceedings of the CORROSION '99 Conference. Paper No. 476. Houston, Texas: NACE International. 1999.
†1lb/ft^3 = 16.02 g/L.

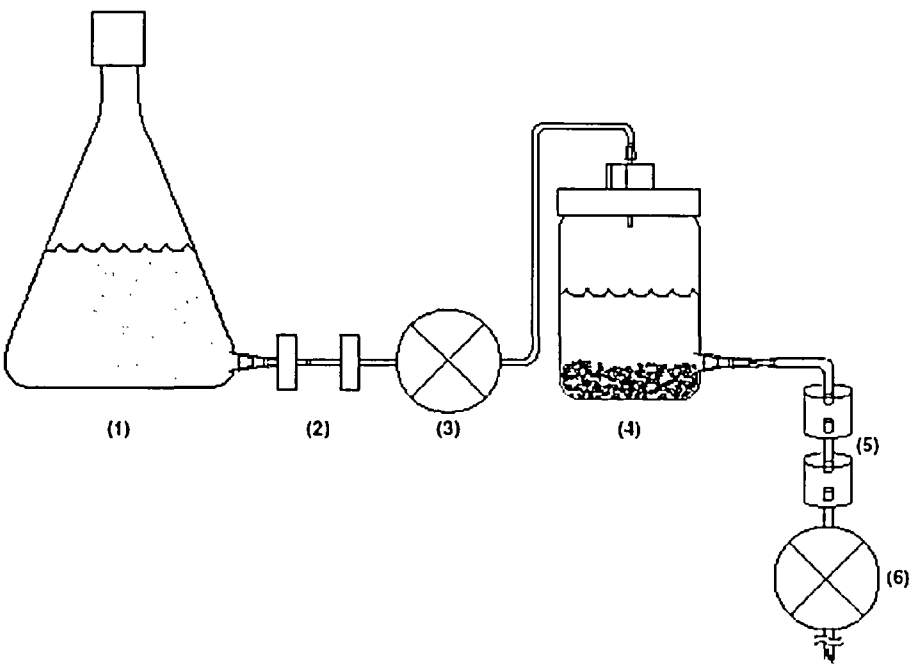

Figure 4-2. Configuration of Microcosms: (1) 1-L [0.26-gal] Reservoir Containing Sterile Media; (2) 0.2-M In-line Filters; (3) Peristaltic Pump; (4) 500-mL [0.13-gal] Modified Spin Flask and Yucca Mountain Tuff and Coupon Material; (5) Media Break Tubes to Prevent Back Contamination; and (6) Second Peristaltic Pump to Regulate the Outlet Flow (Martin, et al., 2004). (Reproduced with Permission from NACE International.)

through the test vessel was maintained at 2 mL/hr [0.07 oz/hr] with the aid of peristaltic pumps. The total residence time for the fluid in the glass vessel was approximately 5 days. The experiments were conducted at 22 °C [72 °F] or 30 °C [86 °F]. For comparison, test specimens were also placed in the same experiment setup shown in Figure 4-2, except the tuff was sterilized (3–4 Mrad/hr irradiation, using a Co-60 gamma source), and the solution was dosed with antibiotics to maintain sterility.

Figure 4-3 shows three Alloy 22 coupons that were (i) unincubated/nonreacted, (ii) exposed to the sterile solution for 43 months, and (iii) exposed to the nonsterile solution for 57 months (Martin, et al., 2004). The coupon exposed to the nonsterile solution at 22 °C [72 °F] clearly shows uniformly distributed arrays of microcavities with sizes ranging from 0.2 to 0.7 μm [7.8×10^{-3} to 2.8×10^{-2} mils]. Similar microcavities were not observed on either the coupons exposed to the sterile solution or the nonreacted coupons. Even though these arrays of microcavities do not have the typical appearance of pitting corrosion, if some of the microcavities continue to grow, they may represent earlier signs of localized corrosion.

Bacteria counts and identification were not reported for these experiments. The cultivation of the tuff from the same Yucca Mountain locations in simulated groundwater (Horn, et al., 2003) has shown that an array of microorganisms can be isolated from the Yucca Mountain rocks. These organisms include the degraders of complex organic compounds such as *Pseudomonas* and *Arthrobacter*, the organic acid producer such as *Microbacterium*, and extracellular polyaccharides producer such as *Bacillus*. Sulfate-reducing bacteria also were identified in the Yucca Mountain rock (see Section 3.2).

4.1.3 Assessment of DOE Approach

Stainless steels are known to be susceptible to microbially influenced corrosion (Amaya, 2003, 1999). Nickel-based alloys, such as Alloys 625 and 825, also were found to be susceptible to localized corrosion in natural seawater when the corrosion potentials were increased as a result of microbial activity (Martin, et al., 2003; Brennenstuhl, et al., 1990). However, there has been no credible evidence for microbially influenced corrosion for Alloy 22. From the extensive studies on the localized corrosion of Alloy 22, the repassivation potential of Alloy 22 at or slightly above the critical temperature {70 °C [158 °F]} is beyond 0.70 V_{SCE} for 5-M $CaCl_2$ -0.1M $NaNO_3$ solution (Bechtel SAIC Company, LLC, 2003b). For temperatures lower than 70 °C [158 °F], no localized corrosion could be initiated at any potentials even in nitrate-free 5-M $CaCl_2$ solutions (Bechtel SAIC Company, LLC, 2003b). For example, no localized corrosion was observed when the potential was scanned to 1.4 V versus Ag/AgCl in pure 5-M $CaCl_2$ brine at 45 °C [113 °F] (Bechtel SAIC Company, LLC, 2003b). It has been reported that microbial activities were responsible for the ennoblement of stainless steels and nickel-based alloys in natural seawater to near 0.40 V_{SCE} (Martin, et al., 2003; Amaya, 2003) and caused the initiation of localized corrosion. However, it is unlikely for localized corrosion to initiate Alloy 22 by the ennoblement microbial activity at low temperatures because the potential required for Alloy 22 is extremely high. The maximum temperature at which mesophilic microorganisms are active is lower than the critical temperature for crevice corrosion in concentrated chloride solutions.

As discussed in Section 4.1, in the 5-month experiment in electrochemical cells (Lian, et al.,1999a), no sign of localized corrosion for Alloy 22 was observed. The corrosion potential of the Alloy 22, and all other metals tested in the experiment, was found to be lower in

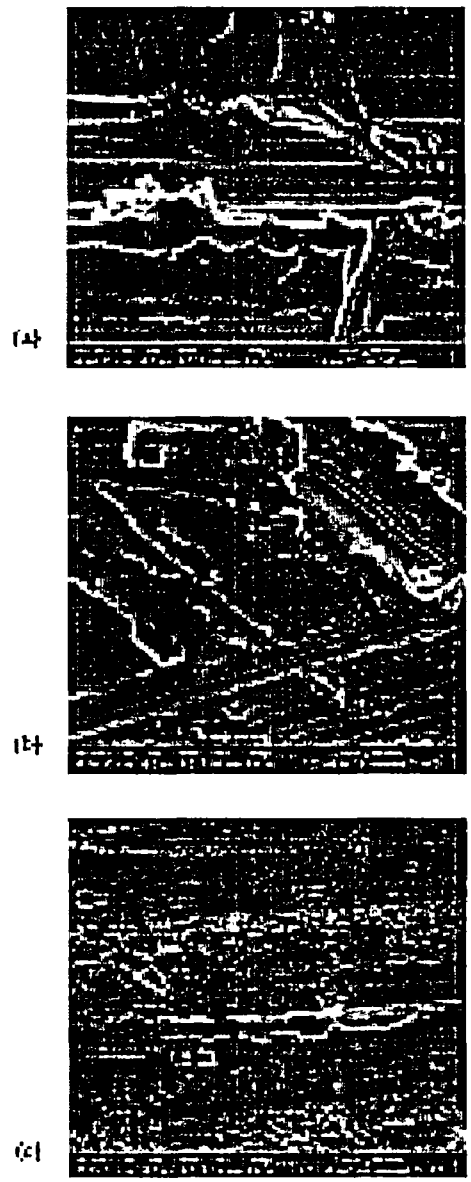

Figure 4-3. Alloy 22 Coupons Incubated at 22 °C [72 °F]: (a) Unincubated/Nonreacted Coupon, (b) Sterile Coupon (43 Months), and (c) Nonsterile Coupon (57 Months). The Micropores on the Nonsterile Coupons Were Ubiquitous and Not Uniform in Shape (c); The Unreacted (a) and Sterile (b) Surfaces Are Similar in Appearance and Are Free of Micropore Features (Martin, et al., 2004). (Reproduced with Permission from NACE International.)

the bacteria-containing solution than in the sterile solution (Bechtel SAIC Company, LLC, 2003c). Based on these observations and the high repassivation potentials of Alloy 22, the microbially influenced corrosion effect on localized corrosion was excluded in the DOE analysis.

However, in the electrochemical experiments (Lian, et al., 1999a), the authors measured a higher corrosion rate with the lineal polarization resistance method for Alloy 22 in the bacteria-containing solution than in the sterile solution. They also observed similar higher corrosion rates in the presence of Yucca Mountain bacteria than in abiotic solutions for other corrosion-resistant metals such as Type 304 SS and Alloy 625. The increases in the electrochemically measured corrosion rates were attributed to general corrosion. Based on this study, DOE uses the microbially influenced corrosion factor, an enhancement factor for general corrosion by microbial activity, to estimate the general corrosion rate in microbial environments (Bechtel SAIC Company, LLC, 2003b). Because the largest microbially influenced corrosion factor measured was two for Alloy 22, the factor was uniformly distributed between one (value in sterile solution) and two in the DOE model analysis to account for uncertainties. Equation (4-1) was applied to the waste package outer barrier general corrosion rate estimation model when the relative humidity at the waste package outer barrier surface is above 90 percent, which is considered as the threshold relative humidity (Section 2.3) for microbially influenced corrosion.

As discussed in Section 4.2, the corrosion rate increases observed by Lian, et al. (1999a) using electrochemical techniques in the presence of sulfate-reducing bacteria may not be a result of the corrosion of the metal. At least part of the increase may be caused by the oxidation reaction of the reducing species produced by the microorganisms. Therefore, the value of the microbially influenced corrosion factor in Eq. (4-1), f_{MIC}, for general corrosion derived from the experiments by Lian, et al. (1999a) is a conservative value because it contains contributions from the oxidation reactions of the chemical species formed by the microorganisms.

On the other hand, microbially influenced corrosion is usually manifested in the form of localized corrosion (Lewandowski, 2000; Little, et al., 2000). Hence, the attribution of a high corrosion rate observed in the presence of microorganisms to general corrosion is not reasonable. If the observed increase in corrosion is true, the possibility of localized corrosion should also be considered. As discussed previously, the increased current density measured using electrochemical methods may be an artifact, and other methods should be used to determine corrosion rates. Solution analysis may be an alternate method for this purpose. Lian, et al. (1999a) reported high values for chromium {1.05 mg/L [1.05 ppm]} and nickel {0.1 mg/L [0.1 ppm]} in the solution containing microorganisms versus values below the detection limits in the sterile solution for Alloy 22. The increase in chromium suggests preferential dissolution, which may, if continued with time, will be an indication of localized corrosion.

In the 56-month immersion test (Martin, et al., 2004), microcavities were observed to have developed on the Alloy 22 specimens in the nonsterile solution. Such microcavities were neither observed in the specimens exposed to the sterile solution nor shown on the nonreacted specimen. While the microcavities are not convincing indicators for pitting corrosion, they may be early signs of susceptibility of pitting corrosion if the microcavities continue to grow. On the other hand, the microorganisms derived from the rocks that were collected at certain locations in the exploratory drift do not include sulfate-reducing bacteria as shown in earlier studies (e.g., Castro, et al., 2004, 1998; Lian, et al., 1999a; and Pitonzo, et al., 2004). These rocks may not contain many other microorganisms that have been shown to be aggressive and may

promote localized corrosion (Section 3), but which may be added during the repository construction phase of development. These microorganisms may be present in the diesel fuels, machinery lubricants, and equipment surfaces, etc., or include native microorganisms that become active as a result of adding water and oxygen, as well as other electron acceptors, during excavation. There is likely a great spatial heterogeneity in the distribution of microorganisms associated with Yucca Mountain rocks. Any specific consortium of organisms may not reflect this heterogeneity. In addition, it is not known if the DOE investigations were limited to annealed specimens. Heat-treated or welded specimen should be included in the test matrix because microbially influenced corrosion often starts from welded areas (Ray, et al., 2002; Borenstein, 1994).

The microbially influenced corrosion effect on localized corrosion was not considered possible by DOE (Bechtel SAIC Company, LLC, 2003b) because the corrosion potential of Alloy 22 measured in the presence of Yucca Mountain bacteria was much lower than the repassivation potential of Alloy 22 (Bechtel SAIC Company, LLC, 2003b). In addition, the temperatures at which the microorganisms are believed to be active are lower than the critical temperature for Alloy 22 to be susceptible to localized corrosion. This consideration does not take into consideration the potential role of thermophilic microorganisms that may be active at temperatures above 60 °C [140 °F]. Little, et al. (1986) demonstrated accelerated corrosion of Nickel 201 at 60 °C [140 °F] as a product of the metabolism of a thermophilic bacterium, whereas, no corrosion occurred during identical conditions at 23 °C [73 °F]. Ford, et al. (1987) reproduced this finding for mild steel. It is possible that all necessary conditions for localized corrosion influenced by microbial activity will exist at temperatures as high as 70 °C [158 °F] when the relative humidity reaches the critical value of 90 percent necessary to support microbial growth (Geesey, 1993).

4.2 CNWRA Investigations

As part of an effort to evaluate the potential susceptibility of Alloy 22 to microbially influenced corrosion, an experimental program was initiated at the Center for Nuclear Waste Regulatory Analyses. The experiments were divided into two parts, an initial study and a full-scale study. The initial study was aimed to evaluate the applicability of electrochemical techniques for the study of microbially influenced corrosion. A second objective was to select a proper microorganism or a consortium of microorganisms known or anticipated to exist at Yucca Mountain for the full-scale study. Because Alloy 22 exhibits an extremely slow corrosion rate and is extremely resistant to localized corrosion at temperatures below 60° C [140° F], stainless steels were used in the initial tests. Sulfate-reducing bacteria were selected because this type of bacteria was one of the identified microorganisms isolated from the Yucca Mountain area (Castro, et al., 2004, 1998; Pitonzo, et al., 2004; Lian, et al., 1999a) and there are examples of the corrosion of stainless steels by sulfate-reducing bacteria available in the literature that can be used for comparison (Ringas and Robinson, 1988a,b). In the full-scale tests, heat-treated Alloy 22 and stainless steels and other nickel-based alloys, including Type 316L SS and Alloy 825, are being tested in parallel cells containing *Pseudomonas*, *Thiobacilli*, *Vibrio Natriegens* (slime former) sulfate-reducing bacteria, or mixtures of these bacteria. Because data from the full-scale tests were not available at the time this report was prepared, only the results from the initial study are presented in the following sections.

4.2.1 Studies in Chloride- and Sulfate-Containing Solutions Inoculated with Sulfate-Reducing Bacteria

Electrochemical methods are sensitive and, beyond their fundamental implications, are usually time-saving for corrosion studies. For example, the susceptibility of a metal to localized corrosion in a given environment can be determined in a few hours by performing electrochemical repassivation measurements. These tests compared favorably with immersion tests during natural corroding conditions that may take many months, even years, for the metal to show any signs of localized corrosion. Measurements of galvanic coupling current and repassivation potential, as well as anodic polarization techniques, were employed in the initial study.

4.2.1.1 Anodic Galvanic Coupling Currents

Figure 4-4 shows the configuration of an electrochemical system used in the experiment for studying microbially influenced corrosion. There were three cells, including a control cell on the left, a test cell on the right, and an aerated cell in the middle. All cells were filled with 500-mL [0.13-gal], 0.5-M NaCl solution that was prepared with reagent grade chemicals and deionized water {18 Mohm-cm [7.1 Mohm-in] resistivity}. The addition of chloride was to initiate localized corrosion during repassivation potential measurement and to assess the effect of microbial activity on repassivation potential. Two salt bridges filled with the same solution were used to connect the control and the test cells to the aerated cell. Large stainless steel electrodes were placed in the aerated cell for coupling with the electrodes in the control and the test cells. Thus, the three-cell system in Figure 4-4 simulates two double-compartment electrochemical cells described by Newman, et al. (1991). The electrochemical potentials of the electrodes in the control and the test cells were raised by coupling them to the large electrodes in the aerated cell, which were used as cathodes. This configuration is used to mimic the situation that engineering metallic components exposed to anaerobic sulfate-reducing bacteria-thriving conditions exhibit when they are electrically connected to the other sections or other components that are exposed to oxygen-rich or other oxidizing environments.

The test cell contained a slime former (*Vibrio Natriegens* ATCC 14048)[1] grown in 1.5-percent NaCl nutrient broth (Table 4-4) and a sulfate-reducing bacterium (*Desulfovibrio vulgaris*

Table 4-4. 1.5-Percent NaCl Nutrient Broth

Chemicals	Amount
Beef Extract	3.0 g*
Peptone	5.0 g
Sodium Chloride	15.0 g
Distilled Water	1,000 mL†
Final pH at 25 °C [77 °F]	7.0 ± 0.3

*1 lb = 454 g
†1 oz = 29.57 mL

[1]ATCC—American Types of Culture and Collection.

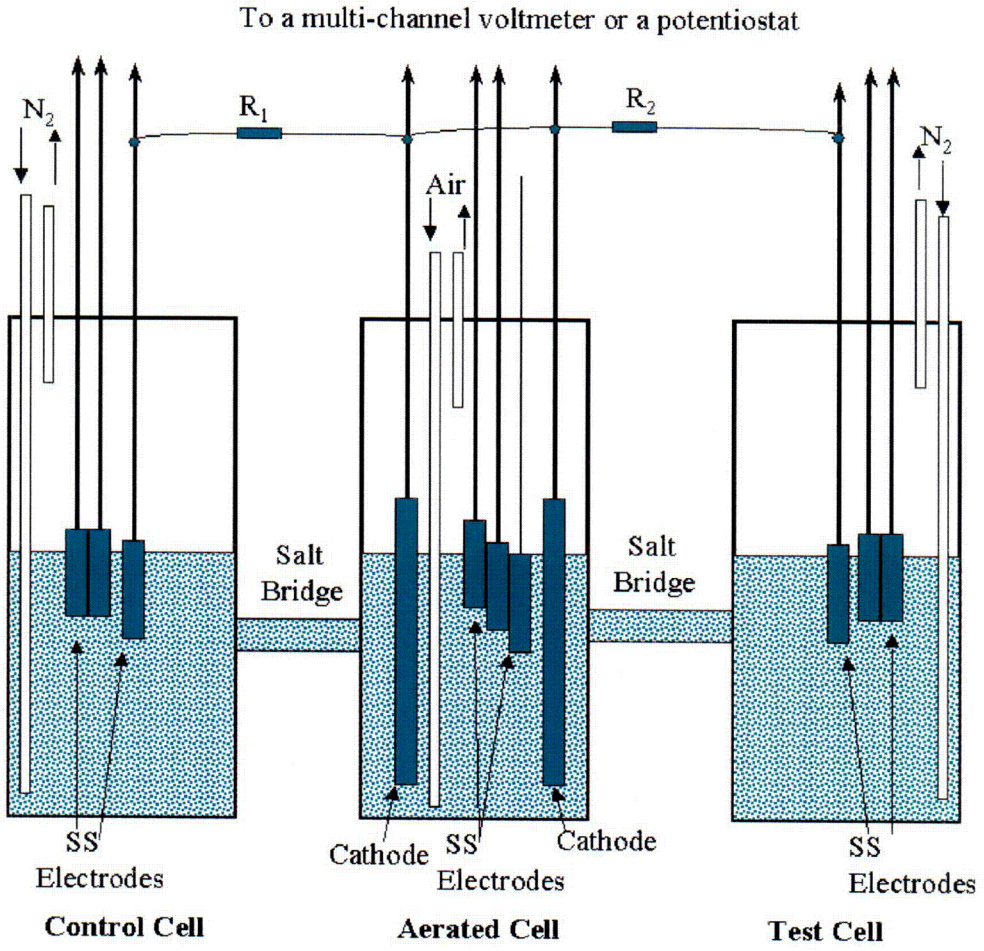

Figure 4-4. Schematic Diagram of the Experimental Cells. Reference and Platinum Electrodes Are Not Shown. R_1 and R_2 Are the Resistors for the Measurements of the Galvanic Coupling Currents to the Cathodes.

ATCC 29579) grown in a modified Baar's Broth medium (Table 4-5), both from Anaerobe System, Morgan Hill, California. The slime former {10 mL [0.34 oz] in 1.5-percent NaCl nutrient broth} and sterile modified Baar's Broth medium {30 mL [1.01 oz]} were added at the beginning of each test. Initial inoculation of the organism into the test system was performed by growing each of the organisms in selective media for an incubation period aimed to achieve log-phase growth (active growth) of each organism type. The *Vibrio Natriegens* was grown in the 1.5-percent nutrient broth at 31 ± 1 °C (87.8 ± 1.8 °F) for approximately 4 hours to achieve a log-phase growth. The sulfate-reducing bacteria were incubated for 48 hours during the same temperature conditions but in an anaerobic environment (Bio Bag Type A, from Becton Dickinson, Franklin Lakes, New Jersey) using modified Baar's Broth medium to achieve a log-phase growth. The sulfate-reducing bacteria {10 mL [0.34 oz] in modified Baar's Broth} were introduced into the test cell approximately 7 days after the addition of the slime former.

The control cell was identical to the test cell except it did not contain any sulfate-reducing bacteria. To maintain the growth of the sulfate-reducing bacteria and the slime former, 10 mL [0.34 oz] sterile Baar's Broth medium was added to the test and control cells

C02

TABLE 4-5. Modified Baar's Broth Medium	
Chemicals	**Amount**
Sodium Chloride	5 g*
Sodium Citrate	5 g
Magnesium Sulfate	2 g
Ammonium Chloride	1 g
Calcium Sulfate	1 g
Potassium Phosphate (Dibasic)	0.5 g
Sodium Lactate (60 wt%)	3.5 mL†
Yeast Extract	1 g
Ferrous Ammonium Sulfate	1 g
Distilled Water	1,000 mL†
Final pH at 25 °C [77 °F]	6.5 ± 0.3

*1 lb = 454 g
†1 oz = 29.57 mL

approximately every 35 hours during the entire test period. Harvest samples of approximately 10 mL [0.34 oz] each from the two cells were taken on a regular basis and cultured for the population counts of both sulfate-reducing bacteria and slime former using a standard serial dilution technique (Collins, et al., 2004). The cell count of the slime former was maintained at 10^5 to 10^{10} cfu (colony forming units)/mL in the two cells. The cell count of the sulfate-reducing bacteria was normally maintained at 10^5 to 10^8 cfu/mL [2.94×10^5 to 2.94×10^{10} cfu/oz]. No sulfate-reducing bacteria were found in the control cell throughout the test.

Reference electrodes, platinum electrodes, and duplicate Types 304 and 304L SS electrodes were placed in the three cells for polarization and repassivation potential measurements. The currents flowing from the stainless steel electrodes in both the test and the control cells to the large stainless steel cathodes in the aerated cell were measured by the voltage drops across the resistors as shown in Figure 4-4. All tests were conducted at room temperature {approximately 24 °C [75 °F]}.

Two types of stainless steel electrodes were used. One was made of Type 304L SS plate with a dimension of 1.27 cm [0.5 in] in width, 5.08 cm [2 in] in length, and 0.21 cm [0.0827 in] thickness (referred to as stainless steel plate electrode). The other type was made of Type 304 SS wire {1-mm [0.039-in] diameter}. The chemical compositions of the stainless steels are listed in Table 4-6. The immersion depth of the plate and the wire electrodes was such that the effective surface areas were approximately 3.2 cm^2 [0.496 in^2]. The wire electrodes were originally used; however, it was difficult to examine their surface appearance optically, hence, the plate electrodes were used. All surfaces of the plate and wire electrodes were polished with 600-grit SiC paper and cleaned with acetone before the experiment. No recleaning or repolishing was performed during the experiments because of difficulties in

Table 4-6. Chemical Compositions (wt%) of the Stainless Steel Materials Used in the Experiment											
Metals	Unified Numbering System for Metals and Alloys	Ni*	Cr	Fe	Mo	Mn	Si	Cu	P	S	C
304 SS	S30400	9.16	18.5	Bal†	0.38	1.10	0.33	0.27	0.019	0.006	0.030
304L SS	S30403	8.29	18.3	Bal	0.4	1.36	0.43	0.26	0.03	0.01	0.02
*Ni—nickel, Cr—chromium, Fe—Iron, Mo—molybdenum, Mn—manganese, Si—silicon, Cu—copper, P—phosphorus, S—sulfur; C—carbon. †Bal: Balance											

maintaining the anaerobic environment. The large cathodes shown in Figure 4-4 were 1-mm [0.039-in]-diameter stainless steel coils made from the same wire used for the electrochemical tests. The surface area of each cathode was approximately 94.2 cm^2 [14.6 in^2]. The cathode-to-anode surface area ratio was 14.7.

Figure 4-5 presents the coupling potential and the galvanic currents from the Type 304L SS plate electrodes in both the test and the control cells to a separate stainless steel cathode in the aerated cell (Figure 4-4). The coupling potential of the stainless steel plate electrodes varied from -0.16 to -0.26 V_{SCE} and was lower than the repassivation potential. The anodic galvanic current from the stainless steel plate electrode in the test cell was slightly higher than that from the control cell. The cause of the current decrease on June 8, 2003, and further increase is not known. Optical examination of the electrode confirmed that pitting corrosion was not initiated during the 30-day test.

The open-circuit steady-state potential of the Type 304 SS in the aerated cell filled with pure NaCl solution varied between -0.03 to -0.15 V_{SCE} (see Section 4.2.1.2). However, its potential dropped by more than 0.10 V after the connection with the small stainless steel sensing electrodes in the deaerated cells, even though the cathode-to-anode surface area ratio was 67. The decrease of the potential of the cathode was probably a result of the poor kinetics of the oxygen-reduction reaction on the stainless steel cathode in the air-saturated sodium chloride solution at room temperature. To simulate the ennoblement of the large cathodes in the aerated cell, a battery was connected in series in each of the cathode-anode circuits as shown in Figure 4-4. The battery output could be adjusted to change the values of the coupling potential. Figure 4-6 shows the responses of the galvanic coupling currents from the two Type 304L SS plate electrodes to the change of potential. The potential was held at approximately -0.235 V_{SCE} for 16 days, -0.12 V_{SCE} for 12 days, and -0.04 V_{SCE} for 21 days. In general, the anodic galvanic coupling currents from the plate electrodes increased with the increase of potential and the anodic coupling current from the electrode in the test cell was higher than that in the control cell.

Figure 4-7 shows that the sulfate-reducing bacteria increased rapidly to 10^8 cfu/mL [2.94 × 10^8 cfu/oz] approximately 10 days after the inoculation and remained at approximately 10^8 cfu/mL [2.94 × 10^8 cfu/oz] after the initial growth by the addition of the medium approximately every 35 hours on average until June 26, 2003. Because the medium was not available and the regular addition was stopped on June 26, 2003, the growth of sulfate-reducing bacteria decreased to 10^4 cfu/mL [3.94 × 10^4 cfu/oz] on July 8, 2003. The regular addition of the

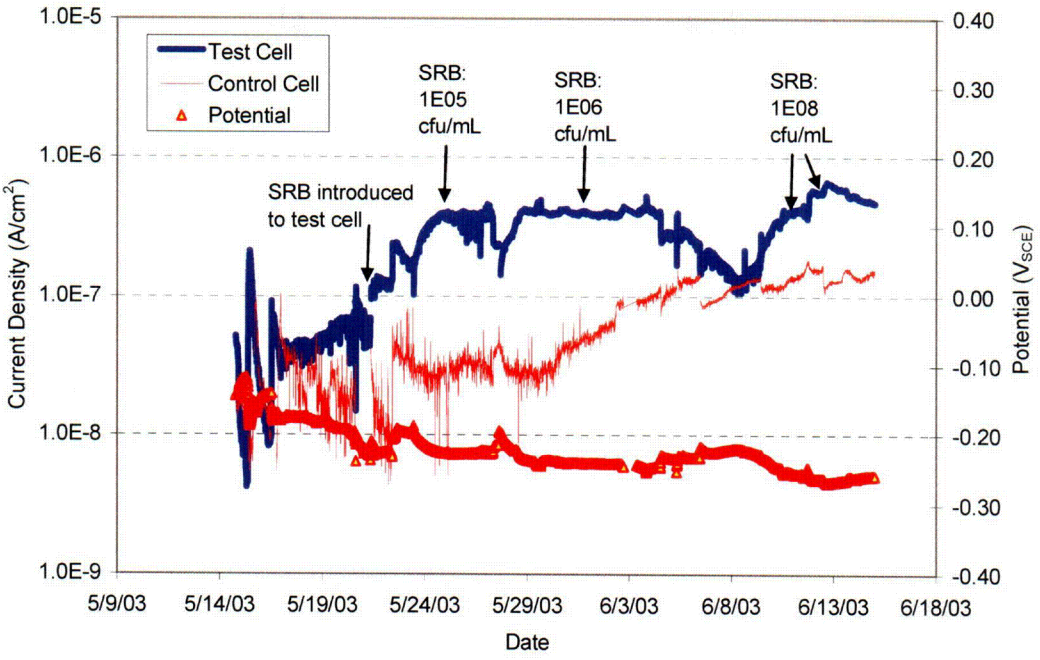

Figure 4-5. Galvanic Coupling Currents from Type 304L SS Plate Electrodes and the Potential During the First 30 Days of Test

NOTE: 1 A/cm² = 9.29 × 10² A/ft²

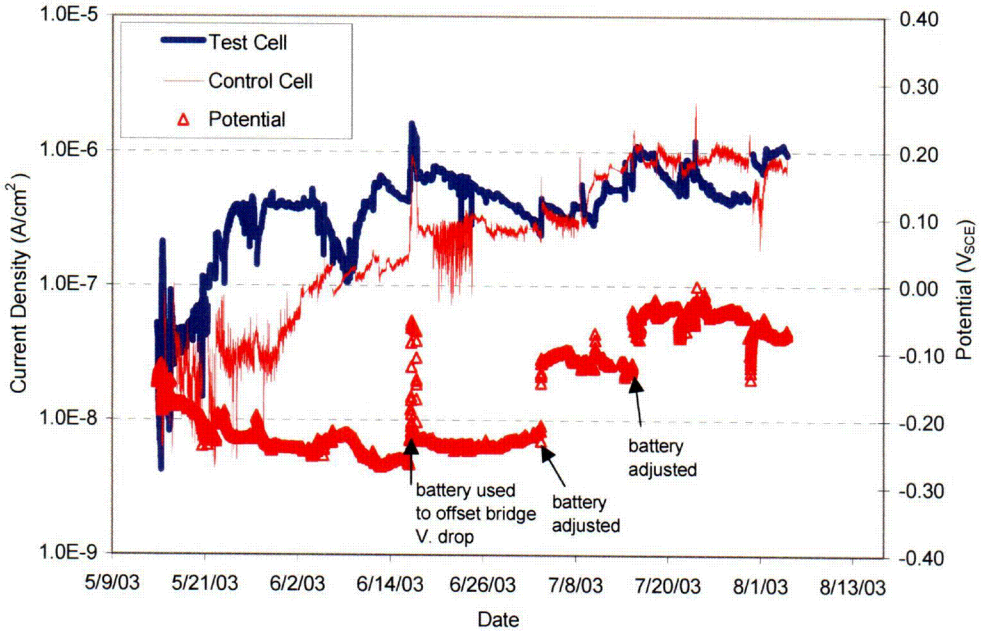

Figure 4-6. Responses of the Galvanic Coupling Currents of the Stainless Steel Plate Electrodes to the Changes of the Coupling Potential

NOTE: 1 A/cm² = 9.29 × 10² A/ft²

C03

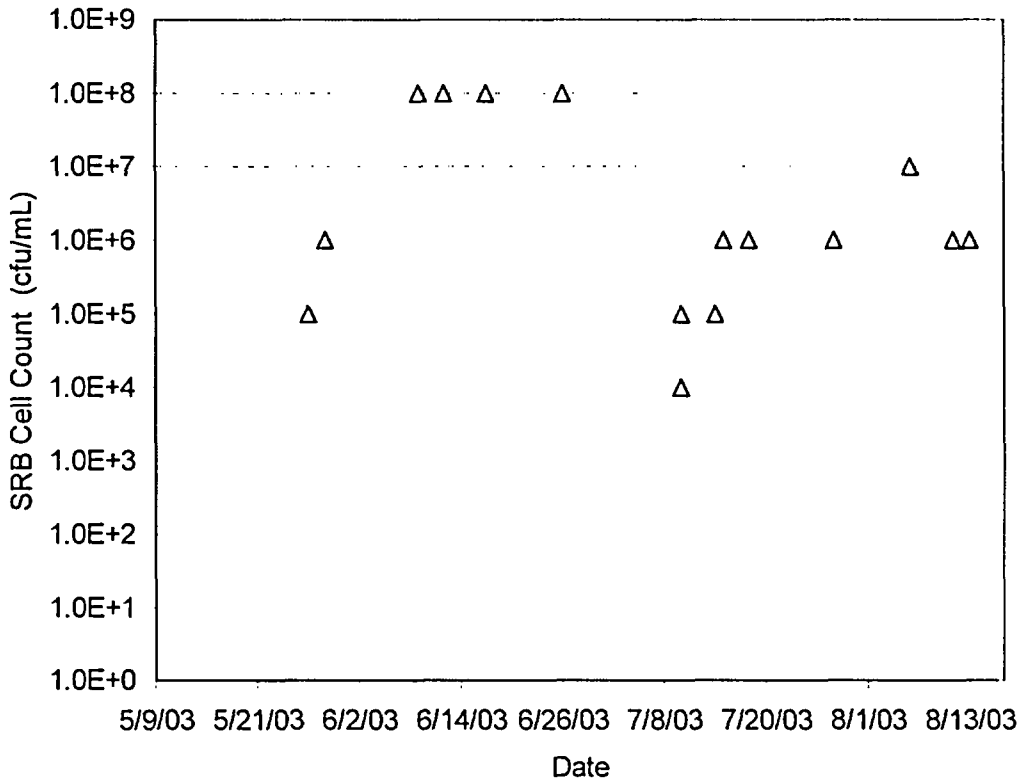

Figure 4-7. Sulfate-Reducing Bacteria Density During the Experiment As Indicated in Figures 4-2 and 4-6. Sulfate-Reducing Bacteria Dropped on June 26, 2004, As a Result of Interruption of Medium Addition.

NOTE: 1 A/cm^2 = 9.29 × 10^2 A/ft^2

medium was resumed, and the growth of sulfate-reducing bacteria increased. The sulfate-reducing bacteria count was maintained at approximately 10^6 cfu/mL [2.94 × 10^6 cfu/oz] until the end of the test. Figure 4-7 seems to show that the galvanic coupling current from the plate electrode in the test cell correlates with the sulfate-reducing bacteria count except at the beginning of the test. The anodic galvanic coupling current was high when the sulfate-reducing bacteria count was more than 10^8 cfu/mL [2.94 × 10^8 cfu/oz], but decreased when the sulfate-reducing bacteria count decreased to approximately 10^4 cfu/mL [2.94 × 10^4 cfu/oz]. The current remained low during the latter stage of the test when the sulfate-reducing bacteria count was approximately 10^6 cfu/mL [2.94 × 10^6 cfu/oz]. If the galvanic coupling current was caused by the anodic dissolution of the stainless steel plate electrode, Figure 4-7 suggests that sulfate-reducing bacteria promote a higher corrosion rate for Type 304L SS.

Visual examination on the Type 304L SS plate electrode after 9 days of exposure showed no pitting on the surface. This result is in agreement with the measurements of pit initiation and repassivation potentials because the potential of the Type 304L SS plate electrodes did not lay between the pit initiation potential (see Section 4.2.1.2) and the repassivation potential (+0.06 to -0.065 V_{SCE}) (see Section 4.2.1.2) for a time sufficient to initiate pitting corrosion.

4.2.1.2 Repassivation and Potentiodynamic Polarization Behaviors

A potentiostat (Model 1287A, from Solartron, United Kingdom) and the associated controlling software (CorrWare, Version 2.2, from Scribner Associates, Southern Pines, North Carolina) were used for the electrochemical measurements. The repassivation potential was determined using a method similar to the one described by Akashi, et al. (1998). The repassivation potential is considered to be the lowest potential at which localized corrosion can be initiated in long-term exposure during naturally corroding conditions (Dunn, et al., 2000). The electrode was potentiodynamically scanned from the open-circuit steady-state potential toward the more noble direction at a rate of 0.5 mV/s. As soon as the anodic current reached 0.2 mA, which indicates the initiation and propagation of pitting corrosion, the current was galvanostatically held at 0.2 mA to allow further propagation of pitting corrosion for 2 hours. Subsequently, the potential was potentiodynamically scanned toward the less noble direction at a rate of 0.167 mV/s until the current reached 0.05 mA and held constant for 2 hours. If the current was higher than 1×10^{-6} A/cm^2 [9.29×10^{-4} A/ft^2] at the end of the 2-hour hold, suggesting continued propagation of pitting corrosion, the potential was lowered by 10 mV and held constant for another 2 hours. If the current was still higher than 1×10^{-6} A/cm^2 [9.29×10^{-4} A/ft^2] at the end of the second 2-hour hold, the potential was lowered by another 10 mV and held for 2 hours. This step sequence was repeated until the current remained below 1×10^{-6} A/cm^2 [9.29×10^{-4} A/ft^2] at the end of a 2-hour hold, suggesting that active pitting corrosion was arrested. To observe the behavior of the cathodic reactions, a modified version of the Akashi method (Jain, et al., 2003) also was used. The modified Akashi, et al. (1998) method is the same as the previously described method except that the potentiodynamic scan toward the less noble direction was allowed to continue until a predetermined low potential so the cathodic current would follow through the electrode. The 2-hour and 10-mV steps were eliminated in the modified Akashi, et al. (1998) method. Unless otherwise specified, the polarization curves presented in this report were obtained using the Akashi, et al. (1998) method.

Typical repassivation polarization curves obtained with the modified Akashi, et al. (1998) method for Types 304 and 304L SS are presented in Figure 4-8. The curves for both the control and the aerated cells are typical of all results obtained throughout the testing period, while the curve for the test cell was obtained only when the sulfate-reducing bacteria count was high. In addition, the curve for the control cell is identical to that from the aerated cell, suggesting that the slime former and the media that contain a wide range of added chemical components (Tables 4-4 and 4-5) in the control cell had little effect on the anodic behavior of stainless steel. However, the typical forward and backward polarization curves obtained in the test cell when the sulfate-reducing bacteria count was high are significantly different. The curves have a distinctive anodic peak at a potential near the repassivation potential (corresponds to the potential at which the current decreased dramatically to below 1×10^{-6} A/cm^2 [9.29×10^{-4} A/ft^2] in Figure 4-8 during a backward potentiodynamic scan) and exhibited a high current density in the passive region. The characteristic parameters of the curves from both the cyclic potentiodynamic polarization and the repassivation potential measurements are as follows:

(i) Repassivation Potential—Figure 4-9 shows the repassivation potentials (E_{rp}) obtained in the three cells for the two types of stainless steel electrodes at different times during the test period of approximately 3 months. The repassivation potentials are all between -0.01 and -0.15 V_{SCE} for the Type 304 SS and between +0.06 and -0.065 V_{SCE} for the Type 304L SS in all cells (test, control, and aerated). The repassivation potential remained unchanged during the course of the test even though the pH of all solutions

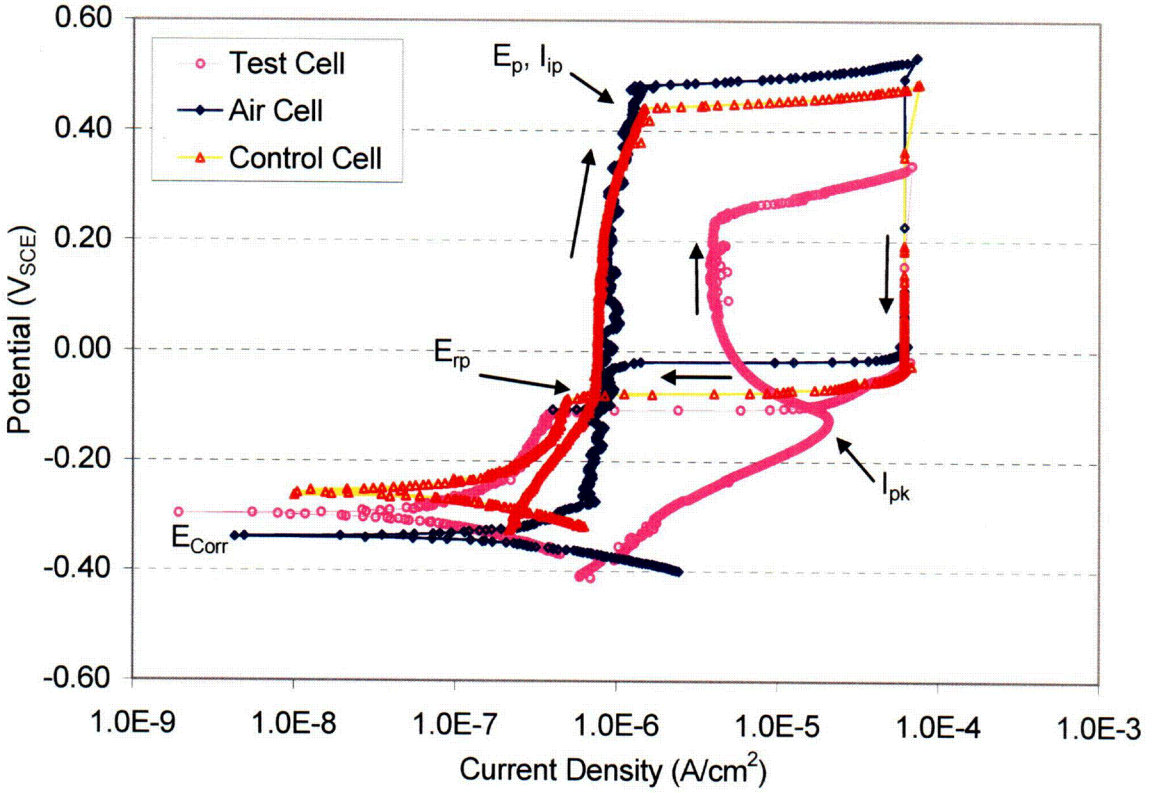

Figure 4-8. Typical Repassivation Polarization Curves Obtained in the Different Electrochemical Cells for Types 304 and 304L SS with Modified Akashi Method

NOTE: 1 A/cm^2 = 9.29 × 10^2 A/ft^2

increased. For example, the solution in the aerated cell changed from a pH of 6.2 at the beginning of the test to a pH of 10.33 at the end of the test. In addition, the repassivation potential measured in the test cell was found to be independent of the sulfate-reducing bacteria count in the solution (Figure 4-7) for both stainless steels. The scattering of the measured repassivation potential data shown in Figure 4-9 is typical for passive alloys.

(ii) Pit Initiation Potential—Pit initiation potential has been widely used as an indicator of the resistance to localized corrosion. Figure 4-10 shows the pit initiation potentials (E_p) obtained in the different cells for the two types of stainless steel electrodes during the experiment. The pit initiation potentials are scattered over a wide range (0.1–0.6 V_{SCE}). However, in most cases, the values obtained from the test cell are lower than those obtained from both the aerated and the control cells for the two types of stainless steel. Most of the values from the test cell lie close to 0.15 V_{SCE}. There is one exceptional low value (0.145 V_{SCE}) measured from the aerated cell [Figure 4-10(b)], which cannot be explained. No apparent correlation between the sulfate-reducing bacteria count (Figure 4-7) and the pit initiation potential of the stainless steel electrodes can be drawn from Figure 4-10. The large scattering of the measured pit initiation potential data shown in Figure 4-10 is typical for passive alloys.

cof

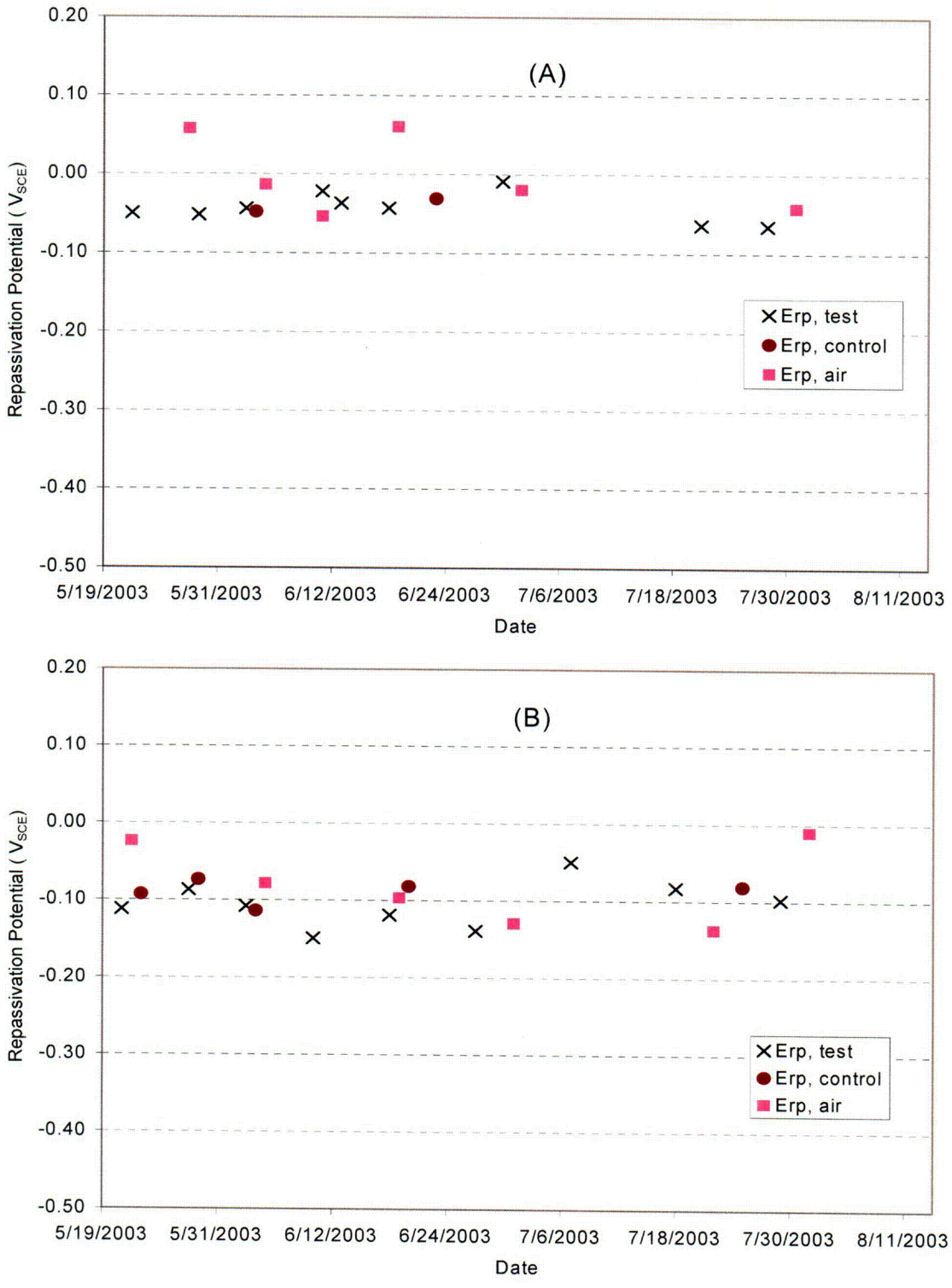

Figure 4-9. Repassivation Potentials of Types (A) 304L and (B) 304 SS Electrodes

C05

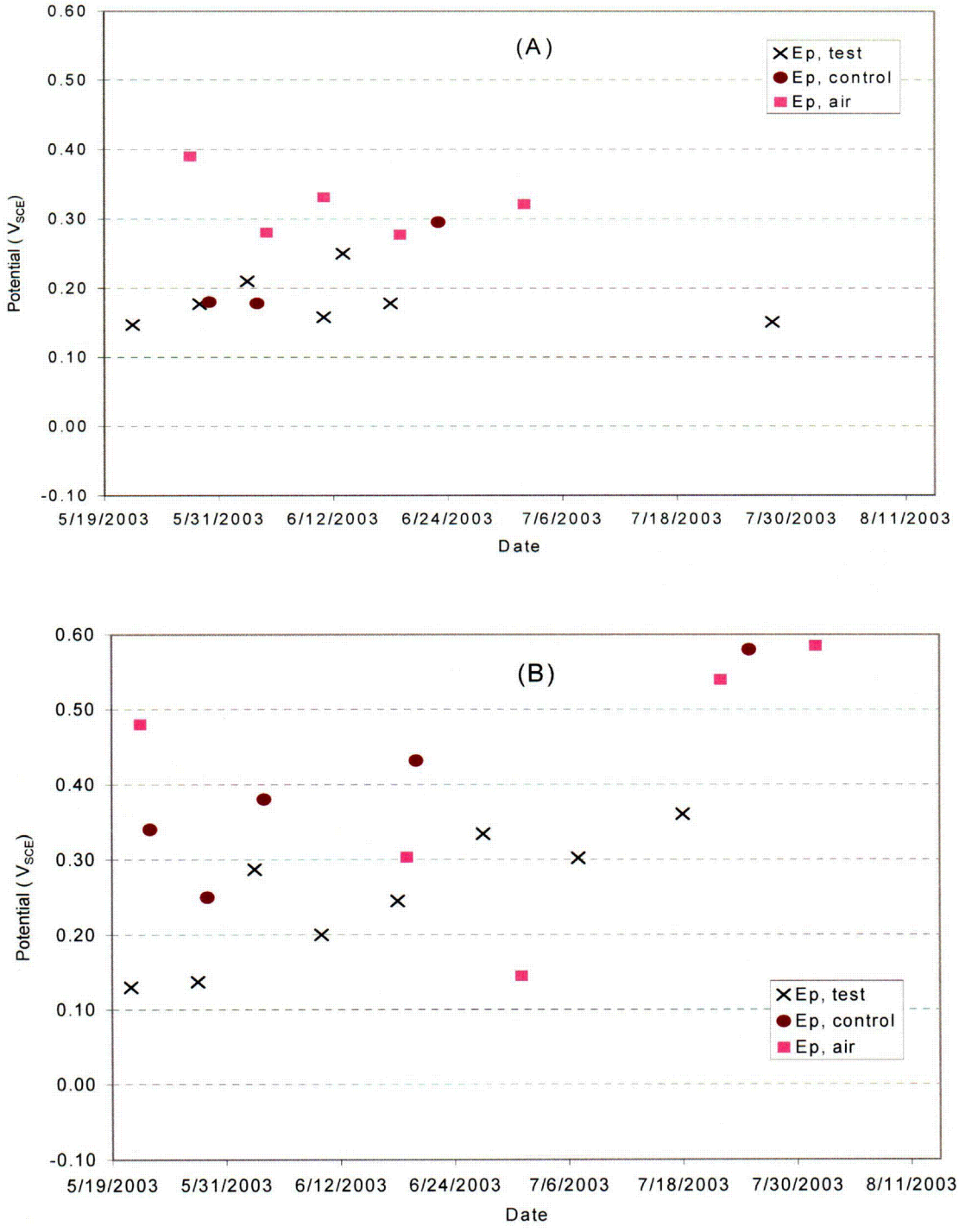

Figure 4-10. Pit Initiation Potentials for Types (A) 304L and (B) 304 SS Electrodes

COC

(iii) Corrosion Potential—Figure 4-11 shows the corrosion potentials (E_{corr}) defined as the potentials at which the net current is zero on the polarization curves (ASTM International, 1999). The values in Figure 4-11 were obtained in the different cells for the two types of stainless steel electrodes during the experiment. The corrosion potentials are between -0.37 and -0.15 V_{SCE} for the Type 304L SS electrodes and between -0.430 and -0.230 V_{SCE} for the Type 304 SS electrodes in all three cells. In general, the corrosion potentials of the test cell are slightly lower than those measured in the control and aerated cells, which is in agreement with the observation for Types 304L, 316, and 316L SS by Ringas and Robinson (1988a). It appears that the corrosion potentials measured from the three cells all decreased with time. This decrease was probably a result of the increase in solution pH (6.2 at the beginning for all cells and 8.8 for the test, 8.3 for the control, and 10.3 for the aerated cells at the end of the test).

(iv) Open-Circuit Potential—Figure 4-12 shows the open-circuit potentials (the steady-state rest potentials measured prior to the potentiodynamic polarization scans) obtained in the different cells for the two types of stainless steel electrodes. As expected, the open-circuit potentials measured in the aerated cell are significantly higher than those obtained in the other two cells because the other two cells were deaerated during the test. Similar to the observation made by Ringas and Robinson (1988a), open-circuit potentials measured from the test cell for the two types of stainless steel are consistently lower than those measured in the control cell even though both cells were deaerated using the same high-purity nitrogen. This difference is much larger than the values that would be caused by the slight difference between the pH in the two cells (8.3 in the control cell and 8.8 in the test cell). However, no apparent correlation between the sulfate-reducing bacteria count and the open-circuit potential of the stainless steel electrodes can be drawn from Figures 4-12 and 4-7.

(v) Anodic Currents—As discussed previously, the typical anodic behavior observed below the pit initiation potential during the forward potential scan in the test cell is significantly different from that in the other two cells (Figure 4-8). Anodic currents have been used as criteria to characterize sulfate-reducing bacteria-influenced corrosion for metals (Ringas and Robinson, 1988a). Other electrochemical methods and parameters have been suggested and used for evaluating the susceptibility of metallic materials to microbially influenced corrosion and monitoring its occurrence (Tuovinen and Cragnolino, 1986). Therefore, the following values were extracted from the polarization curves obtained in the test cell:

Maximum Passive Current (I_{ip}):	The current measured at a potential just below the pit initiation potential
Mean Passive Current (I_{mean}):	The average current for the region between the corrosion potential and the pit initiation potential
Peak Current (I_{pk}):	The peak value as shown in Figure 4-8

These values and the sulfate-reducing bacteria count are plotted in Figure 4-13. It is apparent that all these values, especially the peak current, correlate well with the sulfate-reducing bacteria count. Therefore, they are indications of either a high metal dissolution rate (or corrosion rate) catalyzed by the sulfate-reducing bacteria, as explained by many investigators

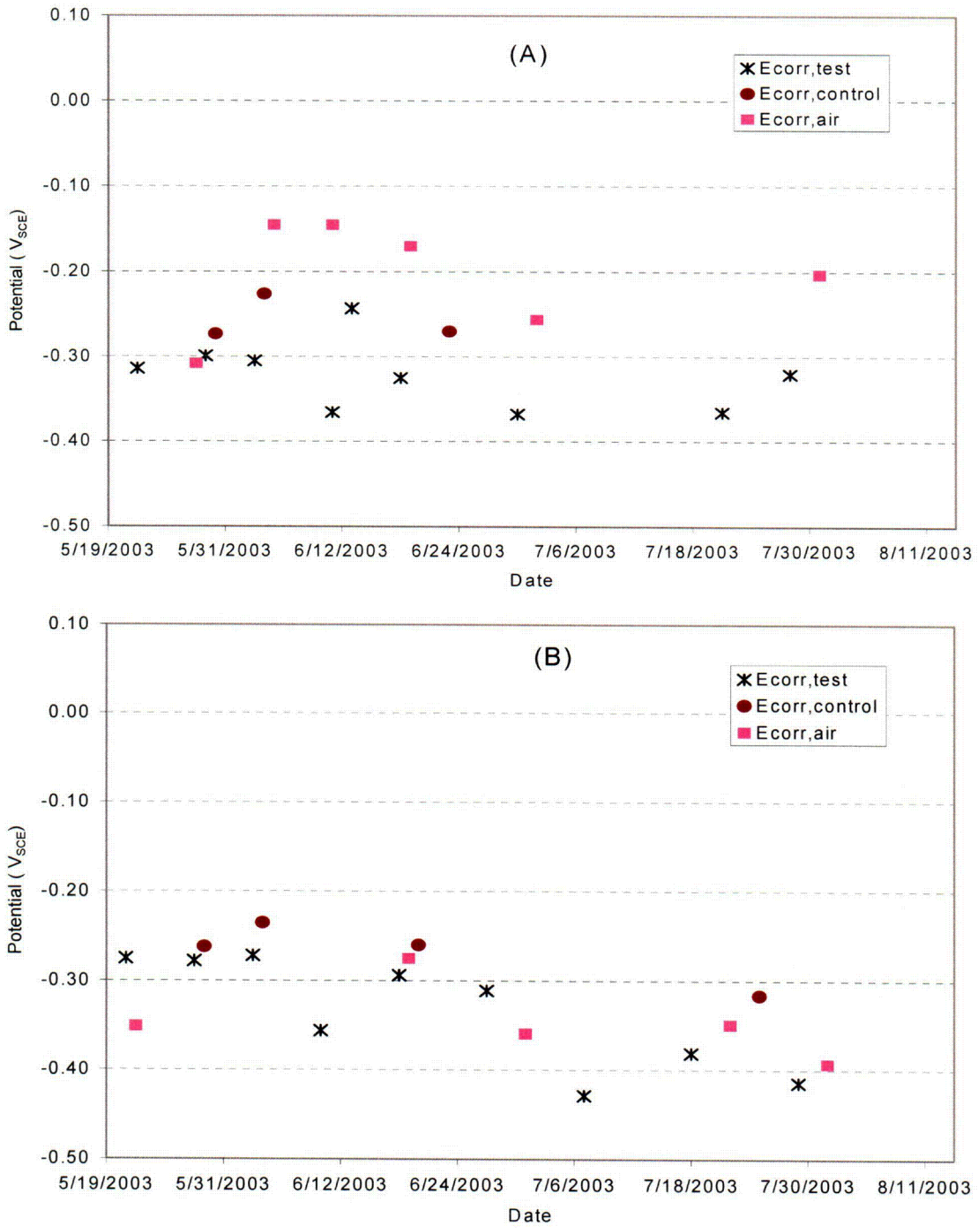

Figure 4-11. Corrosion Potentials for Types (A) 304L and (B) 304 SS Electrodes

C07

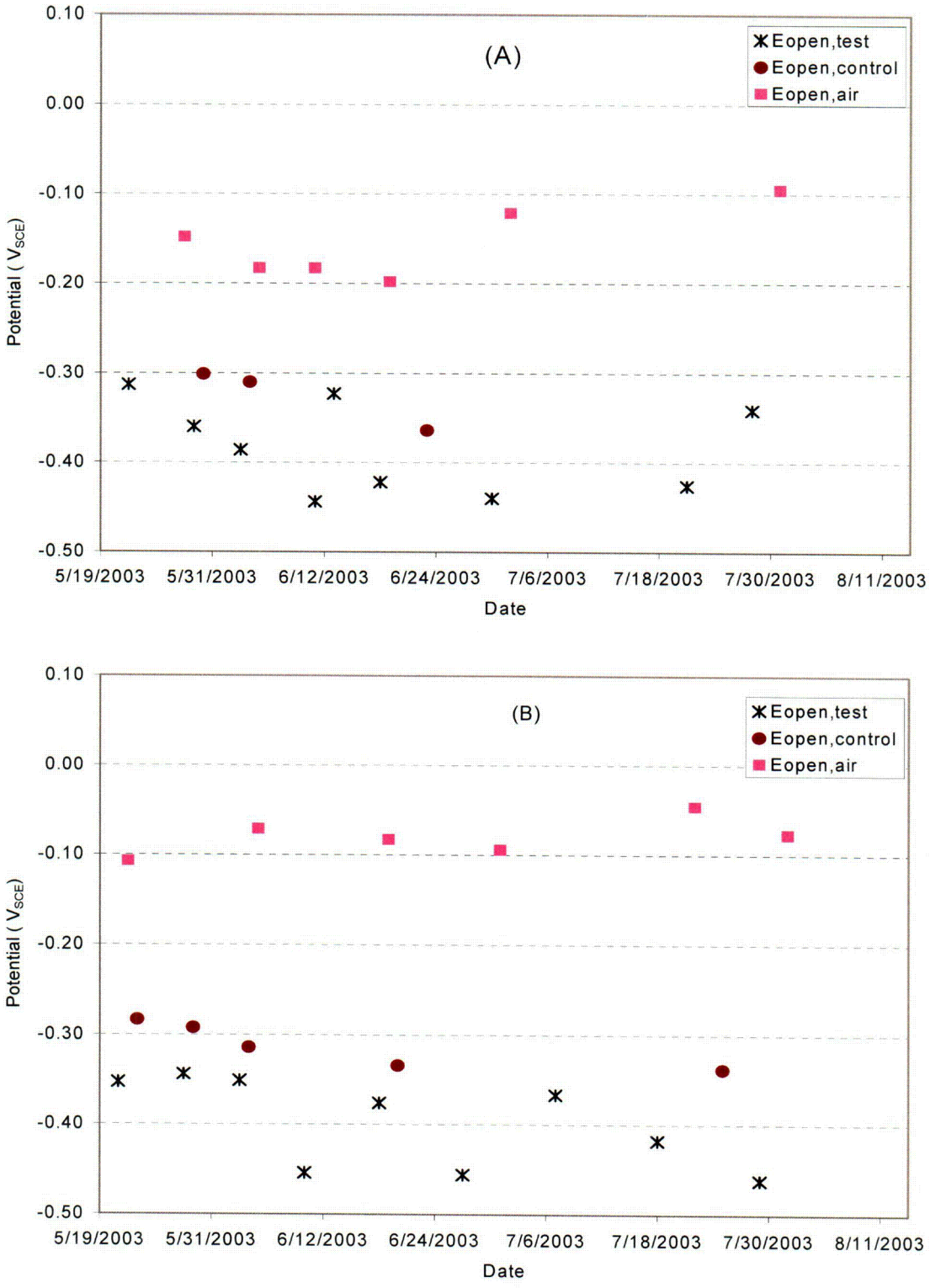

Figure 4-12. Open Circuit Potentials for Types (A) 304L and (B) 304 SS Electrodes

C08

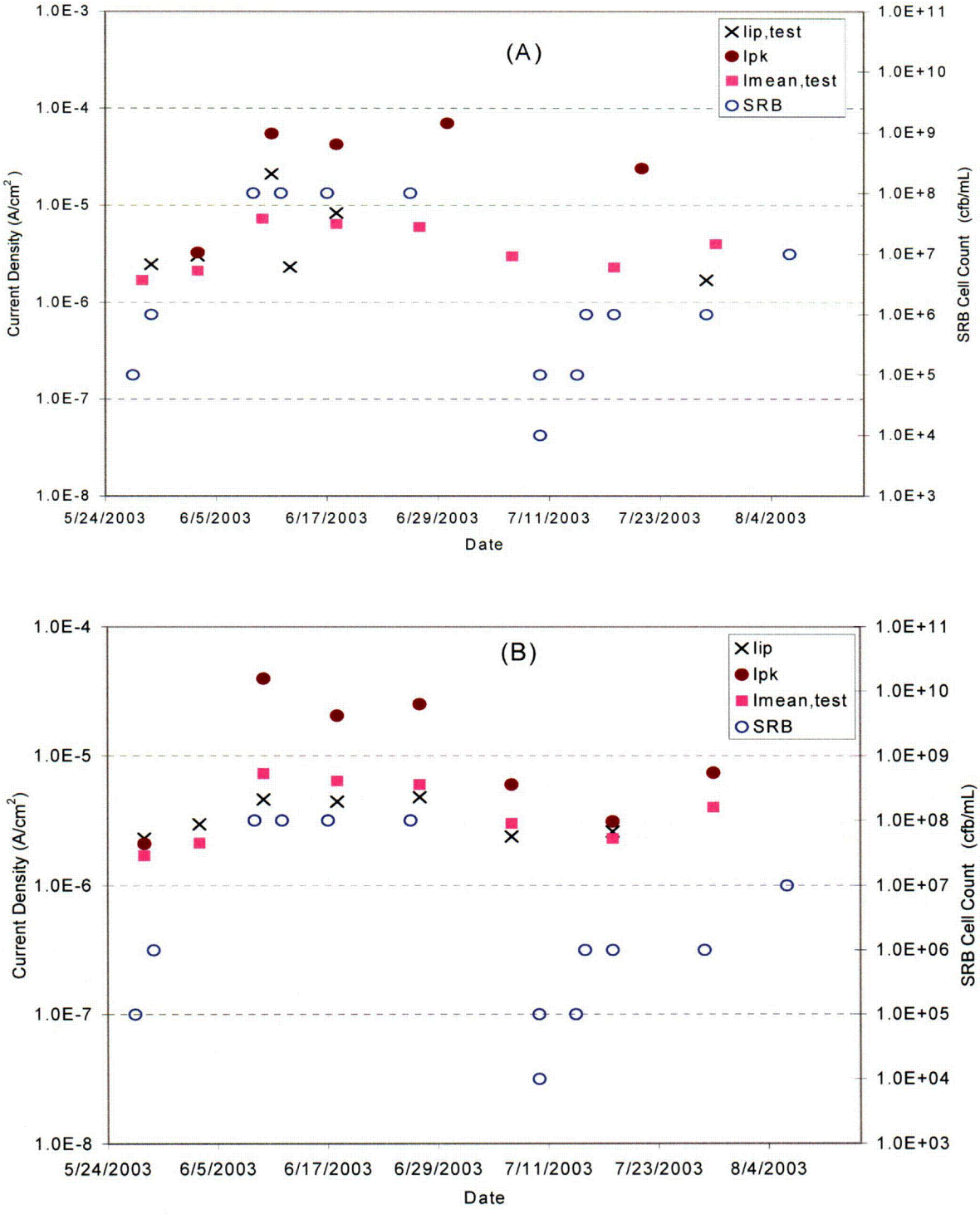

Figure 4-13. Anodic Polarization Currents Below the Pit Initiation Potentials for Types (A) 304L and (B) 304 SS Electrodes

NOTE: 1 A/cm^2 = 9.29 × 10^2 A/ft^2

C09

(Ringas and Robinson, 1988a; Webster, et al., 1990), or a high oxidation rate of certain reduced chemical species that were produced by the sulfate-reducing bacteria in the test cell.

4.2.1.3 Anodic Polarization Currents on Platinum Electrode and Immersion Time Effect on the Peak Currents

The potentiodynamic polarization curves for the Types 304 and 304L SS electrodes show a distinctive anodic peak at potentials above the corrosion potential and significantly higher anodic currents for the sulfate-reducing bacteria-containing test cell than for the sulfate-reducing bacteria-free control cell. The anodic galvanic current from the Type 304L SS plate electrode in the sulfate-reducing bacteria-containing test cell coupled to a large stainless steel cathode in the aerated cell is also slightly higher than those currents obtained in the sulfate-reducing bacteria-free control cell. However, no difference between the repassivation potentials measured from the two cells was observed. To understand the nature of the anodic peak and the high anodic current in the test cell when the sulfate-reducing bacteria count was high, potentiodynamic polarization tests were conducted using platinum electrodes. One platinum electrode was placed in the test cell, and the other was placed in the control cell at the start of the experiment.

Figure 4-14 shows that the anodic polarization curves obtained with the platinum electrodes in the two cells near the end of the experiment are similar to those obtained with the stainless steel plate electrodes (Figure 4-8). No anodic peak was observed with the platinum electrode in the control cell, but a distinctive anodic peak was apparent with the platinum electrode in the test cell at practically the same potential as the peak found on the stainless steel electrodes. Because the dissolution of platinum is unlikely, the peak in Figure 4-14 is probably caused by the oxidation of a chemical species, presumably produced by the sulfate-reducing bacteria. Therefore, it can be concluded that not all the anodic currents discussed in Section 4.2.1.2 for the stainless steel electrodes (peak current, pit initiation current, and mean passive current) were a result of the anodic dissolution. Instead, at least a fraction of each measured current value was a result of the oxidation of chemical species produced by sulfate-reducing bacteria in the test cell. The correlation between these currents and the sulfate-reducing bacteria count indicates that the amount of the reduced chemical species is proportional to the sulfate-reducing bacteria count.

Figure 4-15 shows the effect of the time interval between the potentiodynamic scans on the anodic polarization peak obtained with the platinum electrode in the test cell near the end of the experiment (near the end of August 2003, Figure 4-13). The peak current was approximately 1×10^{-4} A/cm^2 [9.29×10^{-2} A/ft^2] for the initial potentiodynamic polarization test conducted after the electrode was in the sulfate-reducing bacteria-containing solution for 3 months, whereas the peak current obtained 2 days after the first potentiodynamic polarization test was less than 1×10^{-5} A/cm^2 [9.29×10^{-3} A/ft^2]. The peak was not observed in the third scan conducted 5 minutes after the completion of the second scan (Figure 4-15). This observation suggests that the anodic peak is caused by the oxidation of a reducing chemical species accumulated on the surface of the platinum electrode by adsorption or chemical reaction during a considerable length of time in the presence of sulfate-reducing bacteria. The peak was not observed in the third scan because the species attached to the surface of the platinum electrode were oxidized during the second scan and did not have enough time to accumulate on the electrode surface before the start of the third scan.

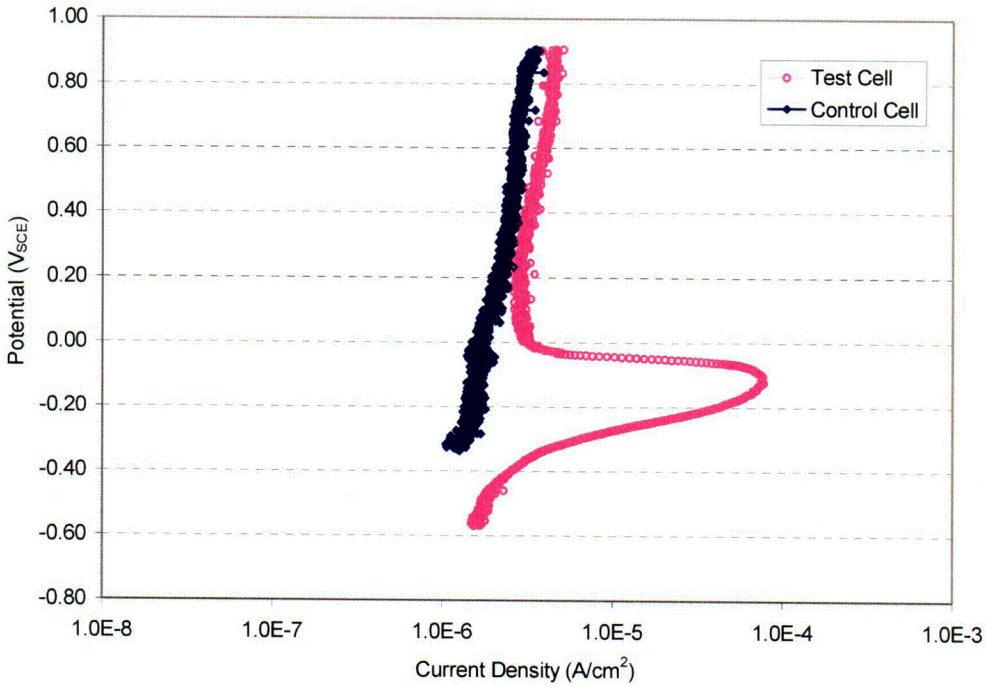

Figure 4-14. Differences Between the Typical Anodic Polarization Curves Obtained with Platinum Electrodes in the Test and in the Control Cells

NOTE: 1 A/cm^2 = 9.29 × 10^2 A/ft^2

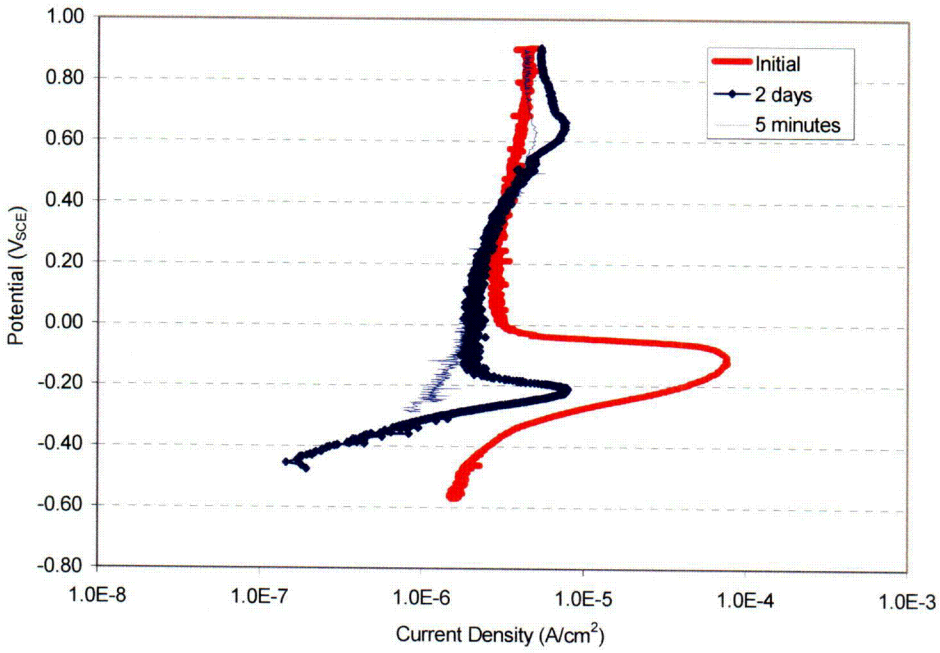

Figure 4-15. Effect of Time Interval Between Potentiodynamic Polarization Scans on the Anodic Peaks of the Polarization Curves Obtained with a Platinum Electrode. The Initial Scan Was Conducted After the Electrode Was in the Solution for 3 Months.

NOTE: 1 A/cm^2 = 9.29 × 10^2 A/ft^2

CID

4.2.1.4 Anodic Polarization Peak Currents on Stainless Steel Electrodes and Immersion Time Effect on the Peak Currents

Figure 4-16 shows the effect of the time interval between the potentiodynamic scans on the anodic peak of the polarization curve obtained with a Type 304L SS electrode in the test cell near the end of the experiment. As in Figure 4-15, the peak is high in the potentiodynamic polarization scan conducted 7 days after a previous potentiodynamic polarization scan on the same electrode. The peak disappeared in the second scan, which was conducted 15 minutes after completion of the first scan. Figures 4-15 and 4-16 suggest that the anodic peaks as shown in Figures 4-8 and 4-16 were at least partially caused by oxidation of reduced chemical species that were accumulated on the surface of the stainless steel electrode in the presence of sulfate-reducing bacteria. Adsorbed atomic sulfur or surface sulfides are suspected to be responsible for the peak currents because of their domain of stability in a potential-pH diagram for the iron-(nickel-)sulfur-water system (Marcus, 1995).

The slightly higher galvanic current obtained with the Type 304L SS electrode in the test cell compared to that in the control cell was probably also a result of the oxidation of the reducing species produced by the sulfate-reducing bacteria.

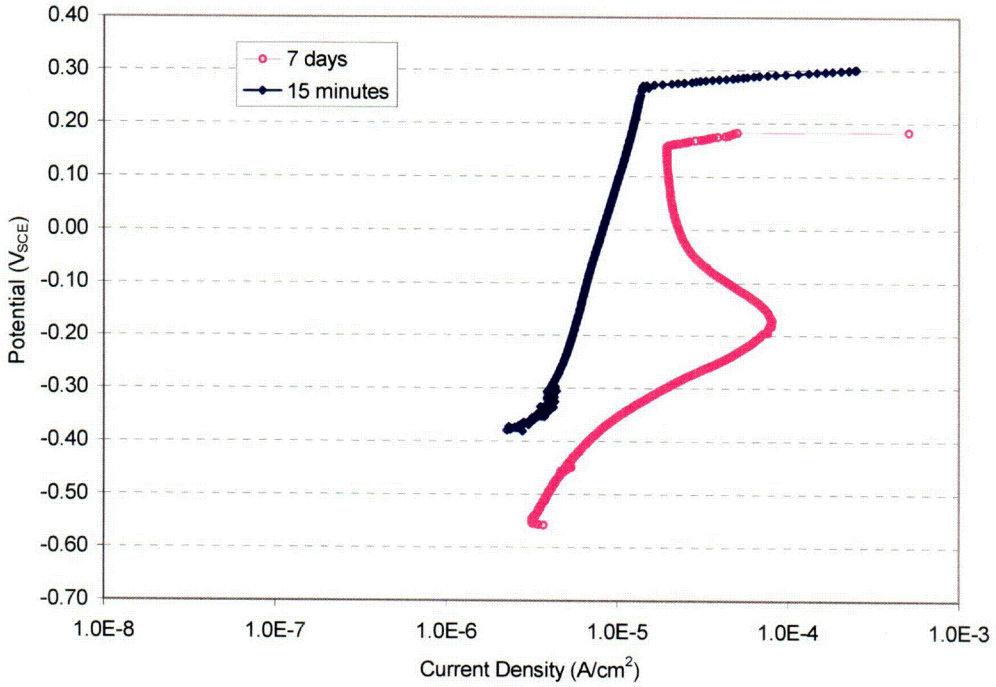

Figure 4-16. Typical Effect of Time Interval Between Potentiodynamic Polarization Scans on the Anodic Peaks of the Polarization Curves Obtained with a Stainless Steel Electrode

NOTE: 1 A/cm^2 = 9.29 × 10^2 A/ft^2

C11

4.2.1.5 Immersion Studies

It appears that the results from the electrochemical tests reported previously, especially the repassivation potential measurement and anodic current results, are in disagreement with the observation of pitting corrosion reported by Rao and Satpathy (2000) and Ringas and Robinson (1988b) for stainless steel exposed to sulfate-reducing bacteria-containing solutions. The open-circuit potentials of the stainless steel specimens lay between -0.13 and -0.43 V_{SCE} in the work by Rao and Satpathy (2000) and below -0.30 V_{SCE} in the work by Ringas and Robinson (1988b). Both teams employed a semicontinuous mode of sulfate-reducing bacteria growth, which is similar to the procedure used in the present study. The medium used in the test by Ringas and Robinson (1988b) did not contain dissolved iron. They observed pitting corrosion on Types 304L, 316, and 316L SS specimens after a 4-month exposure at 30 °C [86 °F]. Rao and Satpathy (2000) noted pitting corrosion on a Type 304 SS specimen after a 25-day exposure. It should be emphasized that no chloride, which promotes localized corrosion, was added in either of the studies. To confirm these observations and understand why no localized corrosion was observed in the short-term tests in 0.5-M NaCl solution, a long-term total immersion test was conducted in a separate flask containing 0.5-M NaCl solution inoculated with the same sulfate-reducing bacteria and slime former used for the short-term tests. Additional studies to confirm the results obtained by Ringas and Robinson (1988b) were conducted in chloride-lean solutions (see Section 4.2.2). The specimen was a Type 304L SS plate that has the same dimension as the stainless steel plate electrode specimen {1.27 by 5.08 by 0.21-cm [0.5 by 2 by 0.0827-in] thickness}. The coupon was totally immersed in the flask, horizontally lying at the bottom of the glass flask during the test in a similar orientation as Figure 4-1 used by Lian, et al. (1999b). As in the test cell shown in Figure 4-4, a nitrogen flow was maintained over the gas space above the liquid level. No electrochemical potential was measured, but it is expected to be lower than -0.3 V_{SCE} according to Figure 4-12. At the end of the test period, the coupon was removed from the flask and stabilized in preparation for scanning electron microscopy following the protocol outlined by Goldstein, et al. (1992), as described in the following paragraphs.

Each sample was immersed into a 2-percent solution of glutaraldehyde in 0.1-M sodium cacodylate (pH = 7.2) at room temperature for a minimum of 12 hours. Following fixation in the glutaraldehyde/cacodylic acid solution, samples were dehydrated in a two-step process whereby liquid water was replaced using a graded ethanol series followed by critical point drying. The percentage of ethyl alcohol used and the durations of exposure were as follows: 25 percent for 30 minutes, 50 percent for 30 minutes, 75 percent for 30 minutes, 100 percent for 30 minutes, and fresh 100 percent for storage.

Critical point drying is based upon the concept that a two-phase state of the majority of volatile liquids (vapor and liquid) vaporizes at a certain temperature and pressure, the so-called critical point. At the critical point for carbon dioxide {31 °C [88 °F] and 1,072 psi [7.39 MPa]}, the liquid and vapor phases are in equilibrium and can coexist. Therefore, the phase boundary disappears, and there is no surface tension between the phases. Drying can proceed without cell disruption.

Within the confines of a high-pressure critical point drying apparatus (Pelco CPD2 Critical Point Dryer), each specimen is passed from 100-percent ethyl alcohol into liquid carbon dioxide, which served as the transitional fluid. In the critical point drying device, liquid carbon dioxide is forced under pressure into the bacterial cells on the metal samples, and the ethyl alcohol is expelled

and vented. After venting the alcohol, the system is closed, and temperature and pressure are raised to the critical point for carbon dioxide. After several minutes at the critical point, the system is slowly vented to allow carbon dioxide gas to escape, thus leaving a stable, dehydrated specimen that retains the structural integrity of its biologic components and is suitable for scanning electron microscopy.

Scanning electron microscopy was performed using a JEOL 840A SEM coupled with an Oxford Instruments energy-dispersive X-ray detector. X-ray data were processed using the Oxford Instruments INCA X-ray analysis software package. A nonquantitative survey of the Type 304 L SS specimen revealed numerous pits near the edge of the specimen. Figure 4-17 shows a typical pit {approximately 50 μm [1.97×10^{-3} in] in diameter} that developed on the specimen surface 157 days after the exposure in a 0.5-M NaCl solution inoculated with sulfate-reducing bacteria and a slime former. Figure 4-17 also shows that the bacteria are clearly visible in a closeup view near the pit center area. This immersion test was conducted during nutrient lean conditions with a long period of no nutrient addition. As such, survival of the bacteria may have been concentrated within pits where large concentrations of cells are visible [Figure 4-17(b)]. The results from the 157-day immersion test confirm that pitting corrosion occurred even though the electrochemical repassivation test results did not indicate it should occur.

4.2.2 Studies in Sulfate-Containing Solutions Inoculated with Sulfate-Reducing Bacteria

As mentioned in Section 4.2.1, pitting corrosion was observed by Rao and Satpathy (2000) and Ringas and Robinson (1988b) on stainless steel specimens exposed to low-chloride solutions inoculated with sulfate-reducing bacteria. No additional chloride was used in these studies with the exception of the chloride contained in the media used for microbial growth. To understand how pitting corrosion of stainless steel specimens occurred in solutions containing low chloride and iron contents, the immersion test conducted by Ringas and Robinson (1988b) was repeated. The test vessel is essentially the same as the test vessel shown in Figure 4-4, with the exception that the salt bridge was eliminated. Type 304L SS plates and Type 304 SS wires, identical to those shown in Figure 4-4, were vertically immersed in the test vessel containing only the medium (Table 4-7) used to grow the sulfate-reducing bacteria. The total concentrations of sulfate, biphosphate, and chloride in the fresh medium were 2,460, 273, and 222 ppm, by weight. The concentration of sulfate was expected to decrease during the test because of the conversion to sulfides and other intermediate sulfur species by the sulfate-reducing bacteria. No slime former was introduced in this test. A small nitrogen flow was maintained over the gas space above the liquid to exclude air.

The average open circuit potentials of the stainless steel specimens and the redox potential on a platinum electrode were measured during the immersion tests (Figure 4-18). The open-circuit potentials of the stainless steel specimens were below $-0.1\ V_{SCE}$ throughout the test period. The platinum potential was below $-0.3\ V_{SCE}$ after the solution was inoculated with the sulfate-reducing bacteria, indicating that the system was under reducing conditions.

The planktonic bacteria count of the sulfate-reducing bacteria was quantified using serial dilution and a five-tube most probable number method (Collins, et al., 2004). Hydrogen sulfide was analyzed using the U.S. Environmental Protection Agency (EPA)-approved methylene blue

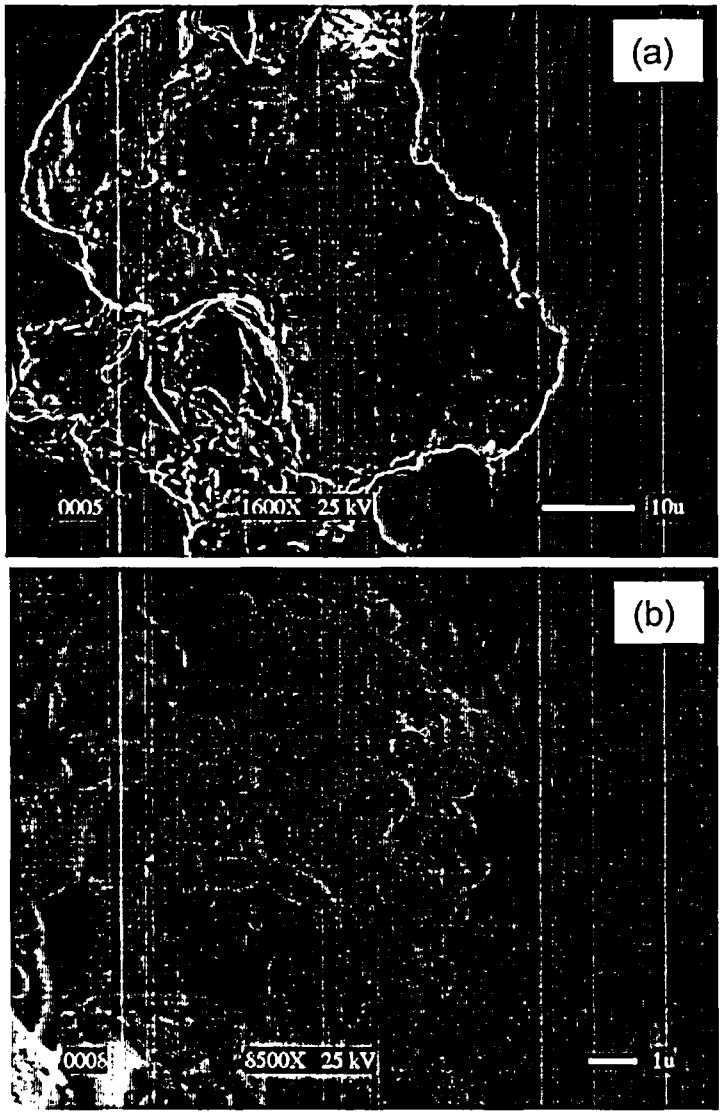

Figure 4-17. A Typical Pit Developed on the Type 304L SS Specimen Surface for 157 Days After the Exposure in a 0.5-M NaCl Solution Inoculated with Sulfate-Reducing Bacteria and a Slime Former (a). A Closeup View at the Pit Center Area Showing Bacteria Cells Clearly Visible (b).

Table 4-7. Ringas Media A*	
Sodium Lactate	7.0 g†
Beef Extract	1.0 g
Peptone	2.0 g
$MgSO_4 7H_2O$	2.0 g
Na_2SO_4	1.5 g
K_2HPO_4	0.5 g
Distilled Water	1000 mL‡
Thoroughly mix above ingredients; autoclave for 15 minutes at 120 °C [248 °F]	
The following heat-sensitive components are prepared separately by dissolving reagents in 100 mL [0.34 oz] distilled water and filter sterilizing.	
Sodium Ascorbate	2.10 g/100 mL
Ammonium Sulfate	2.64 g/100 mL
Prior to inoculation, aseptically add 5.0 mL [0.017 oz] of the sodium ascorbate solution and 5.0 mL [0.017 oz] of the ammonium sulfate solution per liter of media.	

*Ringas, C. and F.P.A. Robinson. "Corrosion of Stainless Steel by Sulfate-Reducing Bacteria-Electrochemical Techniques." *Corrosion*. Vol. 44. pp. 386–396. 1988.
†1 lb = 454 gm
‡1 $ft^3 = 28.32 \times 10^3$ mL

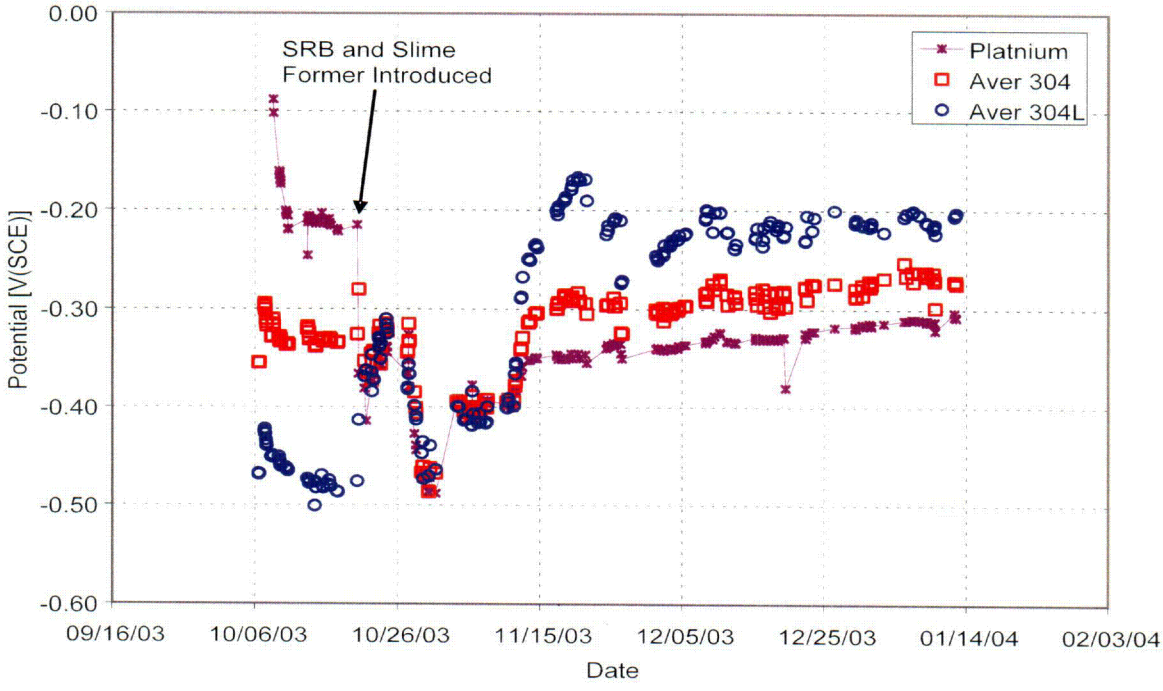

Figure 4-18. Average Open Circuit Potentials of Type 304 and 304L SS Specimens and the Redox Potential of Platinum in the Solution During the Immersion Test

C12

method adapted by HACH as HACH method 8131,[2] and a HACH DR 890 colorimeter. The HACH adaptation is equivalent to EPA method 376.2 or the Standard Method 4500-S^{2-} D for wastewater. The sulfide concentration and the sulfate-reducing bacteria counts are shown in Figure 4-19. The hydrogen sulfide concentration was between 100 and 300 mg/L [2.9 and 8.81mM]. The bacteria count was between 1×10^7 and 2×10^9 cfu/mL [2.94×10^7 and 5.88×10^9. The pH was measured during the test, and the values varied between 7.5 and 8.2. The iron content measured near the end of the test was less than 0.25 mg/L [0.25 ppm by weight].

4.2.2.1 Electrochemical Studies

At the end of the test (between January 18 and January 26, 2004, on Figures 4-18 and 4-19), some of the specimens were used as electrodes for repassivation measurements (see Section 4.2.1). Figure 4-20 shows typical polarization curves obtained using the modified Akashi, et al. (1998) method during the repassivation measurements. Unlike the curves obtained in the chloride-containing solutions inoculated with sulfate-reducing bacteria (see Section 4.2.1), Figure 4-20 appears to indicate that the stainless steel specimens were not susceptible to localized corrosion even at potentials near 1.2 V_{SCE}. However, the anodic current curves during the forward scan are similar to those obtained in the chloride-containing solutions. The anodic currents were high at potentials above 0.0 V_{SCE}. There seems to be an anodic peak at 0.05 V_{SCE} from one of the curves. However, this peak was not observed in the second curve because the anodic peak current density exceeded the maximum allowed current density. The maximum current density was limited to 1.73×10^{-5} A/cm^2 [1.61×10^{-2} A/ft^2] to be consistent and to compare with the repassivation curves obtained using the modified Akashi, et al. (1998) method (see Section 4.2.1). According to the discussion in Section 4.2.1, these high anodic current values observed during the forward scan were caused by the oxidation of the reducing species produced by the bacteria. Ringas and Robinson (1988a) also observed similar anodic curves (with similar peaks) on several alloys, including Type 316 SS, but they attributed the high current to the corrosion of metals.

4.2.2.2 Immersion Studies

The specimens that were not subject to anodic polarization were removed at the end of the test and prepared for scanning electron microscopy analysis as previously described in Section 4.2.1. Numerous pits were formed on the specimen. Figure 4-21 shows that pits {approximately 50 µm [1.97×10^{-3} in] in diameter} were developed on the Type 304L SS specimen surface 98 days after the exposure in the sulfate-containing and chloride-lean solution inoculated with sulfate-reducing bacteria. Bacteria cells on the surfaces inside the pit are clearly visible. Figure 4-21 confirms the localized corrosion observed by Ringas and Robinson (1988b) in the sulfate-containing solution, even though the repassivation potential measurement results suggest that absence of localized corrosion should be expected.

4.2.3 Studies in Solutions Containing Pure Sulfur Species

Reduced sulfur species are considered to be responsible for the enhanced corrosion caused by the sulfate-reducing bacteria (Webster, et al., 1990; Thierry and Sand, 1995; Tuovinen and

---

[2]HACH Company. "Data Logging Colorimeter Handbook." DR820–DR850–DR890. Loveland, Colorado: HACH Company. pp. 495–498.

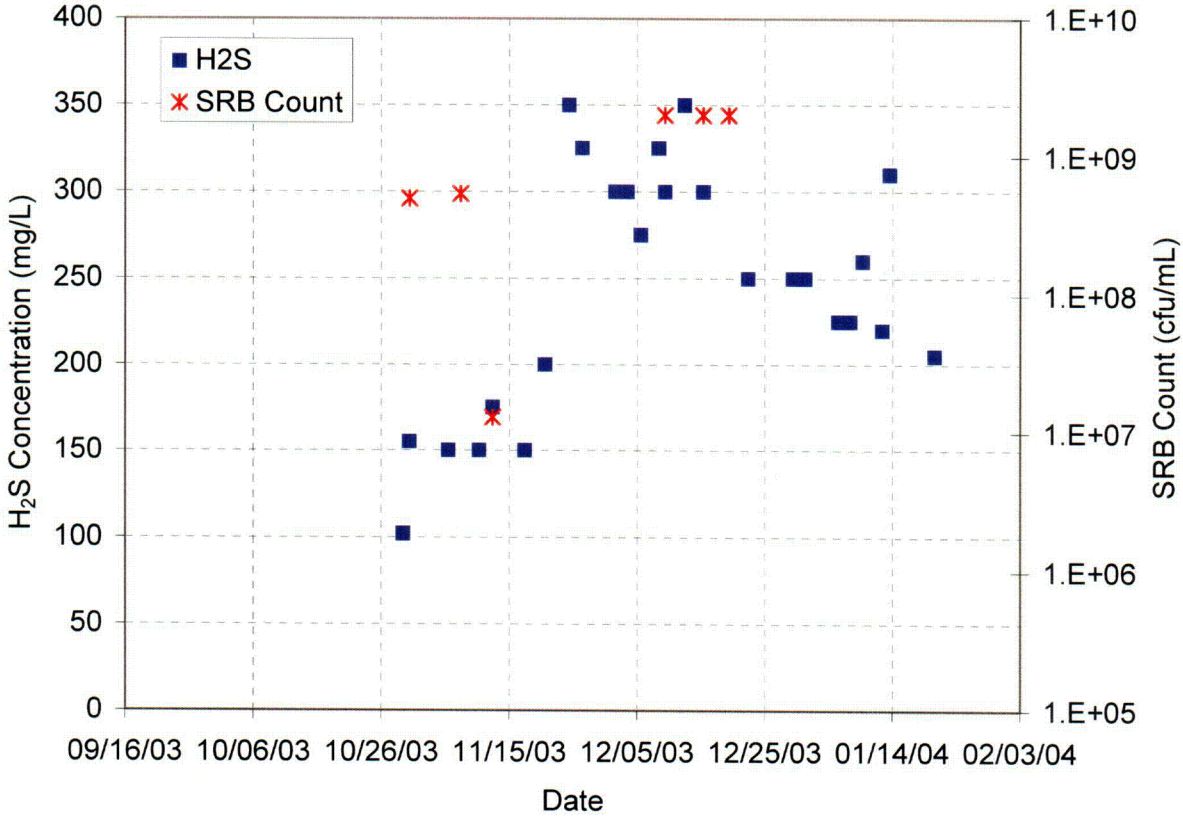

Figure 4-19. Hydrogen Sulfide Concentration and Sulfate-Reducing Bacteria Count During the Immersion Test

Cragnolino, 1986). To understand the microbially influenced corrosion observed in the laboratory and the electrochemical polarization behavior of the stainless steel specimens in the solutions containing sulfate-reducing bacteria, electrochemical studies were performed on platinum electrode and stainless steel specimens in solutions containing pure sulfur species such as H_2S, Na_2S, S^0 (elemental sulfur), and $Na_2S_2O_3$. The electrochemical cells used in these tests were similar to the test cell shown in Figure 4-4, except there was no salt bridge and no coupling to the cathode in the aerated cell. The Na_2S and $Na_2S_2O_3$ solutions were prepared using reagent chemicals. These solutions were continuously purged with pure nitrogen during the electrochemical tests. The H_2S and S^0 solutions were presaturated by the suppliers. The H_2S concentration in the presaturated solution was measured (using the methylene blue method)[3] to be 13.2 mM [450 mg/L]. The concentration of the dissolved elemental sulfur was 0.312 M [10,000 ppm] in the presaturated S^0 solution. These presaturated solutions were not purged because the purging with nitrogen gas may change the concentration of the dissolved H_2S or S^0 in the solutions. Therefore, these solutions are presumably saturated with air. Because the present studies are mainly focused on the anodic processes, the effect of oxygen in the ambient air may not be a concern. A NaOH solution was used to adjust the pH of the H_2S solution from 3.5 to near neutral, and a HCl solution was used to adjust the pH of the Na_2S solution from 11.5 to near neutral.

[3]Ibid.

C13

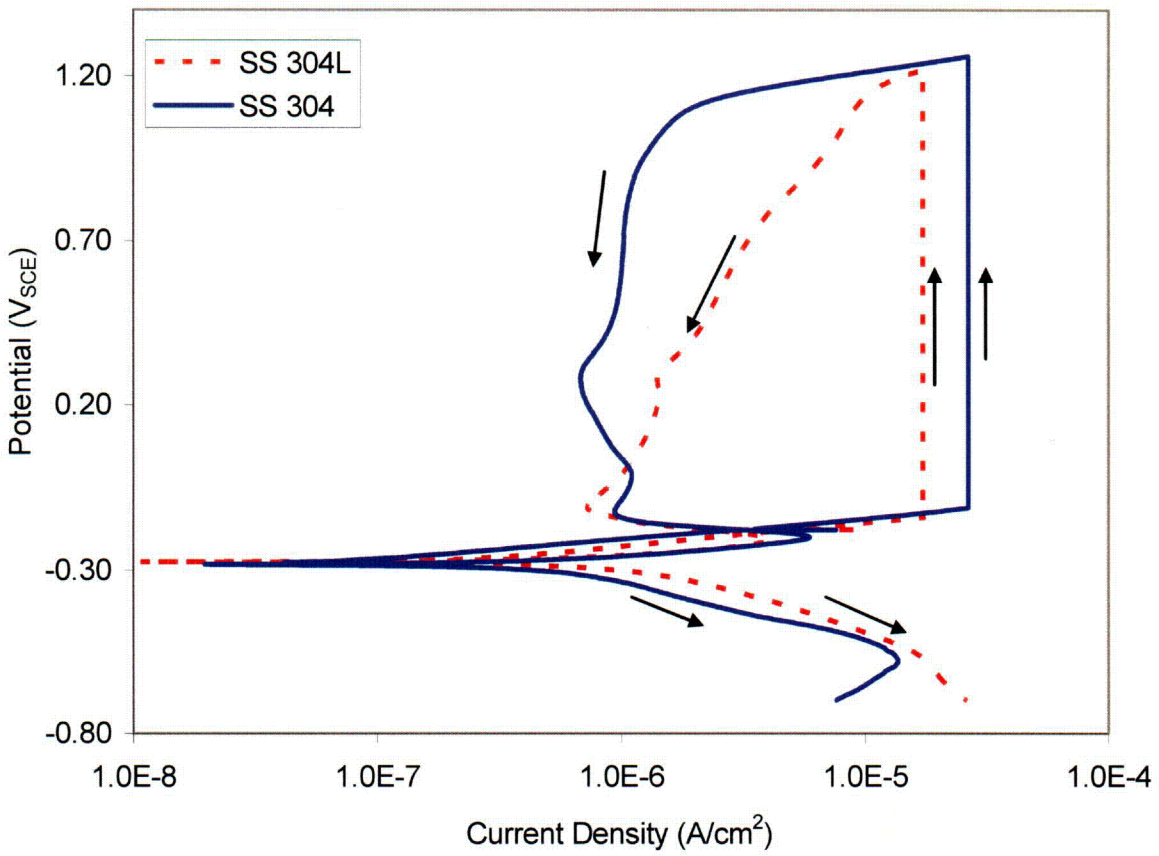

Figure 4-20. Polarization Curves Obtained Using Modified Akashi Method for Stainless Steels in a Sulfate-Containing Solution Inoculated with Sulfate-Reducing Bacteria. The Anodic Curves Reached the Specified Maximum Current Density (1.73×10^{-5} and 2.65×10^{-5} A/cm^2) at Potentials Approximately 0.15 V above the Open Circuit Potentials (Approximately -0.28 V_{SCE}) During the Forward Scan. The Anodic Peak Currents of the Forward Scan Curves Did Not Appear But Are Higher Than the Maximum Current Density Specified for the Tests.

NOTE: 1 A/cm^2 = 9.29×10^2 A/ft^2

4.2.3.1 Polarization Behaviors on Platinum Electrodes

Figure 4-22 shows the current density versus voltage curves on platinum electrodes in 0.5-M NaCl solutions containing the pure elemental sulfur and sulfur-containing species. The electrodes were polarized in the same manner as the stainless steel electrodes in the repassivation potential measurements (described in Section 4.2.1). Both the forward- and backward-scan anodic curves are close to each other in the Na_2S and the $N_2S_2O_3$ solutions, indicating little surface effects. The forward-scan curve was significantly different from the backward-scan curve in the H_2S {13.2 mM [440 ppm by weight]}. There was an anodic peak at approximately -0.2 V_{SCE}. The current of the backward-scan curve is significantly lower than that of the forward-scan curve at potentials below 0.4 V_{SCE}. Comparison between the anodic curve obtained with the platinum electrode in the H_2S solution and those obtained in the solution containing sulfate-reducing bacteria (Section 4.2.1) suggests that the anodic peak currents

C14

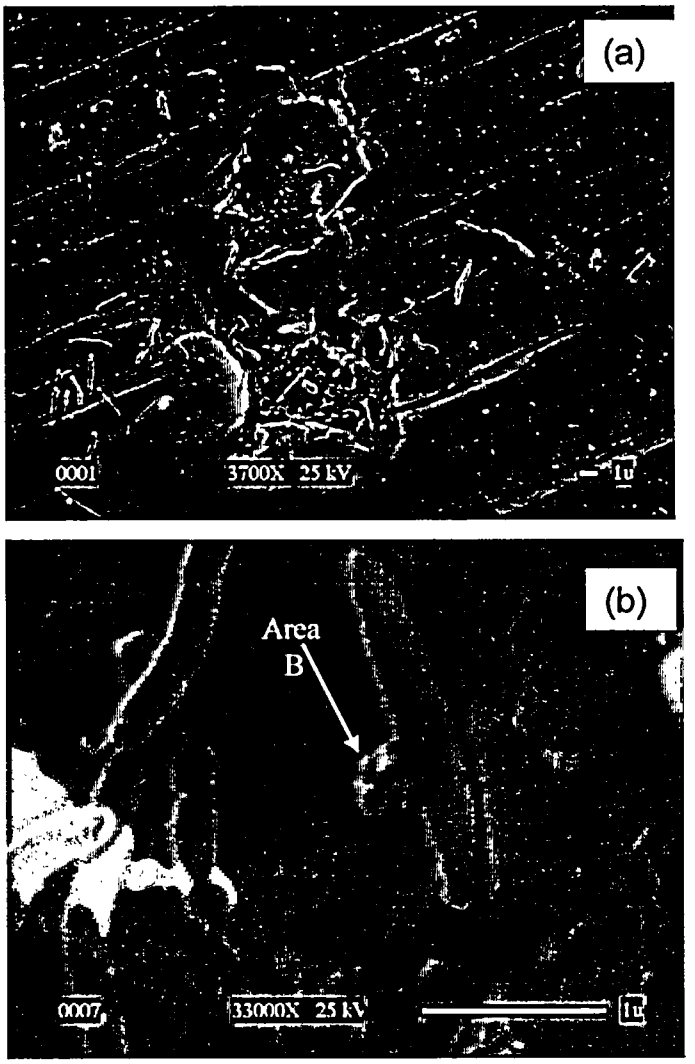

Figure 4-21. (a) Typical Pits Developed on the Type 304L SS Specimen Surface 93 Days After the Exposure in a Sulfate-Containing Solution Inoculated with a Sulfate-Reducing Bacteria, (b) a Closeup View at the Upper Right Corner of the Lower Pit Showing Bacteria Cells Clearly Visible. Sulfide Was Detected at Area B of (b) by Energy Dispersive X-Ray Spectroscopy.

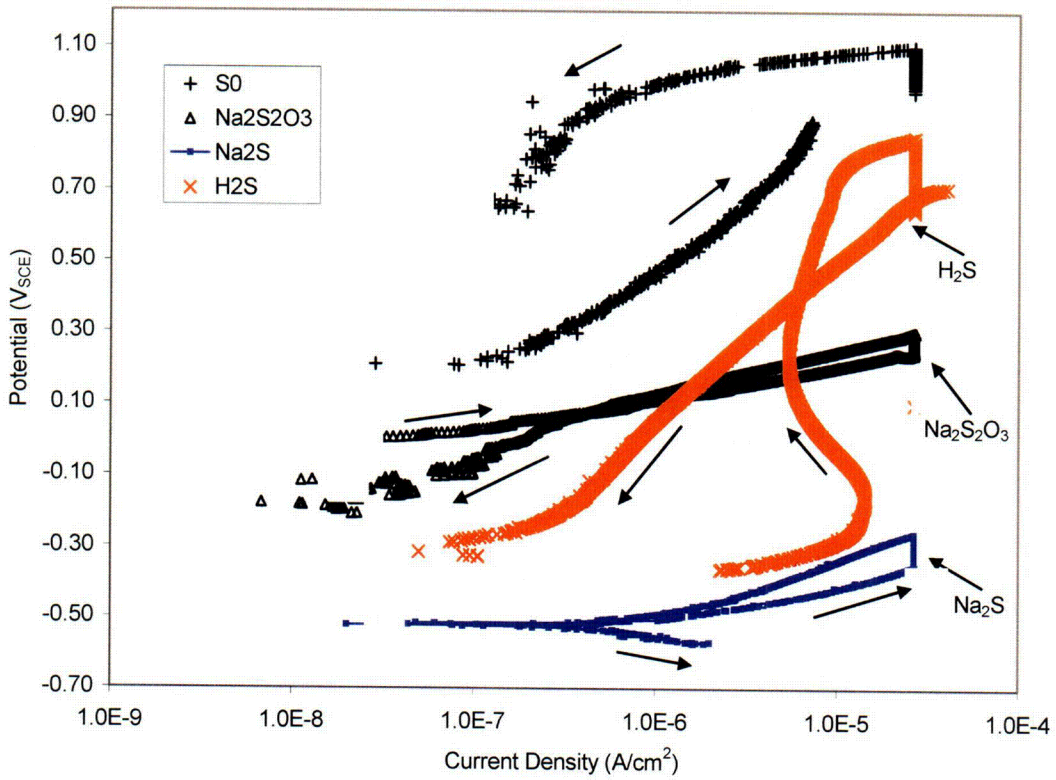

Figure 4-22. Polarization Behavior Obtained Using the Akashi Method for Platinum Electrodes in Solutions Containing Pure Sulfur Element and Sulfur-Containing Species. Ambient Air May Be Present in the Tests with H_2S and Element Sulfur.

NOTE: 1 A/cm^2 = 9.29 × 10^2 A/ft^2

observed in the solution containing sulfate-reducing bacteria was a result of the surface species formed on the platinum electrode in the presence of H_2S. Such surface species are probably adsorbed H_2S.

Anodic current density above 10^{-7} A/cm^2 [9.3 × 10^{-5}/ft^2] was observed in the presence of 0.312-M dissolved elemental sulfur only at high potentials (above 01. V_{SCE}). Compared with the potential-pH diagram for the adsorbed atomic sulfur on the nickel, iron, and chromium metal surfaces (Marcus, 1995), the anodic polarization curve measured in this study in the presence of elemental sulfur suggests that a large overpotential is required to form adsorbed atomic sulfur in aqueous solutions at room temperatures. It appears that the rupture of the chemical bonds in the S_8 molecule of elemental sulfur (Cotton and Wilkinson, 1980) to form adsorbed atomic sulfur is a highly activated process.

4.2.3.2 Polarization Behaviors on Stainless Steel Electrodes

Figure 4-23 shows typical current density versus voltage curves on the stainless steel specimens obtained during the repassivation potential measurements in the 0.5-M NaCl solutions containing pure elemental sulfur and sulfur-containing species. All curves in Figure 4-23 show that localized corrosion was initiated during the forward scan or during the constant current hold at the

C15

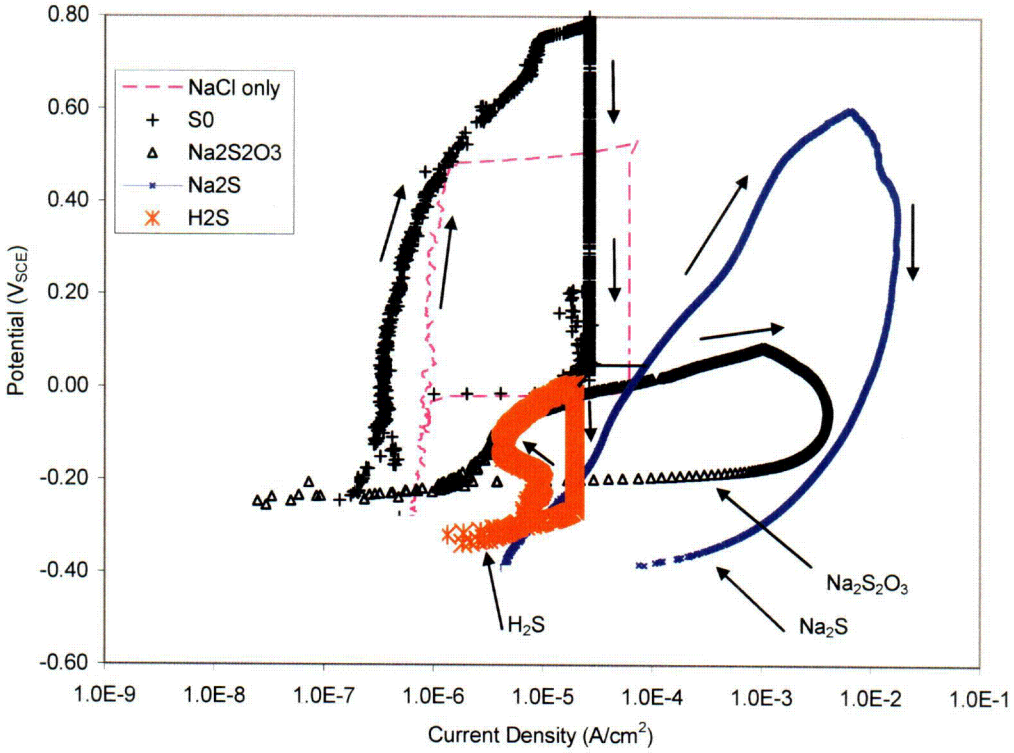

Figure 4-23. Polarization Behaviors Obtained Using the Modified Akashi Method for Stainless Steel Specimens in Solutions Containing Pure Sulfur Element and Sulfur-Containing Species. Note: The Curves for $Na_2S_2O_3$ and Na_2S Were Obtained in a Preliminary Study Using Cyclic Potentiodynamic Polarization Method (Jain, et al., 2003).

NOTE: 1 A/cm^2 = 9.29 × 10^2 A/ft^2

specified current values before the backward scan. According to the results shown in Figure 4-23, the repassivation potentials in the different solutions are presented in Figure 4-24. The repassivation potential was significantly lowered by Na_2S and H_2S and slightly lowered by $Na_2S_2O_3$. The decreased potential is consistent with the phenomena observed by other investigators (Newman, et al., 1982; Rhodes, 2001). However, no effect of dissolved elemental sulfur was observed, which may be the result of the high activation energy for elemental sulfur to dissociate and to be adsorbed as atomic sulfur on the electrodes at room temperature.

By comparing the anodic curves shown in Figure 4-23 for the stainless steel electrodes with those obtained in the solutions containing sulfate-reducing bacteria (Sections 4.2.1 and 4.2.2), it appeared that the anodic peak currents observed in the solutions containing sulfate-reducing bacteria were a result of the surface species formed on the stainless steel electrode in the presence of H_2S.

The lowered repassivation potentials caused by H_2S, which is one of the reduced sulfur species produced by sulfate-reducing bacteria, may confirm why localized corrosion attack was observed in the solutions containing chloride and hydrogen sulfide (Figure 4-17) produced by sulfate-reducing bacteria. Although the solution in the tests shown in Figure 4-24 contains a high chloride concentration, Newman, et al. (1986) observed that 0.003 M (HS + H_2S) would cause

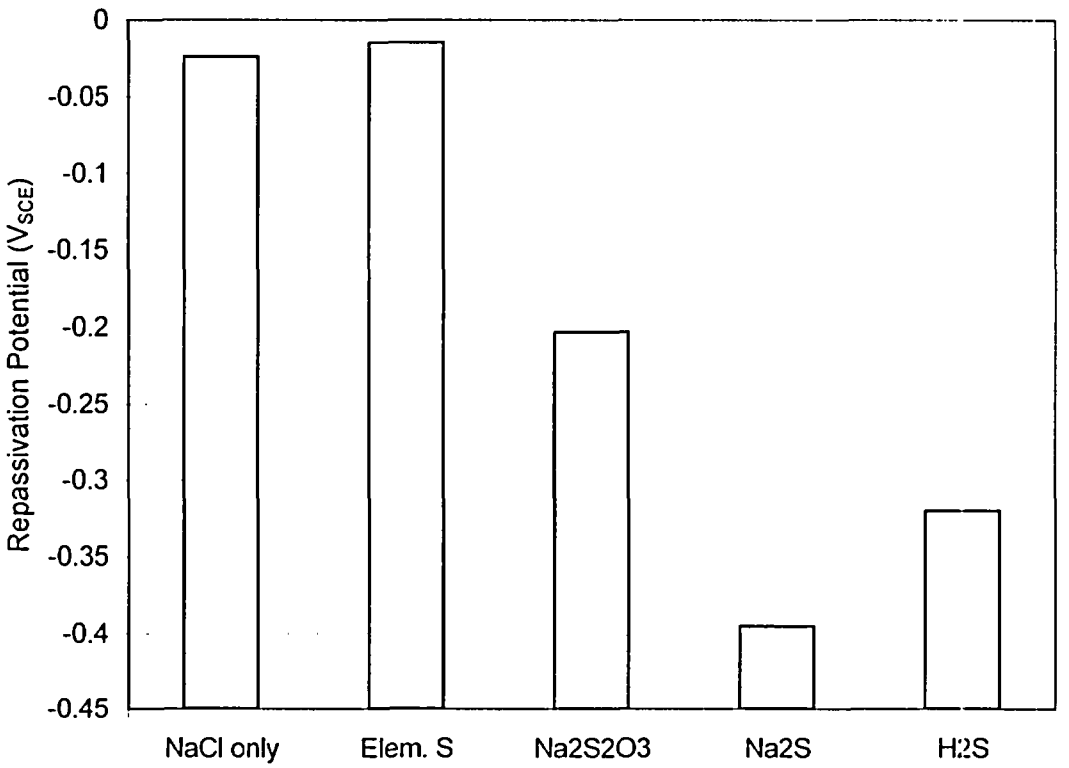

Figure 4-24. Repassivation Potentials of Stainless Steel in Different Solutions

Type 304 SS to pit in the presence of sulfate (0.018 M SO_4^{2-}) after being exposed to air for 7 days at 50 °C [122 °F]. They concluded that pitting corrosion was caused by thiosulfate ($S_2O_3^{-}$), which is a major product of the oxidation of H_2S by oxygen. They also concluded from another study (Newman, et al., 1989), that thiosulfate causes the Type 304 SS to pit as long as there is enough sulfate (even without the presence of chloride), chloride, or the combination of sulfate and chloride. The criteria they derived for pitting of the Type 304 SS to occur was the molar ratio of $[(SO_4^{-} + Cl^{-})/S_2O_3]$ = 10 to 30. The pitting corrosion in the sulfate-containing solution inoculated with sulfate-reducing bacteria is consistent with the observations by Newman, et al. (1986, 1989).

4.3 Repassivation Potential as a Localized Corrosion Susceptibility Criteria in Microbial Environments

Table 4-8 shows that the maximum peak current measured during the forward scan with the Types 304 and 304L SS and platinum electrodes is 3.41×10^{5} A/cm^2 [3.2×10^{-2} A/ft^2] in a solution containing 450 mg/L [450 ppm by weight] of H_2S. The maximum peak current density measured with the stainless steel specimens and the platinum electrode in solutions containing sulfate-reducing bacteria during the forward scan was 1×10^{4} A/cm^2 [9.3×10^{2} A/ft^2] (Figures 4-14 to 4-16). According to Section 4.2.1, the bulk concentration of the dissolved H_2S in the solution containing sulfate-reducing bacteria could be estimated at 100 to 300 mg/L [100 to 300 ppm by weight]. Therefore, the adsorbed H_2S on the metals seems to be higher in the biotic solutions than that in the abiotic solutions containing an even higher amount of dissolved H_2S, suggesting that sulfate-reducing bacteria tend to colonize on the metal surfaces and produce

Table 4-8. Anodic Peak Currents Observed on Different Electrodes in Solutions Containing H_2S				
Cl^- (M)	H_2S (mM)	Electrode	Peak Current (A/cm^2) [A/ft^2]	pH Adjustment
0	1.32	SS 304	1.45×10^{-5} [1.35×10^{-2}]	pH not adjusted (pH = 3 to 4.7)
0	1.32	SS 304L	5.40×10^{-6} [5.02×10^{-3}]	—
0	13.24	SS 304L	3.41×10^{-5} [3.17×10^{-2}]	—
0.5	13.24	Pt	1.42×10^{-5} [1.32×10^{-2}]	NaOH added (pH = 7 to 8.8)
0.5	13.24	SS 304L	9.70×10^{-6} [9.01×10^{-3}]	—
1	13.24	Pt	2.16×10^{-5} [2.01×10^{-2}]	—
1	13.24	SS 304	8.18×10^{-6} [7.6×10^{-3}]	—

more H_2S on or near the metal surface than in the bulk solution. This phenomenon may occur because enzymes used in microbial metabolism are located in the cell envelope, and bacteria can make direct contact between the enzyme and metal surface (Ehrlich, 2002). However, this adsorbed H_2S could be oxidized during the forward scan or during the anodic constant current hold period used in the repassivation potential measurement. By the time the potential was decreased, presumably the H_2S was no longer adsorbed on the electrode to affect the repassivation potential. Because the bulk concentration of the H_2S in the solutions containing the sulfate-reducing bacteria was relatively low {300 mg/L [300 ppm by weight] at the most}, not enough H_2S in the bulk solution was able to reach the electrolytically cleaned electrode during the backward scan to affect the repassivation potential. On the contrary, the dissolved concentration of H_2S in the abiotic solutions was relatively high {450 mg/L 450 ppm by weight]}, and more H_2S was available in the bulk solution to reach the electrode during the backward scan, causing the repassivation potential to be lower.

The higher content of H_2S on or near the metal surface in the solutions containing the sulfate-reducing bacteria is probably the cause for the observed pitting corrosion (Figures 4-17 and 4-22), even though the H_2S effect on localized corrosion of metals could not be detected by measuring the repassivation potential. Therefore, the use of the repassivation potential to determine the susceptibility of a metal to localized corrosion does not seem adequate for environments containing sulfate-reducing bacteria and perhaps for other bacteria too. It appears that long-term immersion tests should be conducted to determine the susceptibility to localized corrosion of corrosion-resistant or passive alloys in microbial environments.

4.4 Electrochemical and Long-Term Immersion Tests for Alloy 22

As discussed in Section 4.2, localized corrosion of Types 304 and 304L SS specimens was observed in the microbial environments even at corrosion potentials lower than the repassivation potentials. Therefore, it appears that the use of repassivation potential and corrosion potential to determine the susceptibility to localized corrosion is not adequate in solutions containing microorganisms. However, the tests conducted by Lian, et al. (1999a) in a consortium of bacteria were too short (5 months) to determine the susceptibility of Alloy 22 to microbially influenced corrosion. Rao and Satpathy (2000) showed only a single pit of nearly round shape {approximately 0.08-mm [3.15×10^{-3}-in] diameter} for a Type 304 SS specimen after 25 days of immersion in a solution containing sulfate-reducing bacteria at room temperature. Ringas and Robinson (1988b) observed pitting corrosion for Type 304L SS specimens after 4 months of immersion in solutions containing sulfate-reducing bacteria at room temperature. This study (Section 4.2) has shown that 59 days of exposure in a solution containing sulfate-reducing bacteria did not result in the initiation of localized corrosion signs. However, the 98-day immersion test developed a significant pit {approximately 0.050-mm [1.97×10^{-3}-in] diameter}. It may take a much longer time for Alloy 22, a much more corrosion-resistant alloy than stainless steels, to show any signs of localized corrosion in the presence of microorganisms

More experiments and longer term experiments should be conducted to verify the dissolution rate of Alloy 22 and to determine if the dissolution rate would continue in the presence of microorganisms. Because it is hard to account for all possible bacteria, including those bacteria native to the drift and those that may be introduced into the repository, bounding case studies should include a test conducted with a consortia of bacteria that are known to cause the severe detrimental corrosion effects. Such consortia of bacteria should include organisms that represent a worse-case scenario of generating corrosive agents and conditions conducive to corrosion (e.g., pH, biofilms, hydrogen sulfide, organic acids, hydrogen peroxide, and hydrogen). Future experiments also should be considered to explore the role of thermophilic bacteria capable of growth at or above 60 °C [140 °F].

5 SUMMARY, CONCLUSIONS, AND RECOMMENDATIONS

5.1 Microbial Activity Effects on Uniform Corrosion of Alloy 22

In the studies on microbially influenced corrosion of Alloy 22 conducted by the U.S. Department of Energy (DOE), anodic current densities measured in the potentiodynamic polarization curves and corrosion rates obtained using the linear polarization resistance method were higher in microbial environments than those obtained in microbial-free environments. In the Center for Nuclear Waste Regulatory Analyses (CNWRA) studies described in this report, higher anodic polarization current densities were obtained on both stainless steel and platinum electrodes in microbial environments compared to those observed in the microbial-free environments. Because platinum is not expected to corrode within the range of potentials included in the polarization scans, the higher anodic current densities observed on platinum and stainless steel electrodes are believed caused by the oxidation of adsorbed surface species produced by the microorganisms (i.e., reduced sulfur species generated by sulfate-reducing bacteria). Results from these initial CNWRA studies suggest that the higher corrosion rates for Alloy 22 measured by DOE using the linear polarization resistance method may be a result of oxidation currents of reduced species produced in the microbial environment rather than an increase in the uniform corrosion rate within the passive range caused by the activity of the microorganisms. Using a microbially influenced corrosion factor derived from the linear polarization resistance measurements to account for microbial activity in the model abstraction for the general corrosion of Alloy 22 tends to overestimate the uniform corrosion rate and, therefore, can be considered a conservative approach if localized corrosion cannot be promoted by bacterial activity.

5.2 Microbial Activity Effects on Localized Corrosion of Alloy 22

From the repassivation potential measurements performed by DOE and CNWRA in microbial-free environments, it can be concluded that the critical temperature for the localized corrosion of Alloy 22, even in concentrated chloride solutions without the presence of inhibiting anions, is higher than the temperature at which the relative humidity on the waste package surface reaches the threshold value of approximately 90 percent required for microbial activity. Based on such repassivation potential measurements, DOE considered that Alloy 22 will not be susceptible to localized corrosion in environments characterized by the presence of microorganisms. However, many microorganisms found in the vicinity of Yucca Mountain are known to produce aggressive environments that could promote localized corrosion of stainless steels and relatively high corrosion-resistant nickel-based alloys.

From these initial CNWRA studies, it is apparent that the effect of microbial activity on the localized corrosion of passive metals such as Type 304 SS is not detectable in short-term tests using repassivation potential measurements. It appears that the high anodic polarization required by the technique to initiate localized corrosion may affect bacterial activity or the concentration of potentially aggressive metabolic products. Even though pitting corrosion of Type 304 SS was detected in a chloride solution with the presence of sulfate-reducing bacteria in the 160-day immersion test, no lowering of the repassivation potential was observed in the short-term electrochemical test in the microbial environments. The repassivation potential method, based on the reverse potentiodynamic scan after initiation of localized corrosion at high anodic potentials, may not be adequate to quantify the effect of bacterial activity on localized corrosion. Therefore, it appears that in environments modified by bacterial metabolism, the repassivation potential method may not be adequate to determine the microbial effect on the

susceptibility to localized corrosion of corrosion-resistant alloys such as Alloy 22, which is far more resistant to this form of corrosion than Type 304 SS. Long-term immersion tests, allowing sufficient time for creating occluded cell conditions in which the appropriate concentration of metabolic products can be reached, could provide a better assessment of the susceptibility to microbially influenced corrosion of a given corrosion-resistant alloy. For this reason, a set of long-term experiments with duplicate specimens made of heat-treated Alloy 22, Type 316L SS, and Alloy 825 is currently being conducted at CNWRA. These experiments are performed in parallel cells containing *Pseudomonas*, *Thiobacilli*, *Vibrio Natriegens*, sulfate-reducing bacteria, or mixtures of these bacteria. At regular intervals, the specimens are removed from the test cells and examined with scanning electron microscope for signs of localized corrosion.

The long-term immersion test solutions inoculated with Yucca Mountain rocks may not contain all the bacteria native to the Yucca Mountain potential repository horizon or may be presumably introduced into the repository during the construction or after waste emplacement because the repository is an open system. For this reason, it would be desirable to conduct long-term tests in solutions that contain all potential detrimental microorganisms that may be present at Yucca Mountain. Although this testing program may seem to be a rather cumbersome endeavor, performance confirmation activities should include this type of testing using not only mill-annealed specimens of Alloy 22 but also heat-treated and welded specimens.

5.3 Future Work

Further evaluation of the effect of microorganisms, particularly bacteria, on the localized corrosion susceptibility of Alloy 22, as well as Type 316L SS, is necessary to assess the performance of the engineered barrier system materials. Although DOE does not take credit for the integrity of the Type 316 nuclear grade stainless steel inner container, the possibility of localized corrosion of the stainless steel following penetration of the Alloy 22 outer container deserves attention. The generation of corrosion products in the annular gap between both containers caused by stainless steel corrosion may introduce substantial stresses in localized areas of the outer container. It is well established that stresses generated by corrosion products are able to induce the initiation or opening of cracks. The opening of stress corrosion cracks is considered to have medium significance to waste isolation (NRC, 2004). An additional reason to include Type 316L SS in future studies is that this alloy will be used as perforated sheets and rock bolts for ground support in the emplacement drifts. The stability of the emplacement drifts is considered to have medium significance to waste isolation (NRC, 2004).

The DOE short-term electrochemical experiments were not adequate to determine the potential susceptibility of Alloy 22 to localized corrosion. The long-term tests show the development of microcavities on Alloy 22 specimens in solutions inoculated with Yucca Mountain rock. If some of these microcavities continue to grow, they could be early signs of localized corrosion. In addition, it is possible that the solutions inoculated with Yucca Mountain rocks collected from the exploratory drift do not contain all the bacteria that may be available in the repository and detrimental to the corrosion of Alloy 22. It is important to note that other bacteria may be introduced during construction or after the emplacement because the repository system is essentially an open system. Microbial communities are highly adaptable to changes in their surroundings. As the environment within the emplacement drifts evolves over time, microorganisms will become adapted to the new conditions of temperature, water, and nutrient

availability. Any bacteria may colonize in the repository system if the conditions become favorable for growth. A broad range of bacteria should be included in future work. The long-term test currently under way may shed light on the approach and the methods needed to conduct a more complete evaluation of the effect of bacteria on corrosion of waste package materials.

6 REFERENCES

Akashi, M., G. Nakayama, and T. Fukuda. "Initiation Criteria for Crevice Corrosion of Titanium Alloys Used for HLW Disposal Overpack." Proceedings of the CORROSION '98 Conference. Paper No. 158. Houston, Texas: NACE International. 1998.

Amaya, H. "Microbially Influenced Corrosion of Stainless Steels in Aerobic Aqueous Environments." *Corrosion Engineering.* Vol. 52. pp. 165–175. 2003.

Amaya, H. and H. Miyuki. "Laboratory Reproduction of Potential Ennoblement of Stainless Steels in Natural Seawater." Proceedings of the CORROSION '99 Conference. Paper No. 168. Houston, Texas: NACE International. 1999.

Anderson, M.J., N.R. Brown, J.D. Cloud, P.R.Z. Russell, and J. Trautner. "Waste Package Design for License Application." Proceedings of the 10th International High-Level Radioactive Waste Management Conference, Las Vegas, Nevada, March 30–April 3, 2003. Section E–7. Published on CD-ROM. La Grange Park, Illinois: American Nuclear Society. pp. 714–720. 2003.

ASTM International. "Standard Practice for Conventions Applicable to Electrochemical Measurements in Corrosion Testing." G3–89 (Reapproved 1999). West Conshohocken, Pennsylvania: ASTM International. 1999.

Bachofen, R. "Multi-Author Review—Microorganisms in Nuclear Waste Disposal." *Experientia: Part II.* Vol. 47. pp. 507–583. 1991.

Bachofen, R. "Multi-Author Review—Microorganisms in Nuclear Waste Disposal." *Experientia: Part I.* Vol. 46. pp. 777–851. 1990.

Barns, S.M., S.L. Takala, and C.R. Kuske. "Wide Distribution and Diversity of the Bacterial Kingdom *Acidobacterium* in the Environment." *Applied and Environmental Microbiology.* Vol. 65. pp. 1,731–1,737. 1999.

Bechtel SAIC Company, LLC. "Technical Basis Document No. 5: In-Drift Chemical Environment." Rev. 1. Las Vegas, Nevada: Bechtel SAIC Company, LLC. 2003a.

——— "Technical Basis Document No. 6: Waste Package and Drip Shield Corrosion." Rev. 1. Las Vegas, Nevada: Bechtel SAIC Company, LLC. 2003b.

———. "General Corrosion and Localized Corrosion of Waste Package Outer Barrier." ANL–EBS–MD–000003. Rev. 00. Las Vegas, Nevada: Bechtel SAIC Company, LLC. 2003c.

Borenstein, S.W. *Microbiologically Influenced Corrosion Handbook.* Cambridge, United Kingdom: Woodhead Publishing Limited. 1994.

Bradford, S.A. *Corrosion Control.* 2nd Edition. Materials Park, Ohio: ASM International. p. 553. 2001.

Brennenstuhl, A.M., P.E. Doherty, P.J. King, and T.G. Dunstall. "The Effects of Biofouling on the Corrosion of Nickel Heat Exchanger Alloys at Ontario Hydro." *Microbially Influenced Corrosion and Biodeterioration.* N.J. Dowling, M.W. Mittelman, and J.C. Danko, eds. Knoxville, Tennessee: The University of Tennessee. pp. 4-25 to 4-31. 1990.

Brock, T.D., ed. "Introduction: An Overview of Thermophiles." *Thermophiles: General, Molecular, and Applied Microbiology.* New York City, New York: John Wiley and Sons. p. 316. 1986.

Castro, P., P.S. Amy, D.A. Jones, G. Southam, R. Donald, and D.B. Ringelberg. "Effect of Rock Surfaces on the Corrosion Capability of Yucca Mountain Bacteria." *Corrosion.* Vol. 60. p. 75. 2004.

Castro, H.F., N.H. Williams, and A. Ogram. "Phylogeny of Sulfate-Reducing Bacteria." *Federation of European Microbiological Societies Microbiology-Ecology.* Vol. 31. pp. 1–9. 2000.

Castro, P., P.S. Amy, D.A. Jones, H.V. Crossen, G. Southam, R. Donald, and D.B. Ringelberg. "The Corrosion of Carbon Steel in Rock Microcosms Containing Native Yucca Mountain Microorganisms." Proceedings of the CORROSION '98 Conference. Paper No. 98284. Houston, Texas: NACE International. 1998.

Collins, C.H., P.M. Lyne, J.M. Grange, and J.O. Falkinham, III. *Collins and Lyne's Microbiological Methods.* 8th Edition. Oxford, England: Butterworth-Heinemann. 2004.

Cotton, F.A. and D. Wilkinson. *Advanced Inorganic Chemistry.* 4th Edition. New York City, New York: John Wiley and Sons. 1980.

CRWMS M&O. Repository Safety Strategy: Plan to Prepare the Safety Case to Support Yucca Mountain Site Recommendation and Licensing Considerations." TDR–WIS–RL–000001. Rev. 04 ICN 01. Las Vegas, Nevada: CRWMS M&O. 2000a.

———. "In-Drift Microbial Communities." ANL–EBS–MD–000038. Rev. 00 ICN 01. Las Vegas, Nevada: CRWMS M&O. 2000b.

Davis, J.R., ed. *Corrosion—Understanding the Basics.* Materials Park, Ohio: ASM International. p. 563. 2000.

Davis, M.A., S. Martin, A. Miranda, and J.M. Horn. "Sustaining Native Microbial Growth with Endogenous Nutrients at Yucca Mountain." Proceedings of the Eighth International Conference on High-Level Radioactive Waste Management, Las Vegas, Nevada, May 11–14, 1998. La Grange Park, Illinois: American Nuclear Society. pp. 662–665. 1998.

Dowling, N.J.E. and J. Guezennec. "Microbially Influenced Corrosion." *Manual of Environmental Microbiology.* C.J. Hurst, G.R. Knudsen, M.J. McInerney, L.D. Stetzenbach, and M.V. Walter, eds. Washington, DC: American Society for Microbiology, ASM Press. pp. 842–855. 1997.

Dunn, D.S., G.A. Cragnolino, and N. Sridhar. "An Electrochemical Approach to Predicting Long-Term Localized Corrosion of Corrosion-Resistant High-Level Waste Container Materials." *Corrosion.* Vol. 56. pp. 90–104. 2000.

Ehrlich, H.L. *Geomicrobiology.* 4th Edition. New York City, New York: Marcel Dekker, Inc. 2002.

Fedors, R., S. Green, D. Walter, D. Farrell, S. Svedeman, F. Dodge, and R. Hart. "Environmental Conditions in Drifts." San Antonio, Texas: CNWRA. 2004.

Ford, T.E., M. Walch, and R. Mitchell. "Corrosion of Metals by Thermophilic Microorganisms." *Materials Performance.* Vol. 26, No. 2. pp. 35–39. 1987.

Geesey, G. "A Review of the Potential for Microbially Influenced Corrosion of High-Level Nuclear Waste Containers." CNWRA 93-014. San Antonio, Texas: CNWRA. 1993.

Geesey, G. and G.A. Cragnolino. "A Review of the Potential for Microbially-Influenced Corrosion of High-Level Nuclear Waste Containers in an Unsaturated Repository Site." The 1995 International Conference on Microbially Influenced Corrosion. P. Angell, S.W. Borenstein, R.A. Buchanan, S.C. Dexter, N.J.E. Dowling, B.J. Little, C.D. Lundin, M.B. McNeil, D.H. Pope, R.E. Tatnall, D.C. White, and H.G. Ziengenfuss, eds. Houston, Texas: NACE International. pp. 76/1–76/20. 1995.

Goldstein, J.I., D.E. Newbury, P. Echlin, D.C. Joy, A.D. Romig, Jr., C.E. Lyman, C. Fiori, and E. Lifshin. *Scanning Electron Microscopy and X-Ray Microanalysis.* 2nd Edition. New York City, New York: Plenum Press. p. 820. 1992.

Halberg, K.B. and E.B. Lindstrom. "Characterization of *Thiobacillus caldus sp. nov.*, A Moderately Thermophilic Acidophile." *Microbiology.* Vol. 140. pp. 3,451–3,456. 1994.

Hamilton, W.A. "Biofilms and Microbially Influenced Corrosion." *Microbial Biofilms.* H.M. Lappin-Scott and J.W. Costerton, eds. Cambridge, United Kingdom: Cambridge University Press. pp. 171–182. 1995.

Harrar, J.E., J.F. Carley, W.F. Isherwood, and E. Raber. "Report to the Committee to Review the Use of J–13 Well Water in Nevada Nuclear Waste Storage Investigations." UCRL–ID–21867. Livermore, California: Lawrence Livermore National Laboratory. 1990.

Horn, J.M., B.A. Masterson, A. Rivera, A. Miranda, M.A. Davis, and S. Marlin. "Bacterial Growth Dynamics, Limiting Factors, and Community Diversity in a Proposed Geological Nuclear Waste Repository Environment." *Geomicrobiology Journal.* Vol. 21. pp. 273–287. 2004.

Horn, J., C. Carrillo, and V. Dias. "Comparison of the Microbial Community Composition at Yucca Mountain and Laboratory Test Nuclear Repository Environments." Proceedings of the CORROSION 2003 Conference. Paper No. 03556. Houston, Texas: NACE International. 2003.

Horn, J.M., S. Martin, and B. Masterson. "Evidence of Biogenic Corrosion of Titanium After Exposure to a Continuous Culture of *Thiobacillusferrooxidans* Grown in Thiosulfate Medium." Proceedings of the CORROSION 2001 Conference. Paper No. 01259. Houston, Texas: NACE International. 2001.

Horn, J.M., S. Martin, A. Rivera, P. Bedrossian, and T. Lian. "Potential Biogenic Corrosion of Alloy 22, A Candidate Nuclear Waste Packaging Material Under Simulated Repository Conditions." Proceedings of the CORROSION 2000 Conference. Paper No. 387. Houston, Texas: NACE International. 2000.

Horn, J., S. Martin, B. Masterson, and T. Lian. "Biochemical Contributions to Corrosion of Carbon Steel and Alloy 22 in a Continual Flow System." Proceedings of the CORROSION '99 Conference. Paper No. 162. Houston, Texas: NACE International. 1999.

Horn, J.M., A. Rivera, T. Lian, and D.A. Jones. "MIC Evaluation and Testing for the Yucca Mountain Repository." Proceedings of the CORROSION '98 Conference. Paper No. 152. Houston, Texas: NACE International. 1998.

Horn, J.M., R.D. McCright, and B. Economides. "Initial Studies to Assess Microbial Impacts on Nuclear Waste Disposal." High-Level Radioactive Waste Management: Proceedings of the Seventh Annual International Conference, Las Vegas, Nevada, April 29–May 3, 1996. La Grange Park, Illinois: American Nuclear Society. pp. 7–8. 1996.

Jain, V., D.S. Dunn, N. Sridhar, and L. Yang. "Effect of Measurement Methods and Solution Chemistry on the Evaluation of Localized Corrosion of Candidate High-Level Waste Container Materials." Proceedings of the CORROSION 2003 Conference. Paper No. 03690. Houston, Texas: NACE International. 2003.

Jorgensen, B.B., M.F. Isaksen, and H. Jannasch. "Bacterial Sulfate-Reduction Above 100 °C in Deep-Sea Hydrothermal Vent Sediments." *Science*. Vol. 258. pp. 1,756–1,757. 1992.

Lewandowski, Z. "MIC and Biofilm Heterogeneity." Proceedings of the CORROSION 2000 Conference. Paper No. 00400. Houston, Texas: NACE International. 2000.

Lian, T., S. Martin, D. Jones, A. Rivera, and J. Horn. "Corrosion of Candidate Container Materials by Yucca Mountain Bacteria." Proceedings of the CORROSION '99 Conference. Paper No. 476. Houston, Texas: NACE International. 1999a.

Lian, T., D. Jones, S. Martin, and J. Horn. "A Quantitative Assessment of Microbiological Contributions to Corrosion of Candiate Nuclear Waste Package Materials." Scientific Basis for Nuclear Waste Management XXII. Symposium Proceedings 556. D.J. Wronkiewicz and J.H. Lee, eds. Warrendale, Pennsylvania: Materials Research Society. pp. 1,175–1,182. 1999b.

Little, B., R. Rope, and R. Ray. "Localized Corrosion and Bacterial Attraction Determined by Surface Analytical Techniques." Proceedings of the CORROSION 2000 Conference. Paper No. 00395. Houston, Texas: NACE International. 2000.

Little, B., P. Wagner, S.M. Gerchakov, M. Walch, and R. Mitchell. "The Involvement of a Thermophilic Bacterium in Corrosion Processes." *Corrosion.* Vol. 42, No. 9. pp. 533–536. 1986.

Liu, Y., T.M. Karnauchow, K.F. Jarrell, D.L. Balkwill, G.R. Drake, D. Ringelberg, R. Clarno, and D.R. Boone. "Description of Two New *Thermophilic Desulfotomaculum* spp., *Desulfotomaculum Putei* sp. nov., from a Deep Terrestrial Subsurface, and *Desulfotomaculum Luciae* sp. nov. From a Hot Spring." *International Journal of Systematic Bacteriology.* Vol. 47. pp. 615–621. 1997.

Love, C.A., B.K.C. Patel, P.D. Nicholas, and E. Stackebrandt. "*Desulfotomaculum australicum*, sp. nov., A Thermophilic Sulfate-Reducing Bacterium Isolated from the Great Artesian Basin of Australia." *Systematic and Applied Microbiology.* Vol. 16. pp. 244–251. 1993.

Maier, R.M., I.L. Pepper, and C.P. Gerba. *Environmental Microbiology.* San Diego, California: Academic Press. p. 585. 2000.

Manaia, C.M. and E.R.B. Moore. "*Pseudomonas thermotolerans* sp. nov., A Thermotolerant Species of the Genus *Pseudomonas* sensu stricto." *International Journal of Systematic and Evolutionary Microbiology.* Vol. 52. pp. 2,203–2,209. 2002.

Manaia, C.M., O.C. Nunes, and B. Nogales. "*Caenibacterium thermophilum* gen. nov., sp. nov., Isolated from a Thermophilic Aerobic Digester of Municipal Sludge." *International Journal of Systematic and Evolutionary Microbiology.* Vol. 53. pp. 1,375–1,382. 2003.

Marcus, P. "Sulfur-Assisted Corrosion Mechanisms and the Role of Alloyed Elements." *Corrosion Mechanisms in Theory and Practice.* P. Marcus and J. Oudar, eds. New York City, New York: Marcel Dekker, Inc. p. 239. 1995.

Marshall, K.C. "Colonization, Adhesion, and Biofilms." *Manual of Environmental Microbiology.* C.J. Hurst, G.R. Knudsen, M.J. McInerney, L.D. Stetzenbach, and M.V. Walter, eds. Washington, DC: American Society for Microbiology, ASM Press. pp. 842–855. 1997.

Martin, S., J. Horn, and A.C. Carrillo. "Micron-Scale MIC of Alloy 22 After Long-Term Incubation in Standard Nuclear Waste Repository Microcosms." Proceedings of the CORROSION 2004 Conference. Paper No. 04596. Houston, Texas: NACE International. 2004.

Martin, F.J., P.M. Natishan, K.E. Lucas, E.A. Hogan, A.M. Grolleau, and E.D. Thomas. "Crevice Corrosion of Alloy 625 in Natural Seawater." *Corrosion.* Vol. 59. pp. 498–504. 2003.

Newman, R.C., B.J. Webster, and R.G. Kelly. "The Electrochemistry of SRB Corrosion and Related Inorganic Phenomena." *Iron Steel Institute of Japan International.* Vol. 31. pp. 201–209. 1991.

Newman, R.C., W.P. Wong, H. Ezuber, and A. Garner. "Pitting of Stainless Steels by Thiosulfate Ions." *Corrosion.* Vol. 45. pp. 282–287. 1989.

Newman, R.C., W.P. Wong, and A. Garner. "A Mechanism of Microbial Pitting in Stainless Steel." *Corrosion.* Vol. 42. pp. 489–491. 1986.

Newman, R.C., H.S. Isaacs, and B. Alman. "Effects of Sulfur Compounds on the Pitting Behavior of Type 304 Stainless Steel in Near-Neutral Chloride Solutions." *Corrosion.* Vol. 35. pp. 261–265. 1982.

NRC. "Risk Insights Baseline Report." Rev. 00. Washington, DC: NRC. April 2004.

———. NUREG–1762, "Integrated Issue Resolution Status Report." Washington, DC: NRC. July 2002.

———. "Issue Resolution Status Report, Key Technical Issue: Container Life and Source Term." Rev. 3. Washington, DC: NRC. 2001.

Okabe, S., T. Itoh, H. Satoh, and Y. Watanabe. "Analyses of Spatial Distributions of Sulfate-Reducing Bacteria and Their Activity in Aerobic Wastewater Biofilms." *Applied and Environmental Microbiology.* Vol. 65. pp. 5,107–5,116. 1999.

Peck, H.D. Jr., and J. LeGall. *Inorganic Microbial Sulfur Metabolism, Methods in Enzymology.* Vol. 243. San Diego, California: Academic Press. p. 682. 1994.

Pitonzo, B.J., P.S. Castro, G. Amy, D.A. Southam, D.A. Jones, and D. Ringelberg. "Microbiological Influenced Corrosion Capability of Bacteria Isolated from Yucca Mountain." *Corrosion.* Vol. 60. p. 64. 2004.

Postgate, J.R. *The Sulphate-Reducing Bacteria.* Cambridge, United Kingdom: Cambridge University Press. p. 151. 1979.

Rao, T.S. and K.K. Satpathy. "Studies on Pitting Corrosion of Stainless Steel (SS-304) by a Marine Strain of Sulfate Reducing Bacteria (*Desulfovibrio vulgarious*)." Microbial Corrosion: Proceedings of the 4th International EFC Workshop, European Federation of Corrosion. C.A.C. Sequira, ed. Publication No. 29. London, England: IOM Communications. p. 79. 2000.

Ray, I.R., B.J. Little, and J. Jones-Meehan. "A Laboratory Evaluation of Stainless Steels Exposed to Tap Water and Seawater in Microbially Influenced Corrosion." Proceedings of the Corrosion 2002 Research Topical Symposium. B.J. Little, ed. pp. 133–144. Houston, Texas: NACE International. 2002.

Rhodes, P.R. "Environment-Assisted Cracking of Corrosion-Resistant Alloys in Oil and Gas Production Environments: A Review." *Corrosion.* Vol. 57. pp. 923–966. 2001.

Ringas, C. and F.P.A. Robinson. "Corrosion of Stainless Steel by Sulfate-Reducing Bacteria-Electrochemical Techniques." *Corrosion.* Vol. 44. pp. 386–396. 1988a.

Ringas, C. and F.P.A. Robinson. "Corrosion of Stainless-Steel by Sulfate-Reducing-Bacteria Total Immersion Test-Results." *Corrosion.* Vol. 44. p. 671. 1988b.

Sanbongi, Y., M. Ishii, Y. Igarashi, and T. Kodama. "Amino Acid Sequence of Cytochrome c-552 from a Thermophilic Hydrogen-Oxidizing Bacterium *Hydrogenbacter thermophilus.*" *Journal of Bacteriology.* Vol. 171. pp. 65–69. 1989.

Santegoeds, C.M., T.G. Ferdelman, G. Muyzer, and D. de Beer. "Structural and Functional Dynamics of Sulfate-Reducing Populations in Bacterial Biofilms." *Applied and Environmental Microbiology.* Vol. 64. pp. 3,731–3,739. 1998.

Shooner, F., J. Bousquet, and R.D. Tyagi. "Isolation, Phenotypic Characterization, and Phylogenetic Position of a Novel, Facultatively Autotrophic, Moderately Thermophilic Bacterium, *Thiobacillus thermosulfatus* sp. nov." *International Journal of Systematic Bacteriology.* Vol. 46. pp. 409–415. 1996.

Stetter, K.O. "Archeoglobus Fulgidus gen. nov., sp. nov, A New Taxon of Extremely Thermophilic Archaea." *Systematic and Applied Microbiology.* Vol. 13. pp. 24–28. 1988.

Stetzenbach, L.D. DOE/NV/10872–T238. "Identification of Subsurface Microorganisms at Yucca Mountain." Quarterly Report. July 1–September 30, 1995. Washington, DC: DOE. 1995.

Sundaram, T.K. "Physiology and Growth of Thermophilic Bacteria." *Thermophiles: General, Molecular, and Applied Microbiology.* T.D. Brock, ed. New York City, New York: John Wiley and Sons. p. 316. 1986.

Takai, M., K. Kamimura, and T. Sugio. "A New Iron Oxidase from a Moderately Thermophilic Iron Oxidizing Bacterium Strain TI-1." *European Journal of Biochem*istry. Vol. 268. pp. 1,653–1,658. 2001.

Teilzel, G.M. and M.R. Parsek. "Heavy Metal Resistance of Biofilm and Planktonic *Pseudomonas Aeruginosa*." *Applied and Environmental Microbiology.* Vol. 69. pp. 2,313–2,320. 2003.

Thierry, D. and W. Sand. "Microbially Influenced Corrosion." *Corrosion Mechanisms in Theory and Practice.* P. Marcus and J. Oudar, eds. New York City, New York: Marcel Dekker, Inc. p. 457. 1995.

Tiller, A.K. "Is Stainless Steel Susceptible to Microbial Corrosion?" Microbial Corrosion: Proceedings of the Conference. London, United Kingdom: The Metals Society. pp. 104–109. 1983.

Tuovinen, O.H. and G. Cragnolino. "A Review of Microbiological and Electrochemical Techniques in the Study of Corrosion Influenced by Sulfate-Reducing Bacteria." Corrosion Monitoring in Industrial Plants Using Nondestructive Testing and Electrochemical Methods. G.C. Moran and P. Labine, eds. Special Technical Publication 908. West Conshohocken, Pennsylvania: ASTM International. pp. 412–432. 1986.

Vroom, J.M., K.J. De Grauw, H.C. Gerritsen, D.J. Bradshaw, P.D. Marsh, G.K. Watson, J.J. Birmingham, and C. Allison. "Depth Penetration and Detection of pH Gradients in Biofilms by Two-Photon Excitation Microscopy." *Applied and Environmental Microbiology.* Vol. 65. pp. 3,502–3,511. 1999.

Webster, B.J., R.G. Kelly, and R.C. Newman. "The Electrochemistry of SRB Corrosion in Austenitic Stainless Steel." *Microbially Influenced Corrosion and Biodeterioration.* H.J. Dowling, M.W. Mittelman, and J.C. Danko, eds. Houston, Texas: NACE International. pp. 2.9–2.17. 1990.